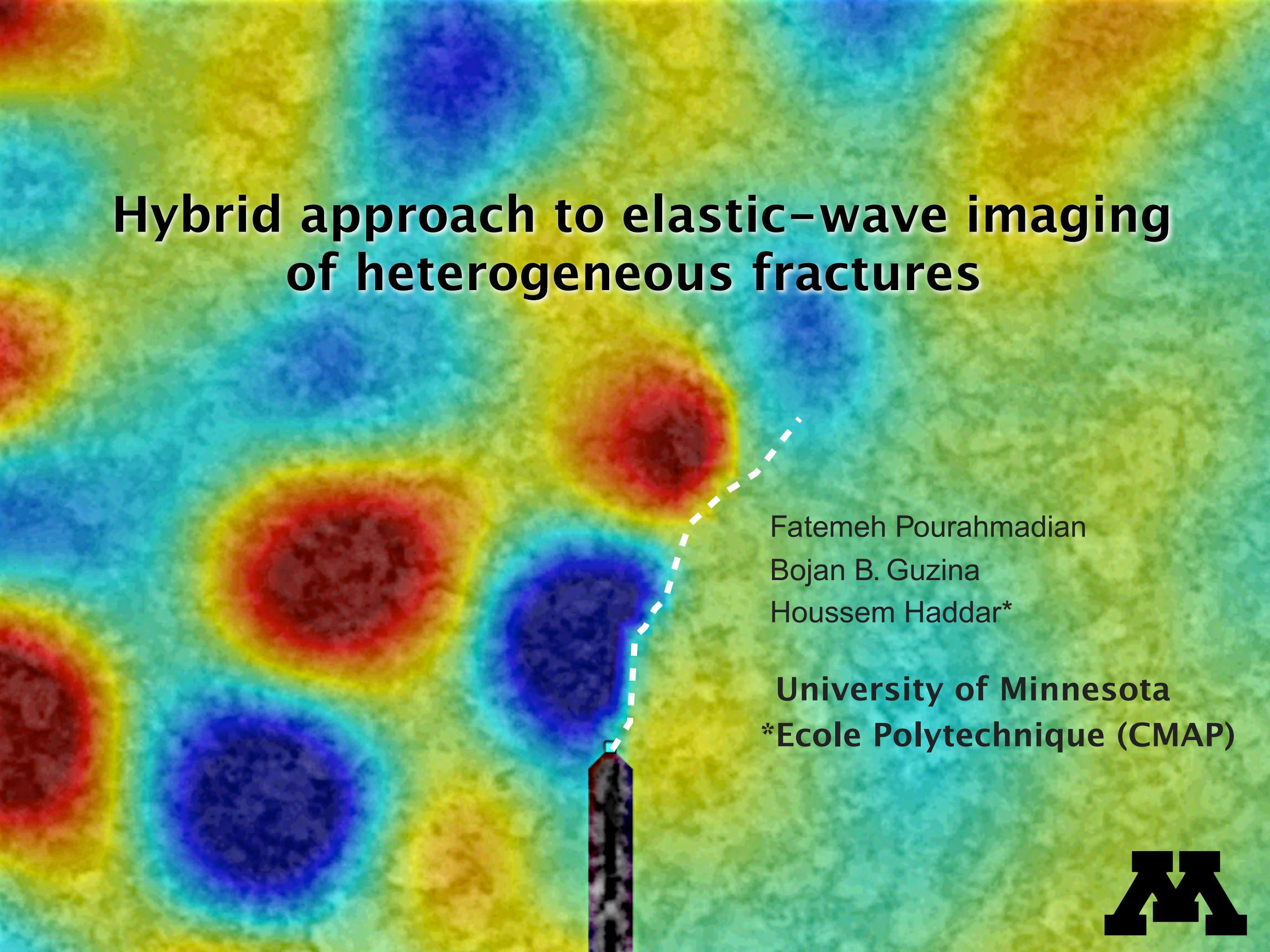
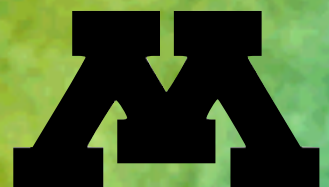


Hybrid approach to elastic-wave imaging of heterogeneous fractures



Fatemeh Pourahmadian
Bojan B. Guzina
Houssem Haddar*

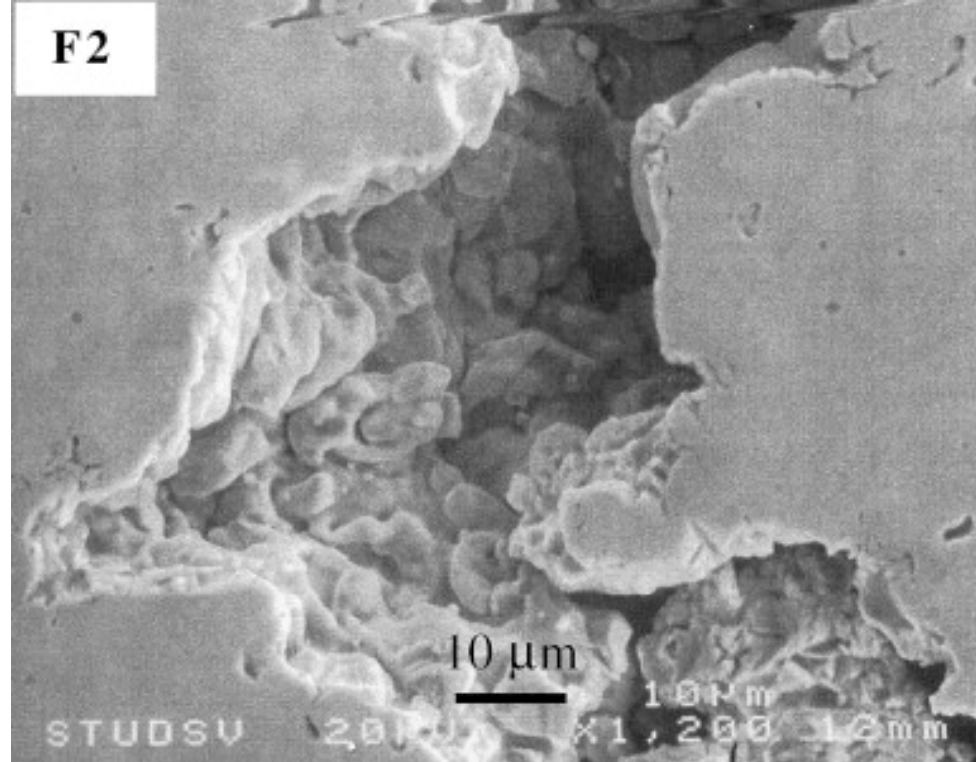
University of Minnesota
*Ecole Polytechnique (CMAP)



Heterogeneous fractures

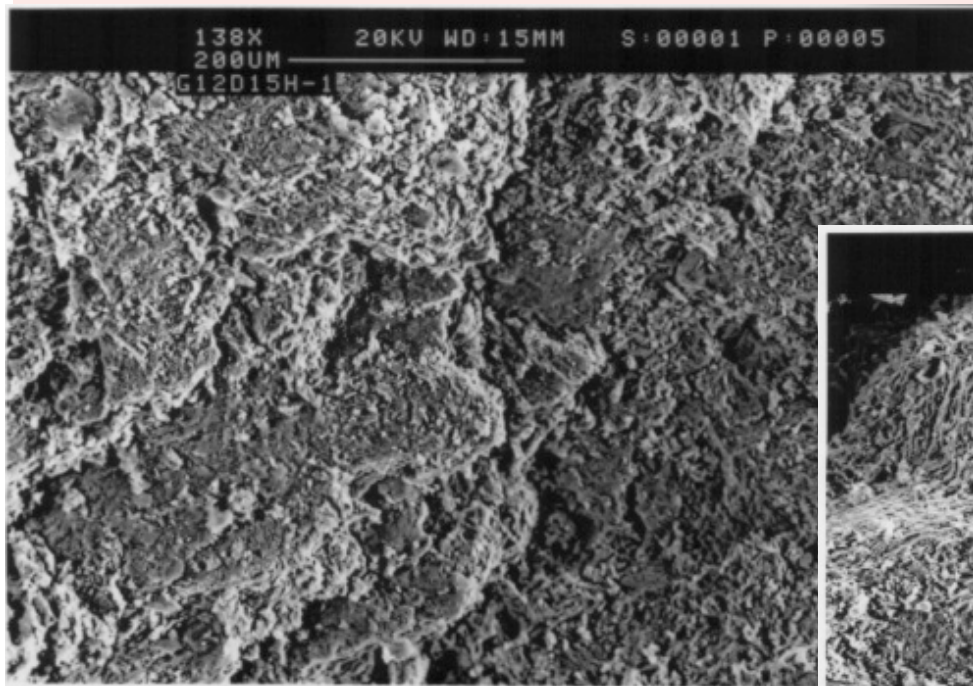
Fracture surface topography

F2

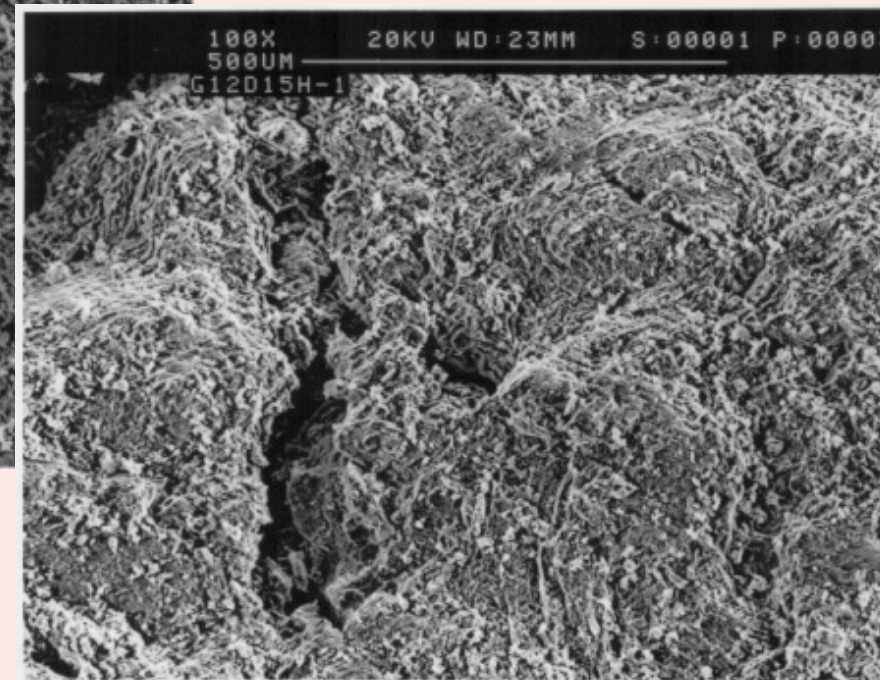


C. Pecorari, Int. J. Eng. Sc.(2008)

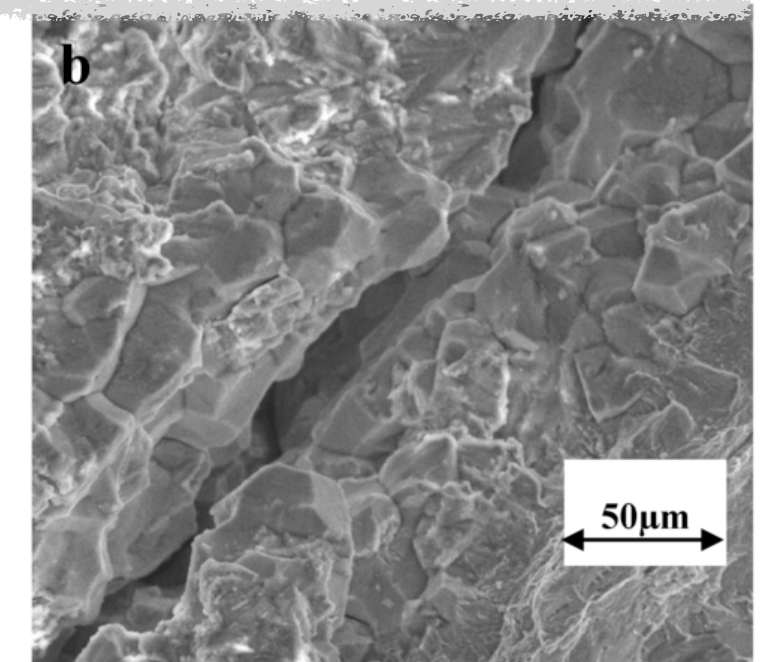
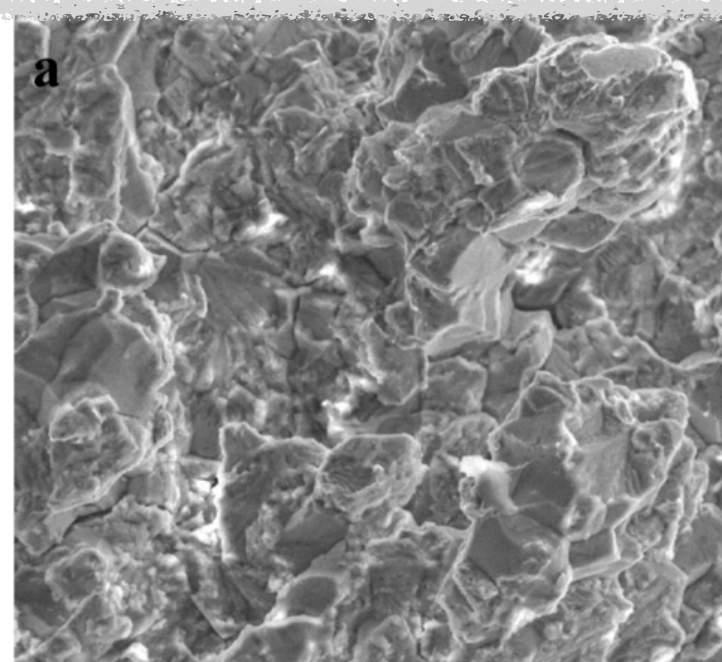
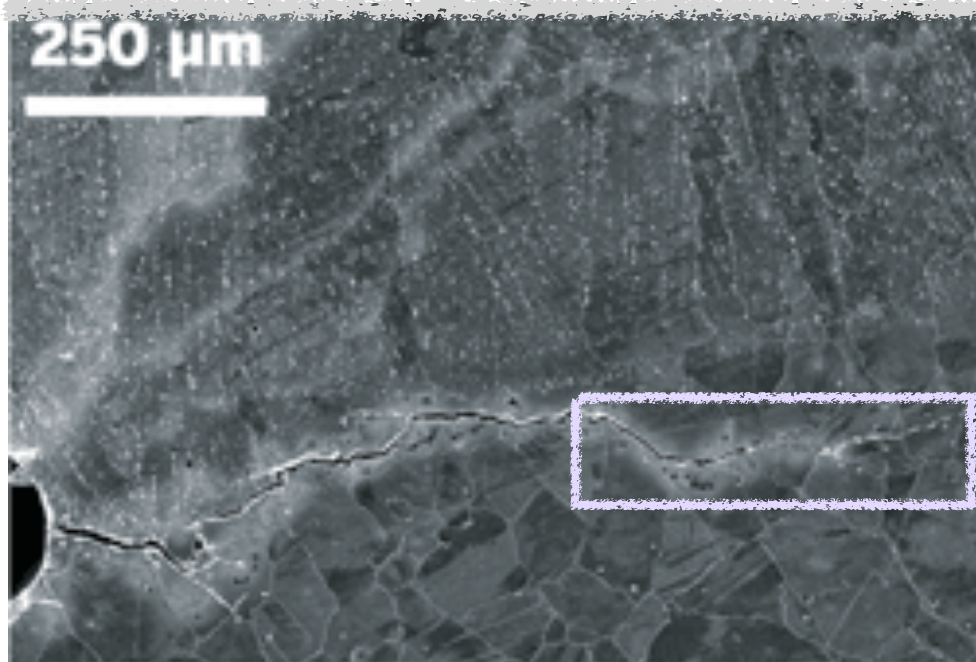
Micrographs of the fracture surface of IM1-24 graphite



M. J. Holt



Stress corrosion cracking in nuclear reactors

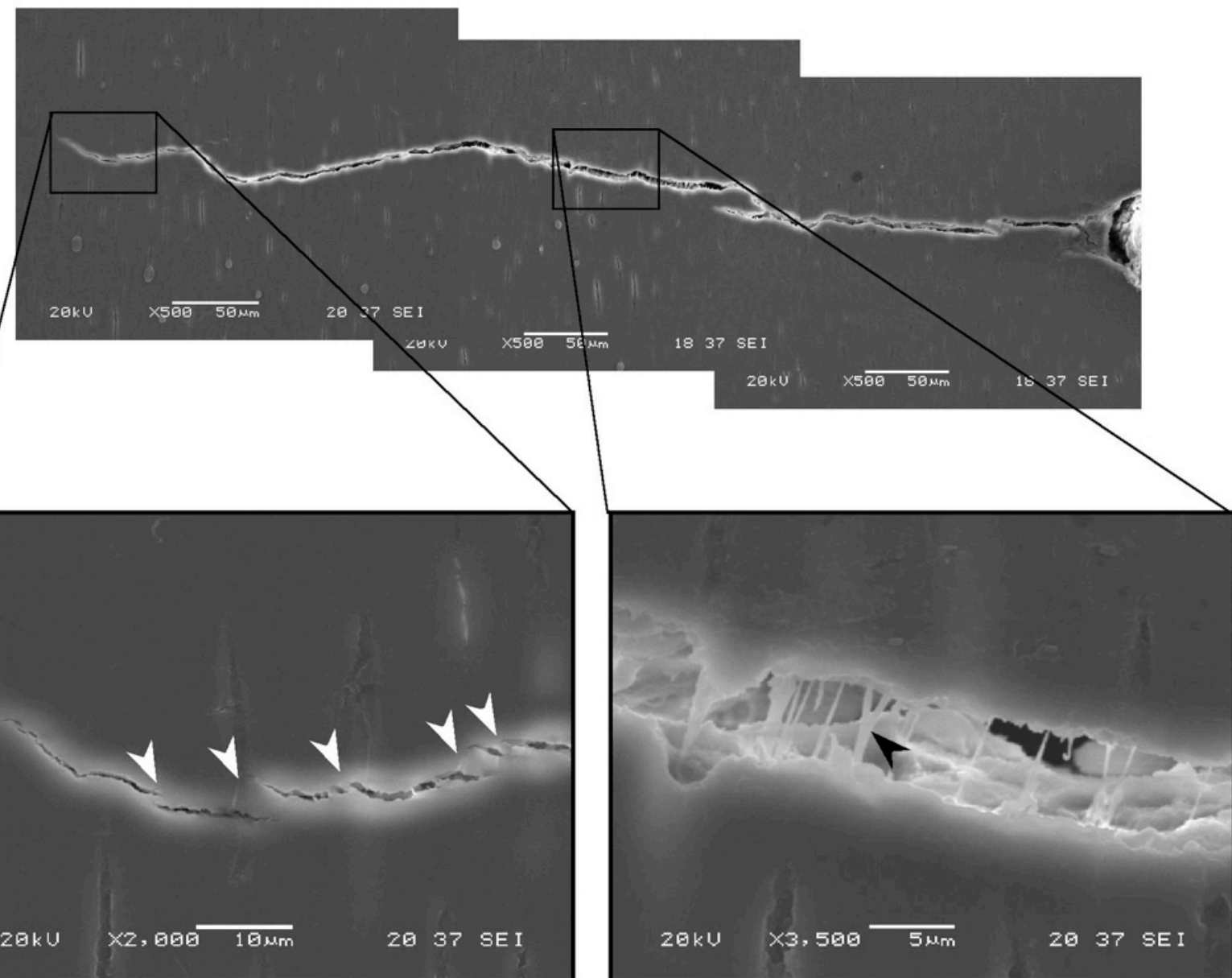


B. Alexandreanu, Argonne National Lab

R. K. Singh Raman, Materials (2014)

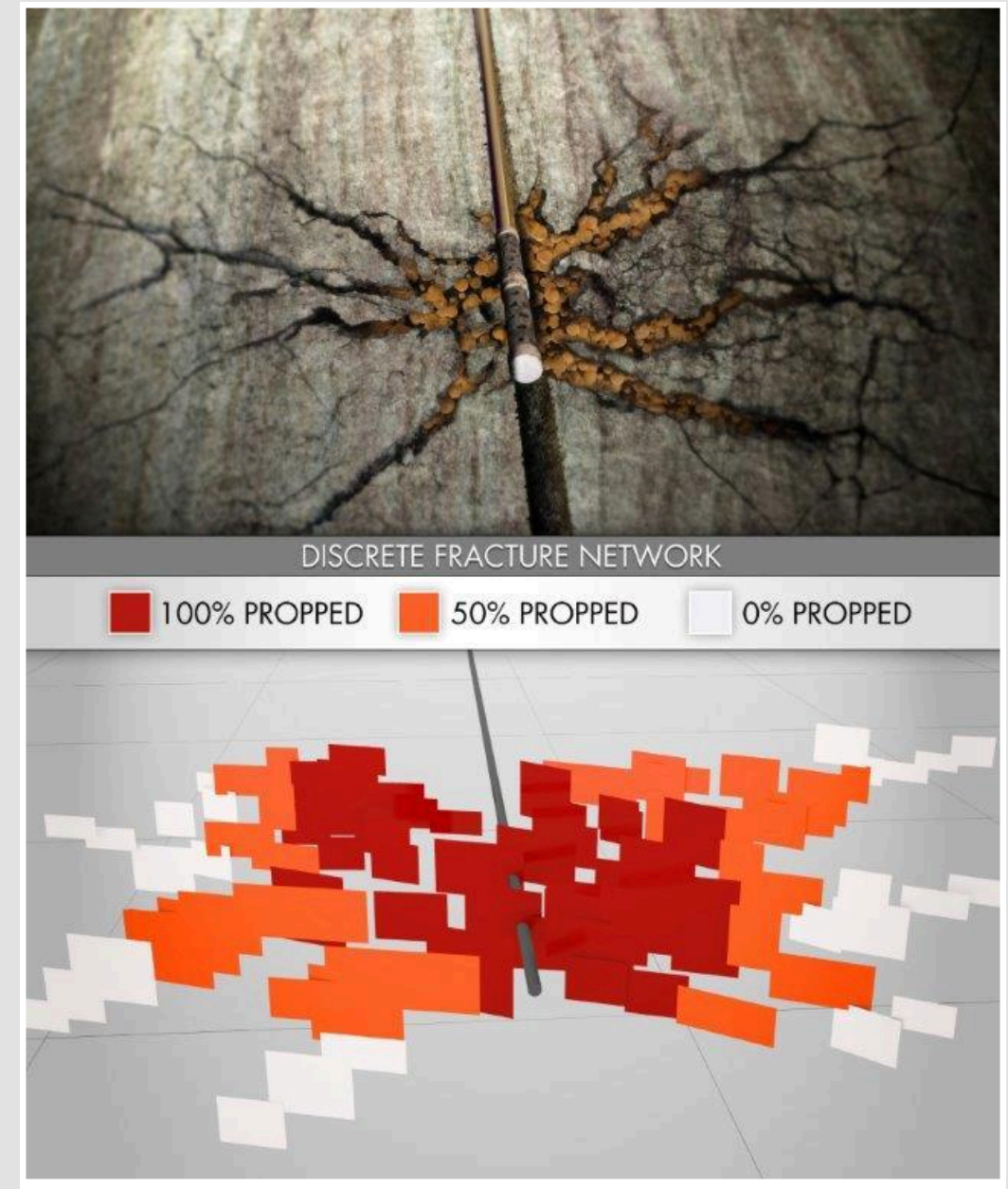
Heterogeneous fractures

Fracture propagation mechanisms

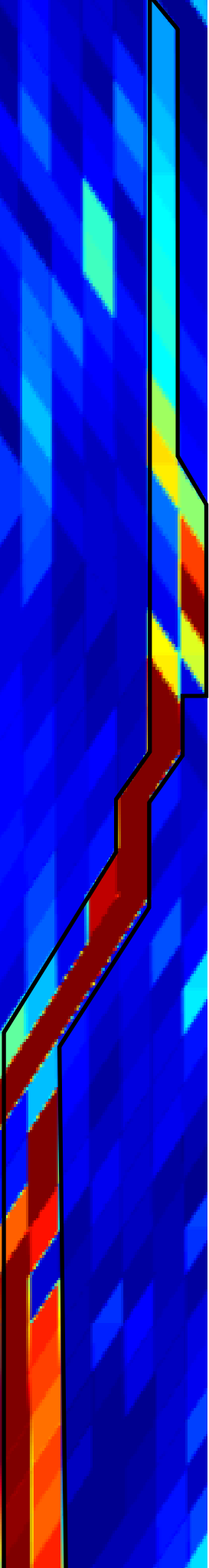


D. Bajaj, J. Biomed. Mater. Res. B (2008)

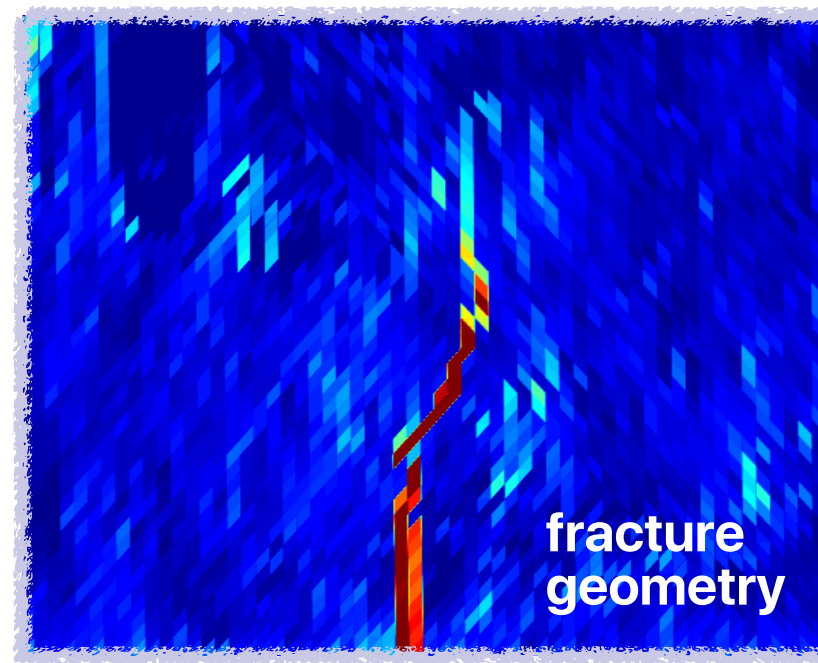
Proppant injection process



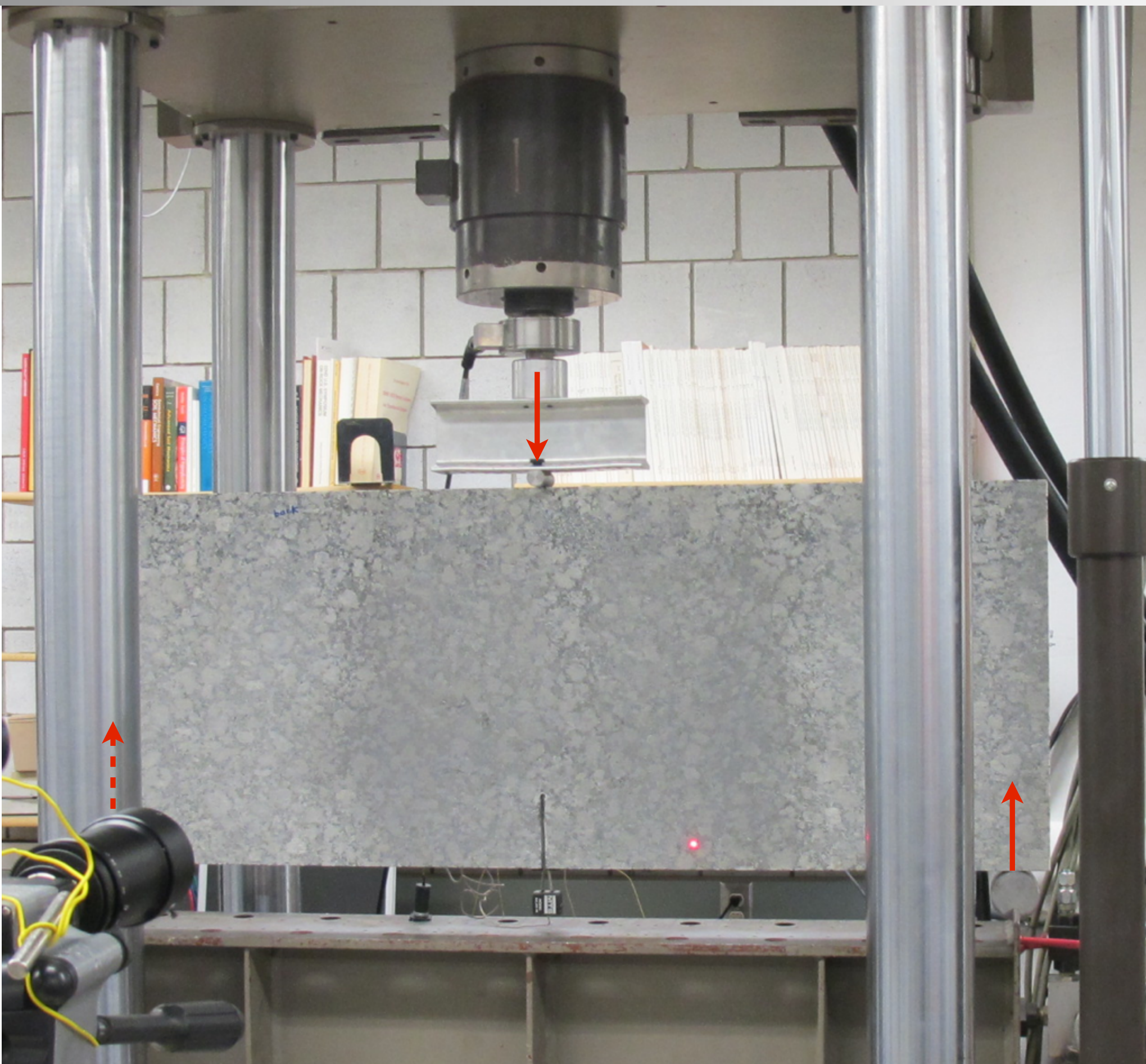
Microseismic Inc. (2013)



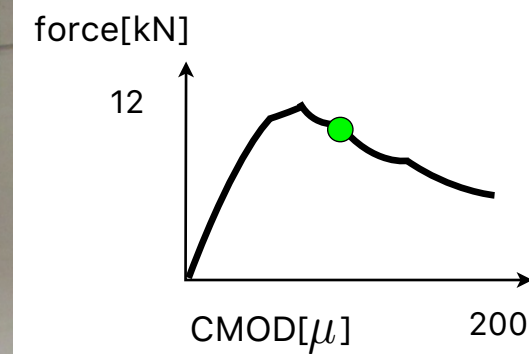
Experimental study of the forward scattering problem



3-point bending configuration

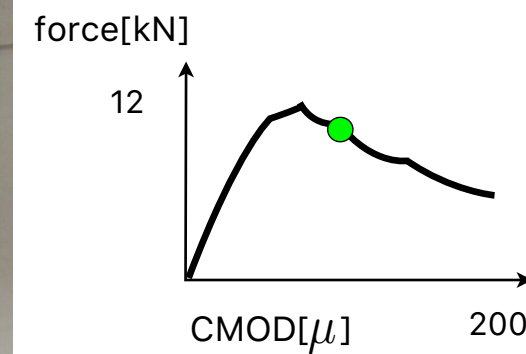
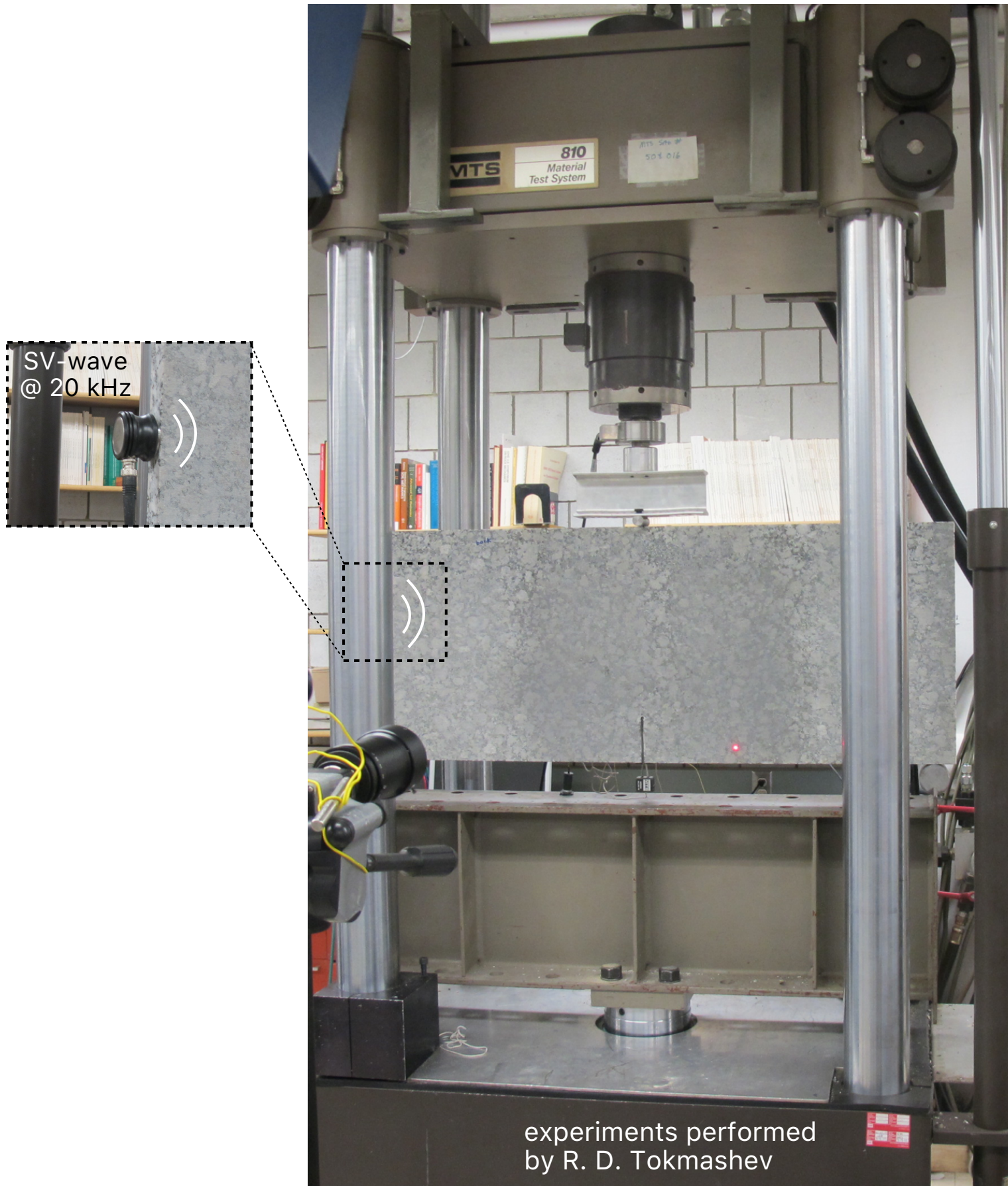


SLDV measurements



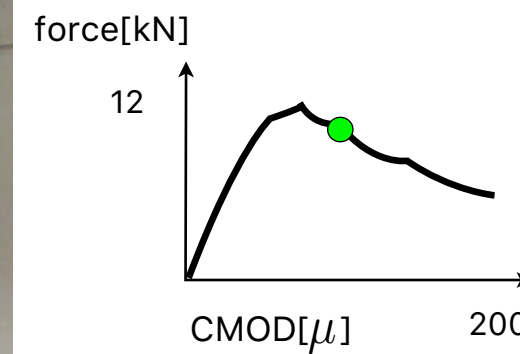
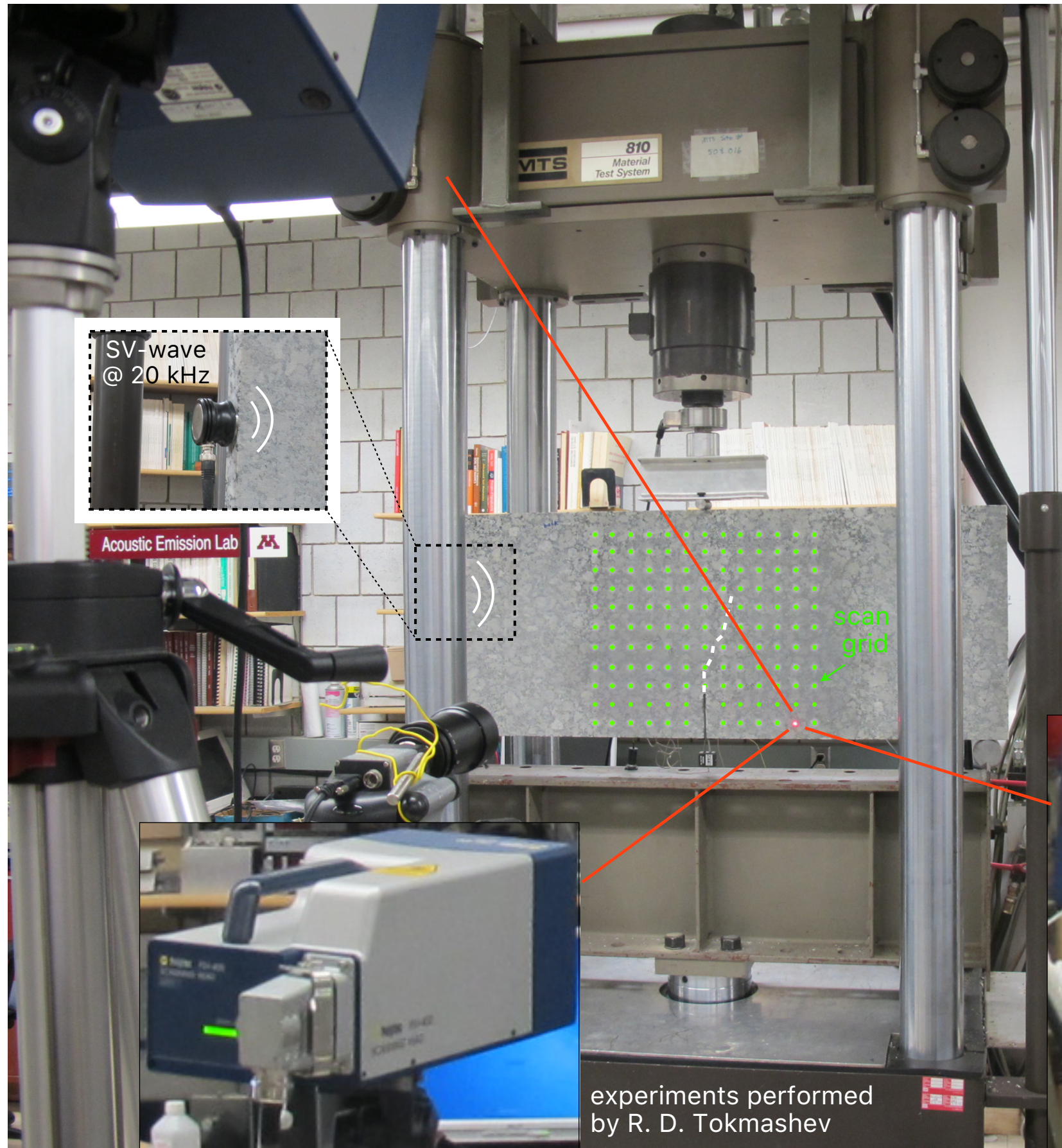
experiments performed
by R. D. Tokmashev

SLDV measurements



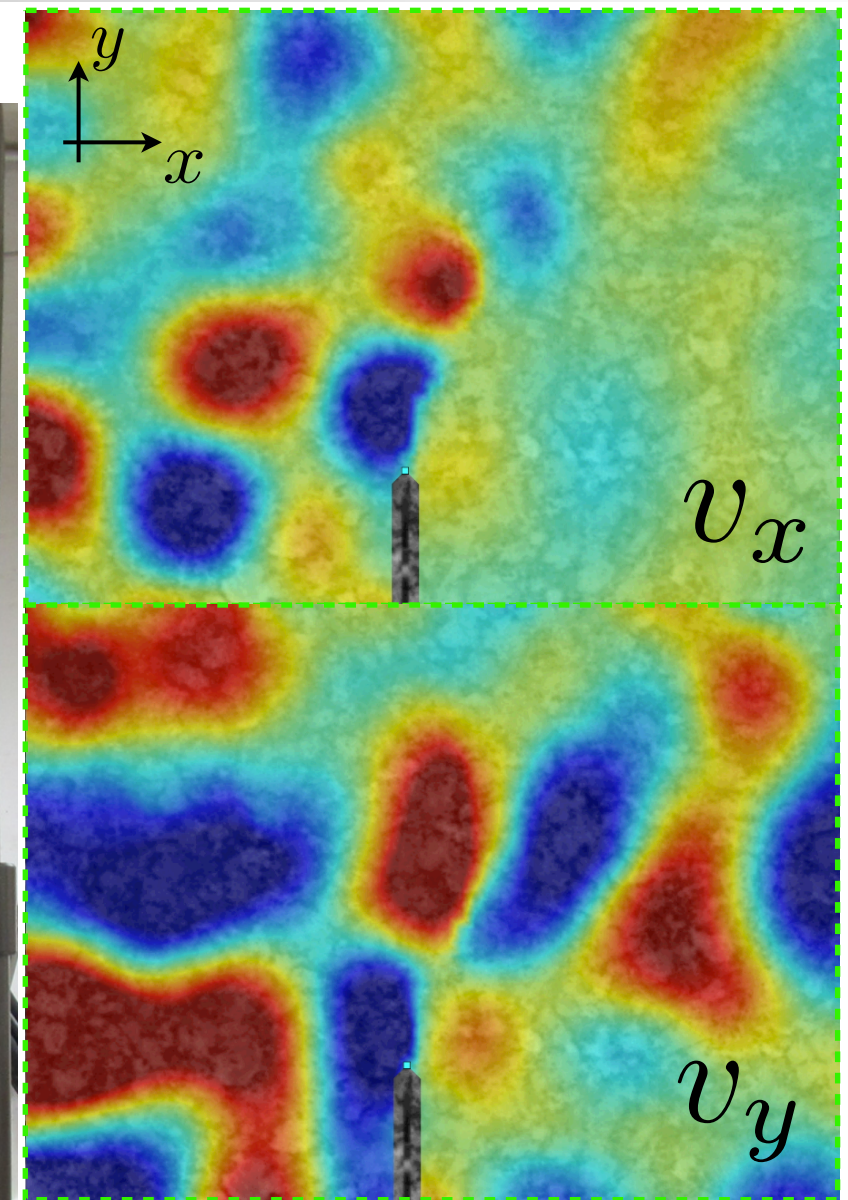
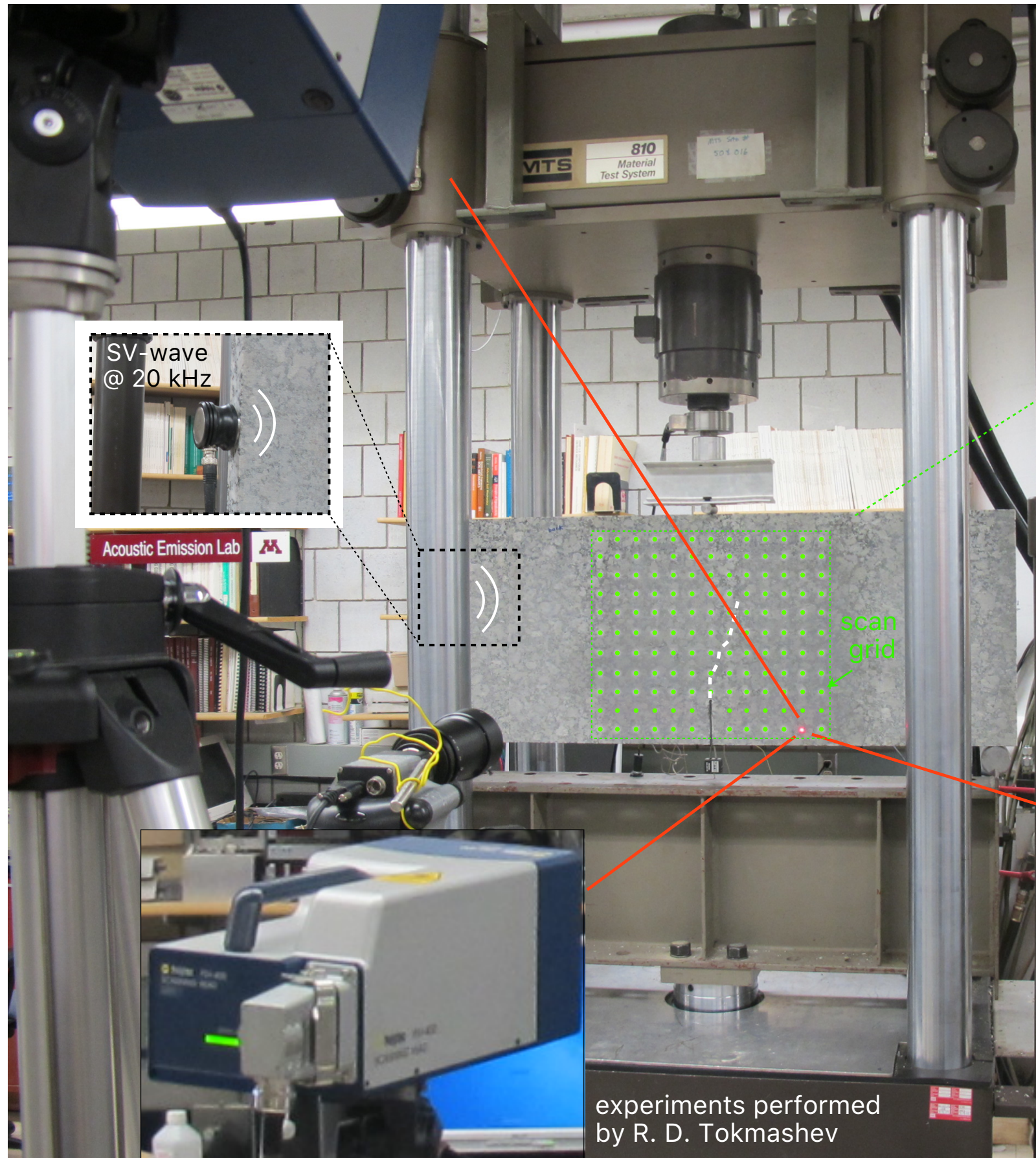
experiments performed
by R. D. Tokmashev

SLDV measurements



experiments performed
by R. D. Tokmashev

SLDV measurements

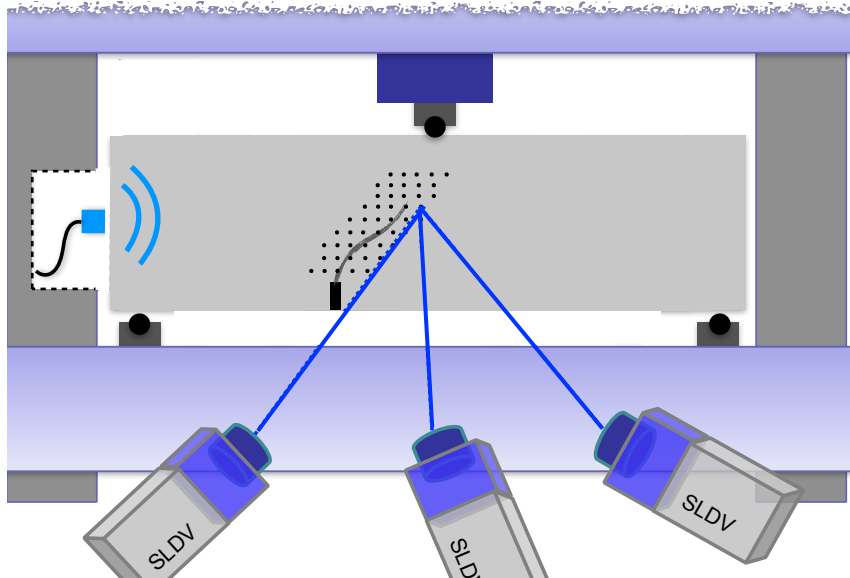


experiments performed
by R. D. Tokmashev

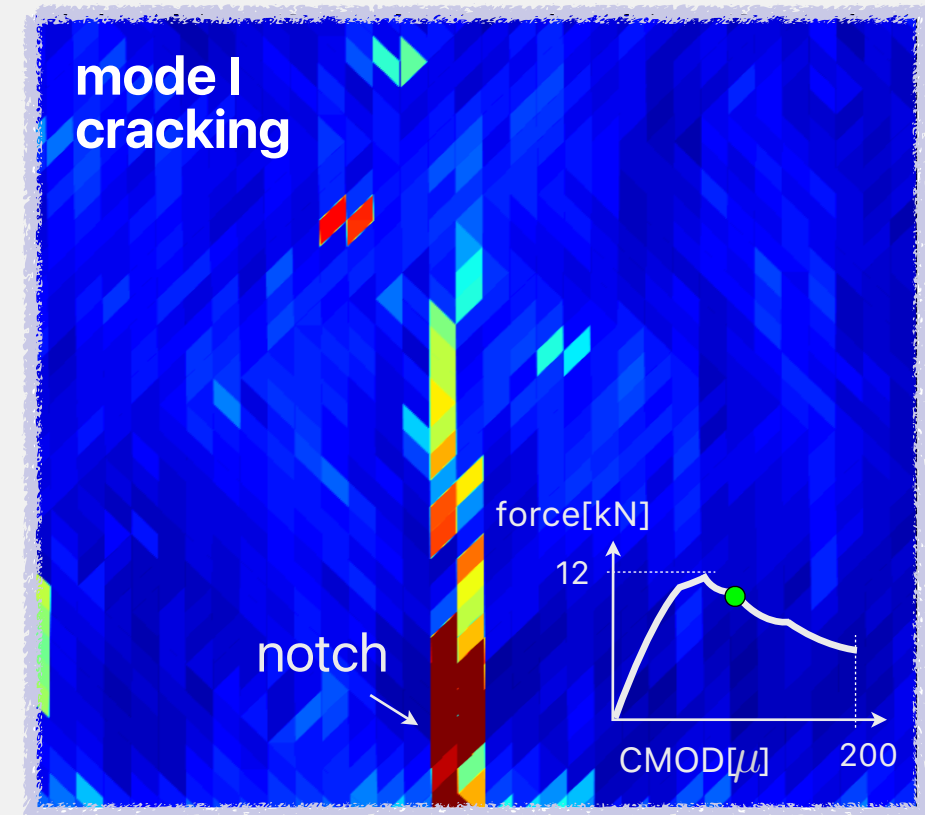


Geometric reconstruction

absolute value of velocity jump along x and y
summed and averaged over time

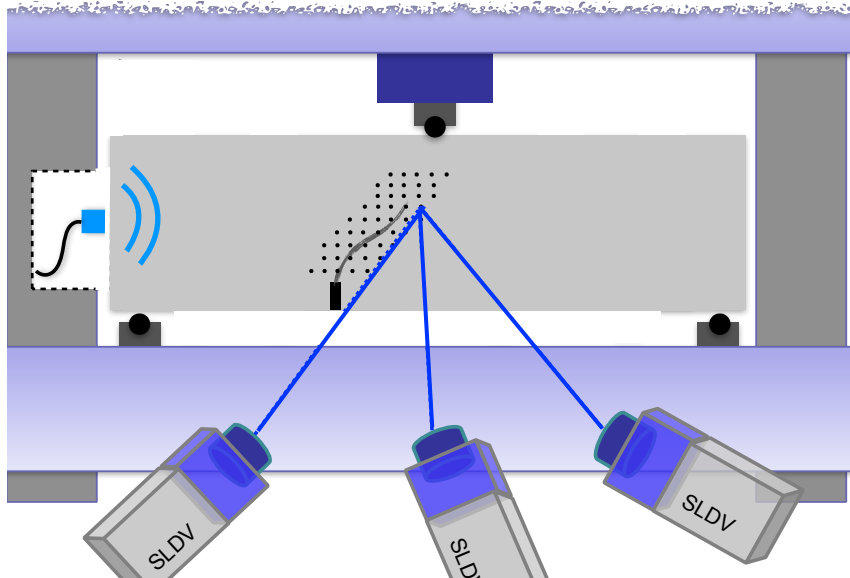


65% post peak

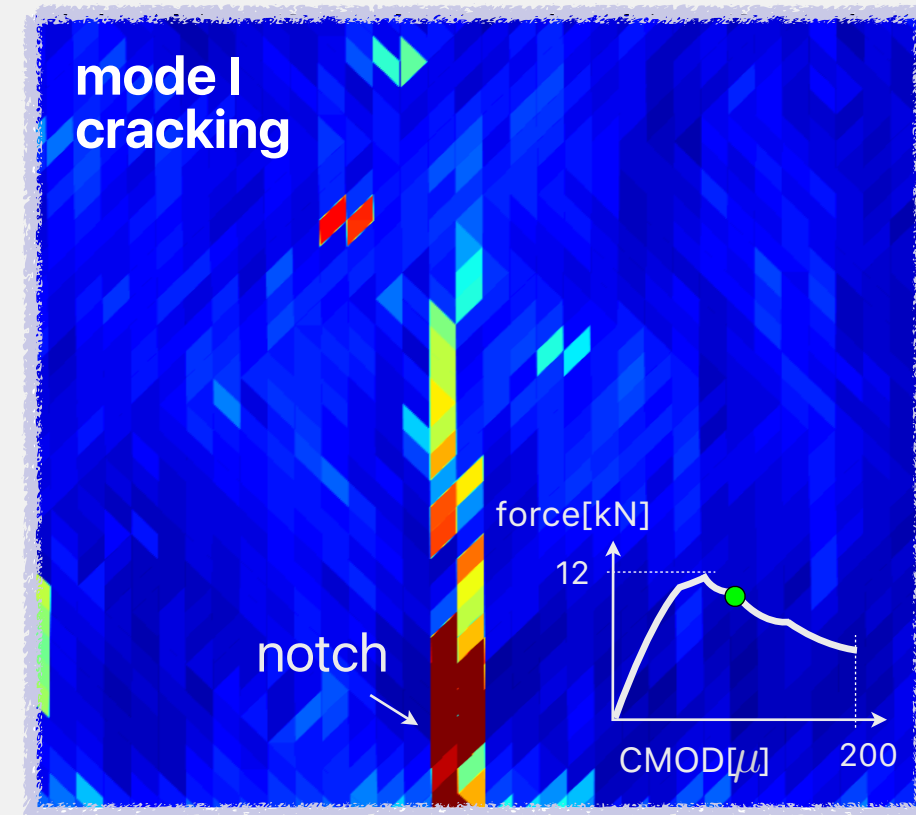


Geometric reconstruction

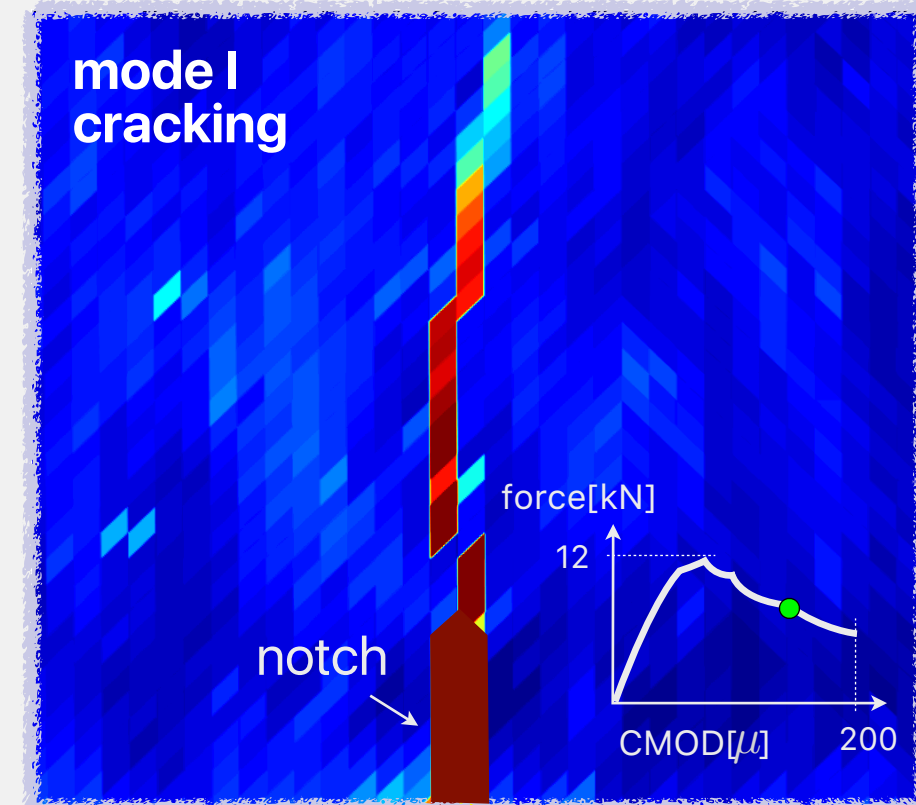
absolute value of velocity jump along x and y
summed and averaged over time



65% post peak

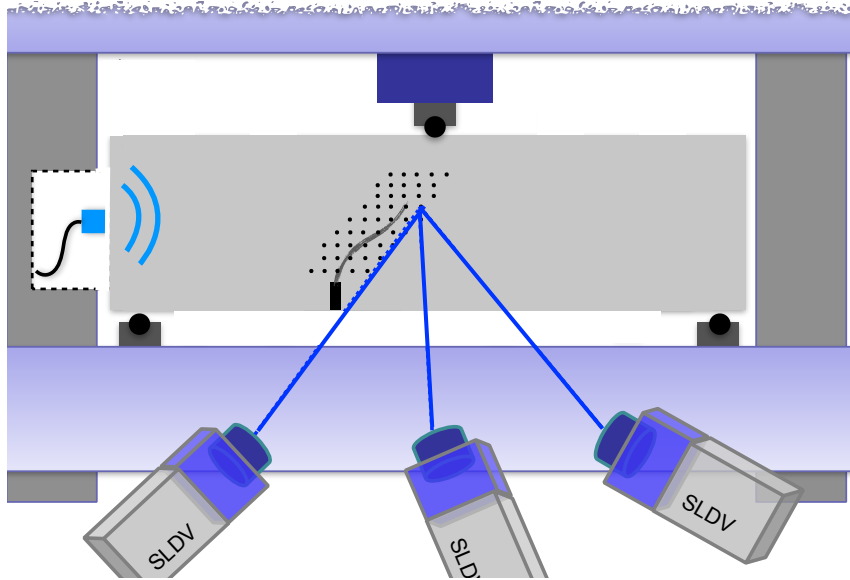


50% post peak

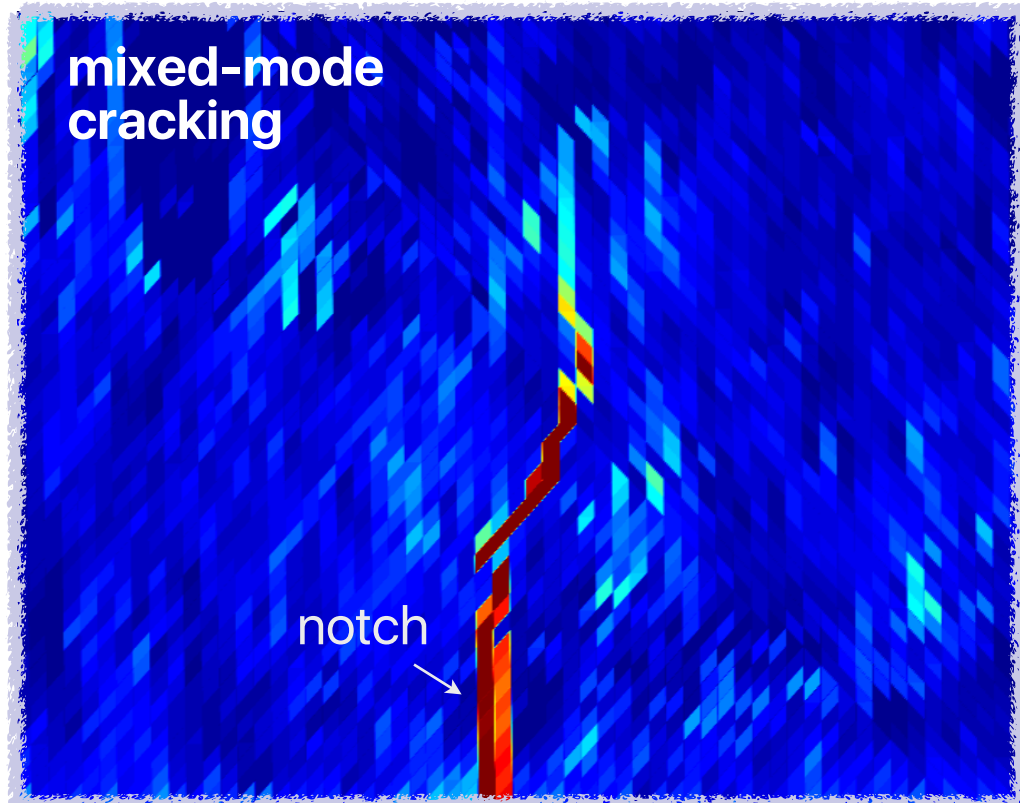


Geometric reconstruction

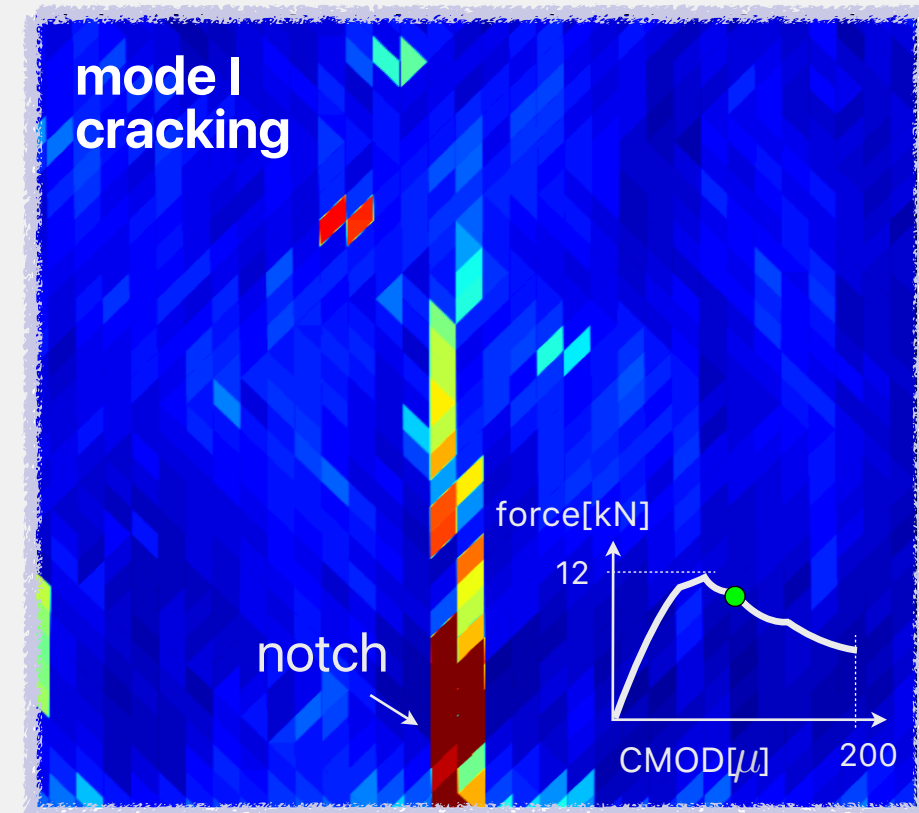
absolute value of velocity jump along x and y
summed and averaged over time



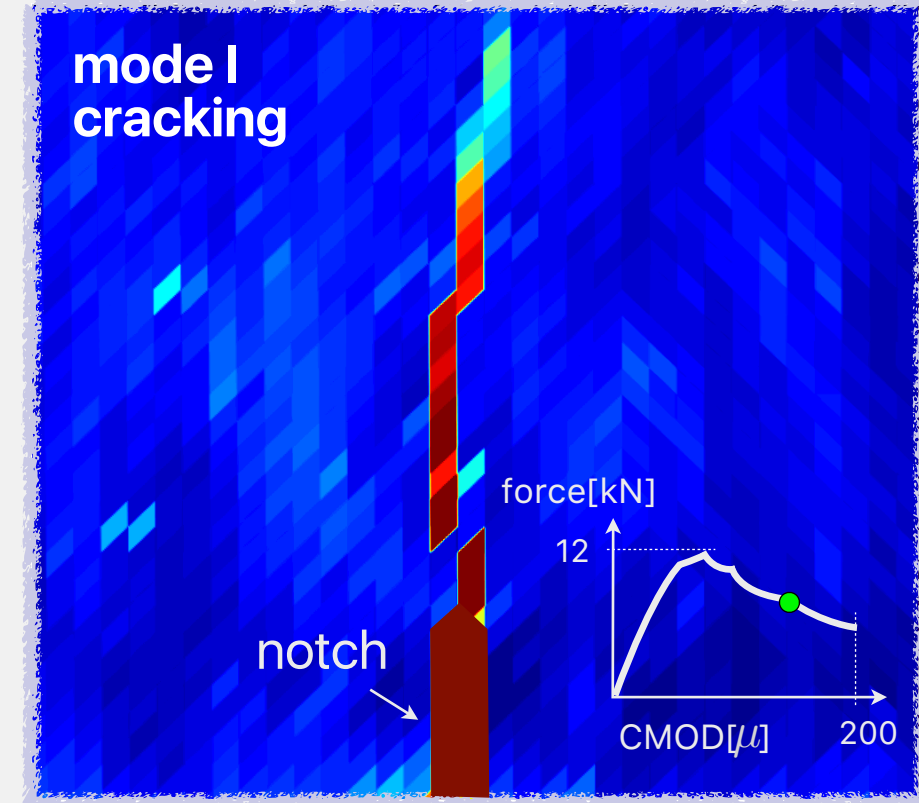
70% post peak



65% post peak



50% post peak



Signal processing displacement

SLDV velocity field



denoising in time

band-pass filtering
@ **every** scan point



numerical integration

displacement field



**fixing integration
error**

high-pass filtering
@ **every** scan point



displacement field

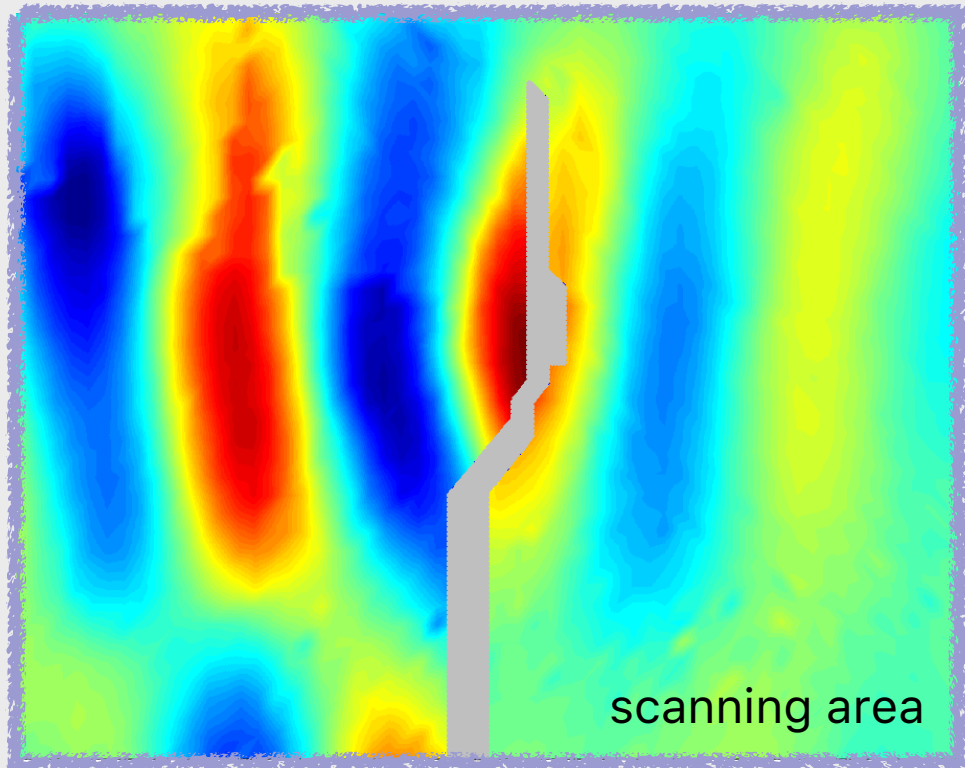


denoising in space

Fourier series fitting in
both x and y directions
(up to 7 harmonics)

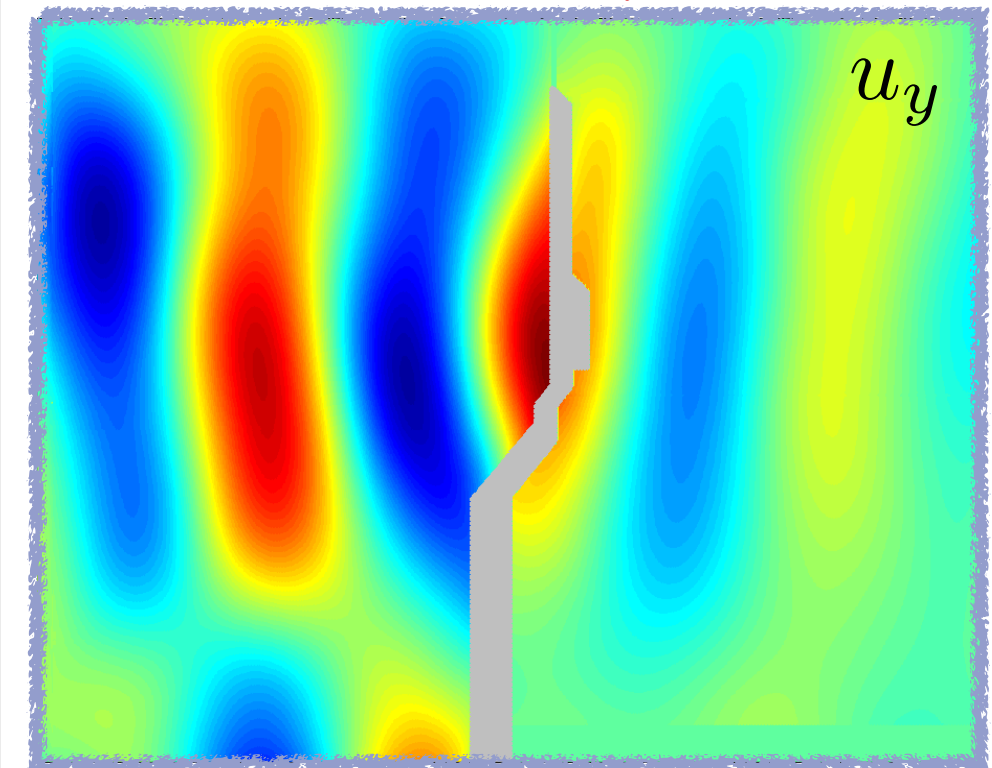
before

displacement field in y direction

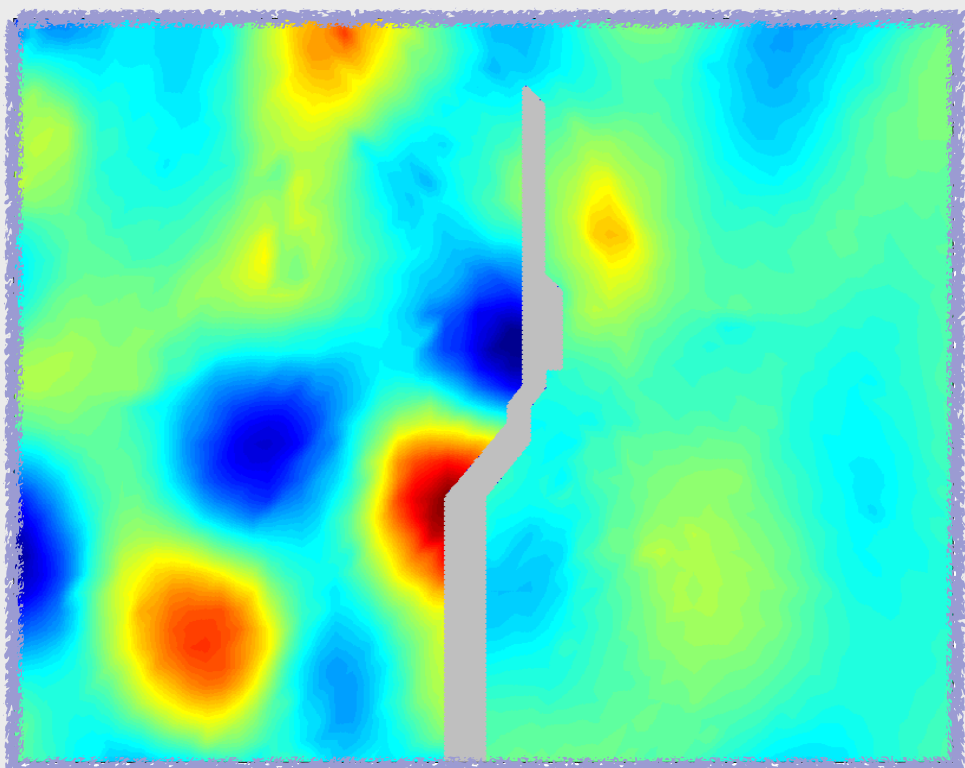


after

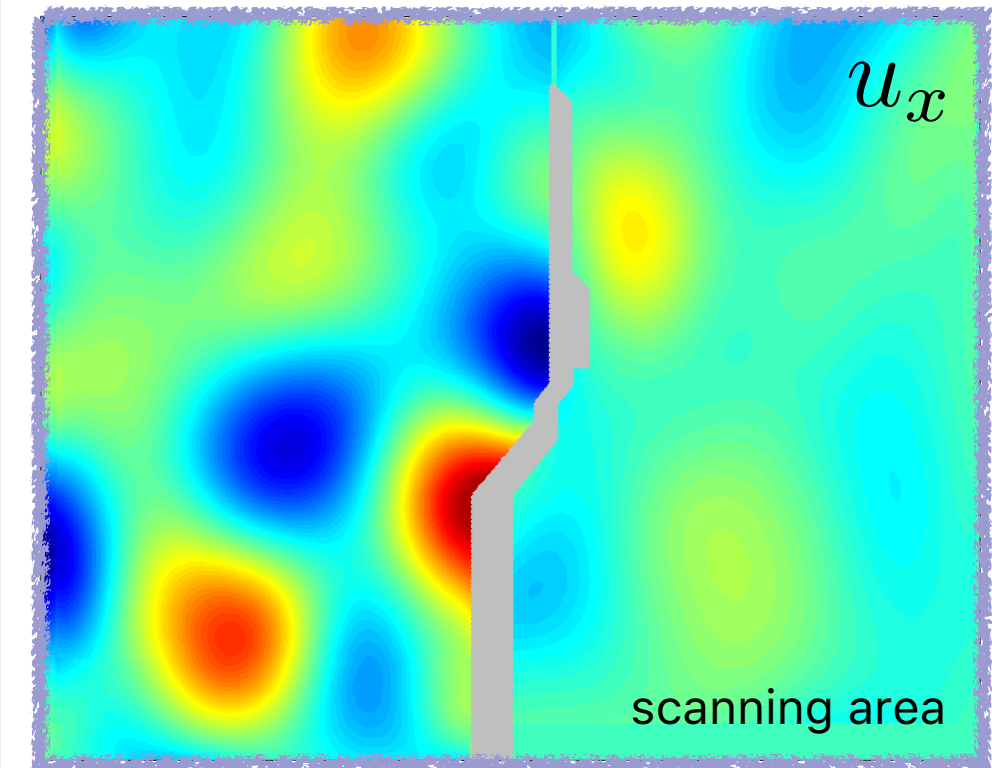
displacement field in y direction



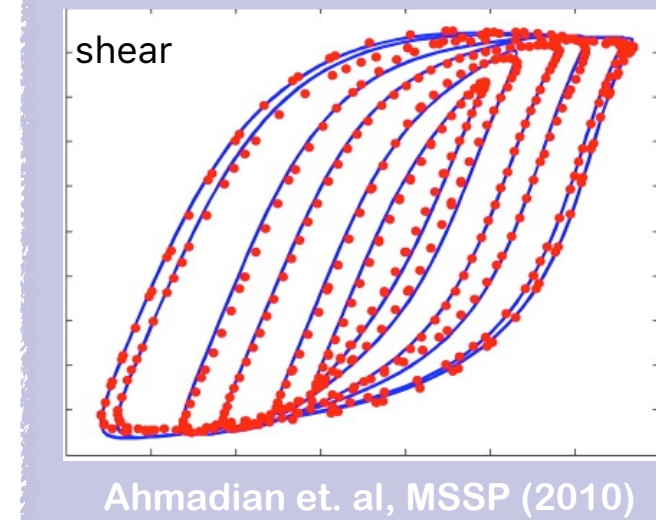
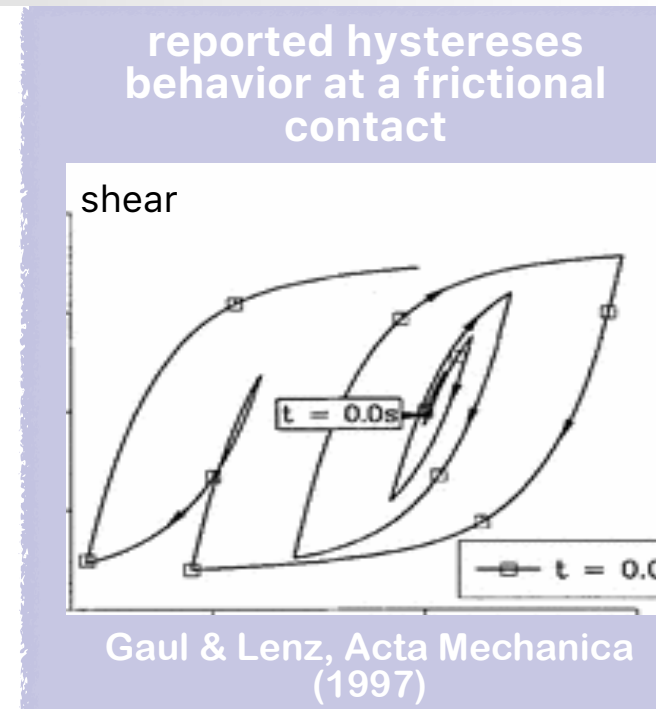
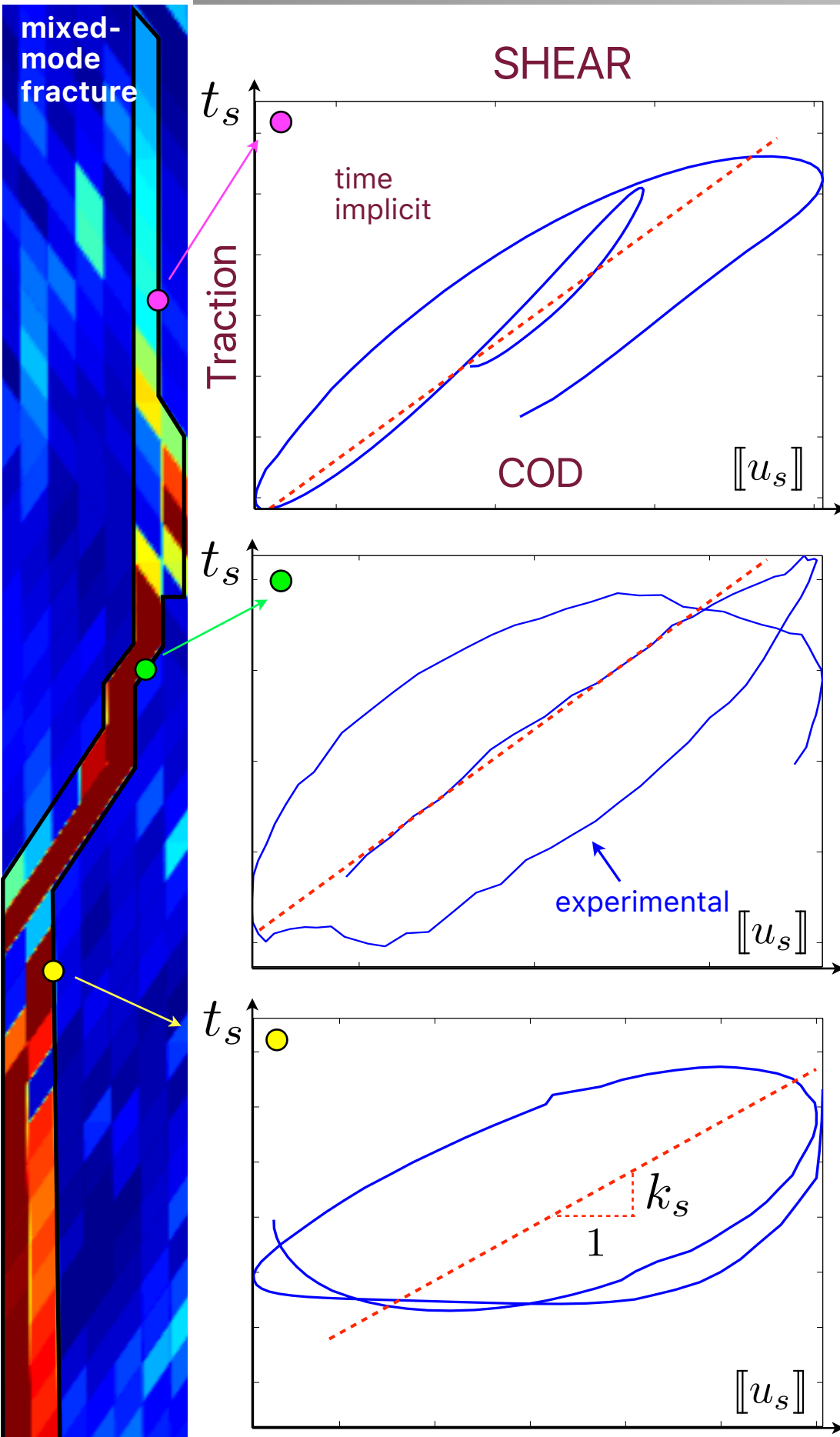
displacement field in x direction



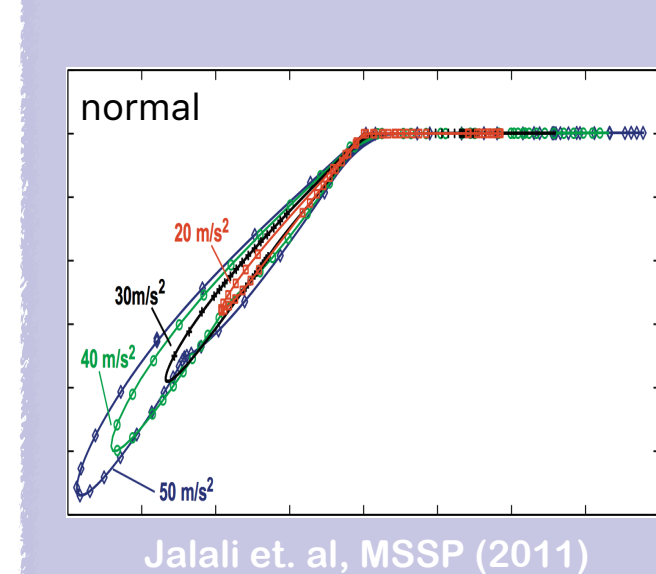
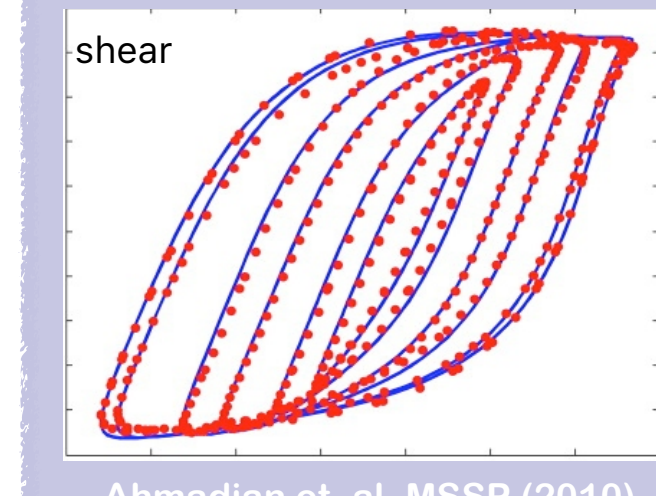
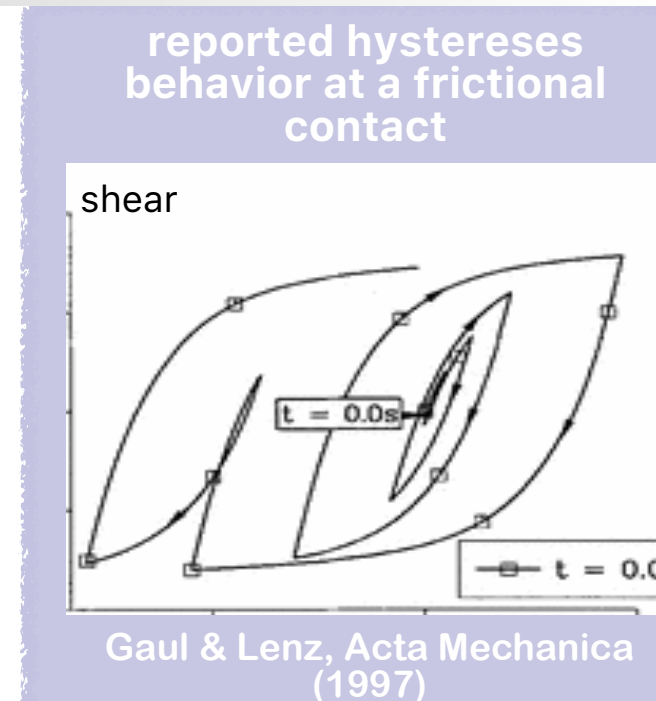
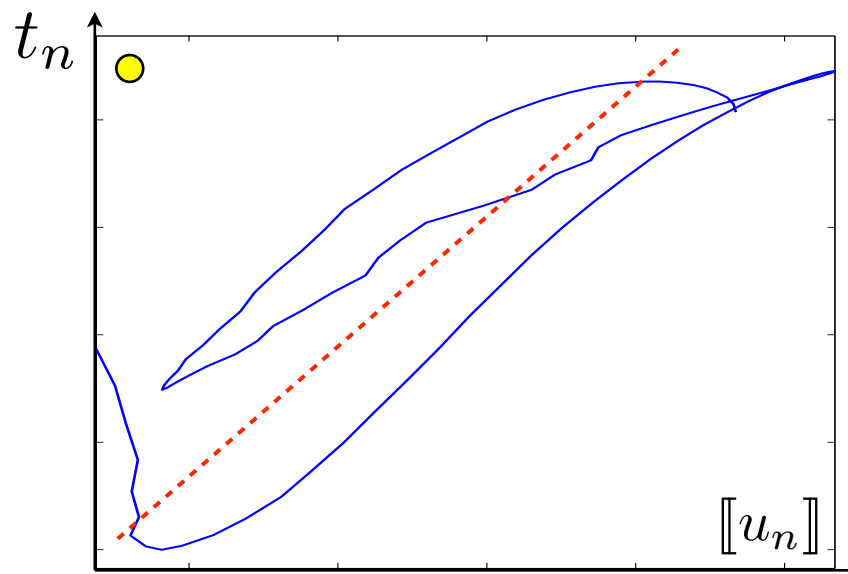
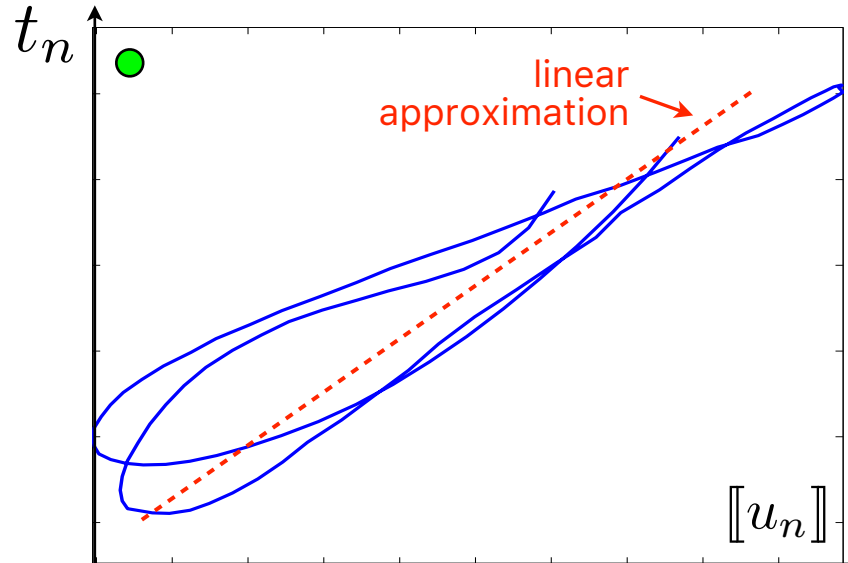
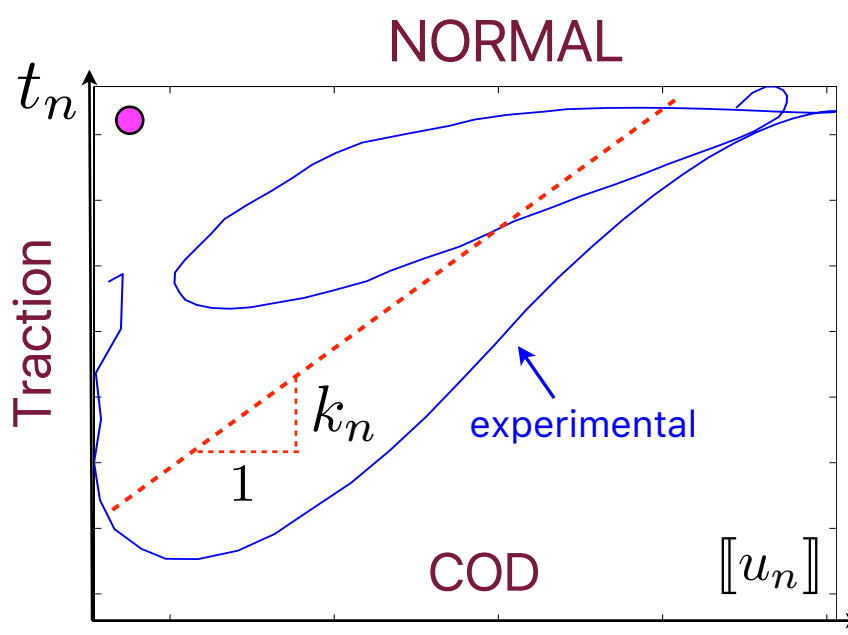
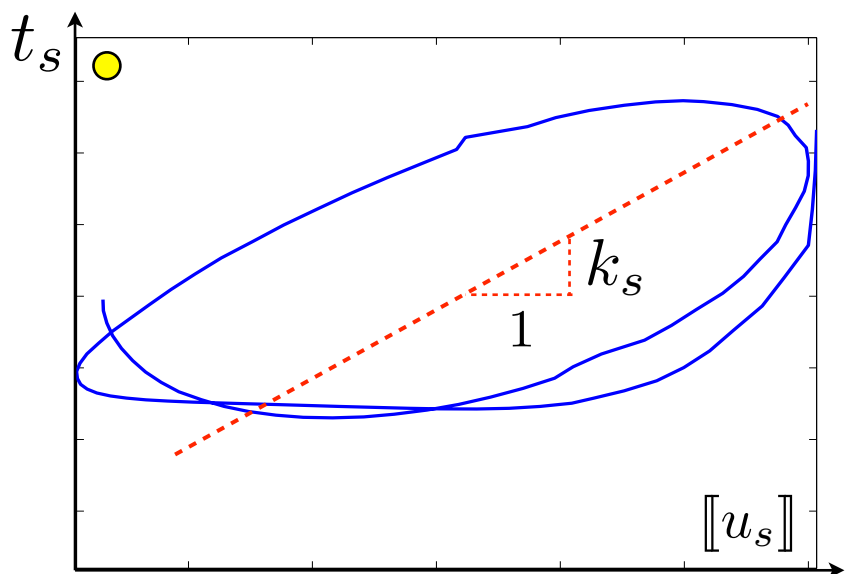
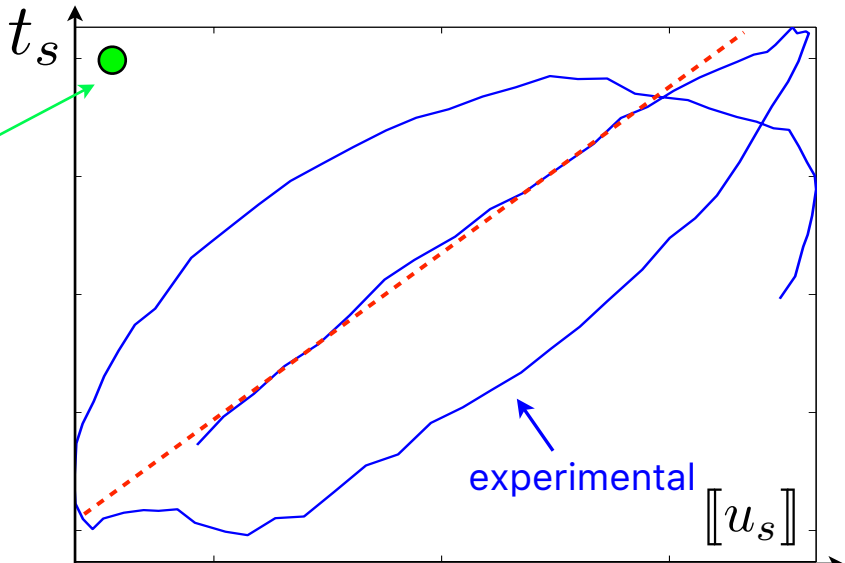
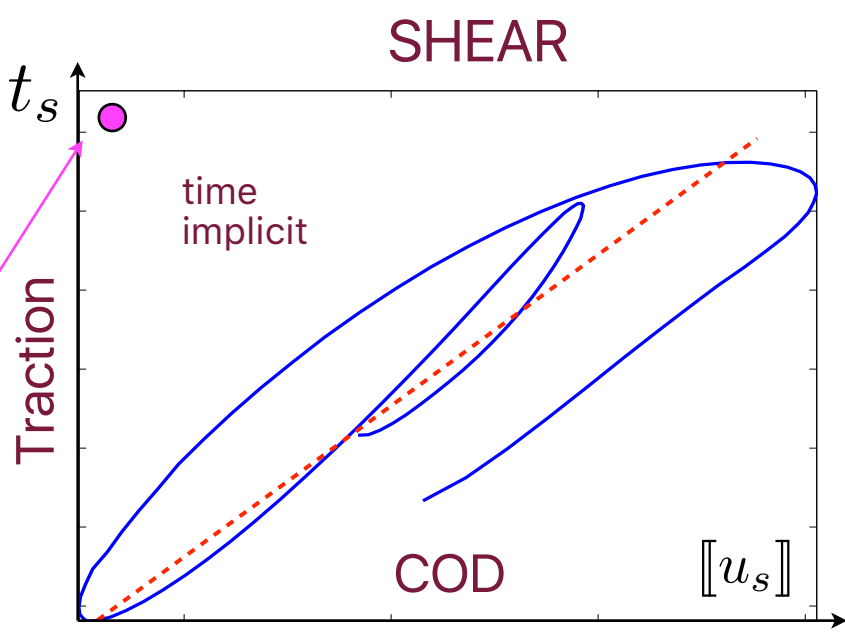
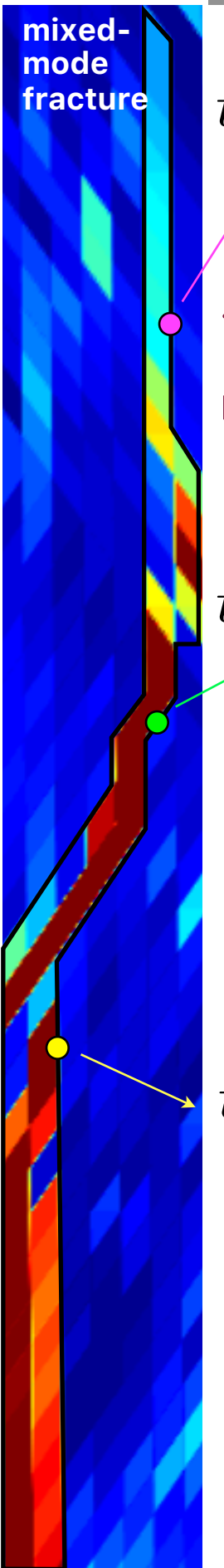
displacement field in x direction



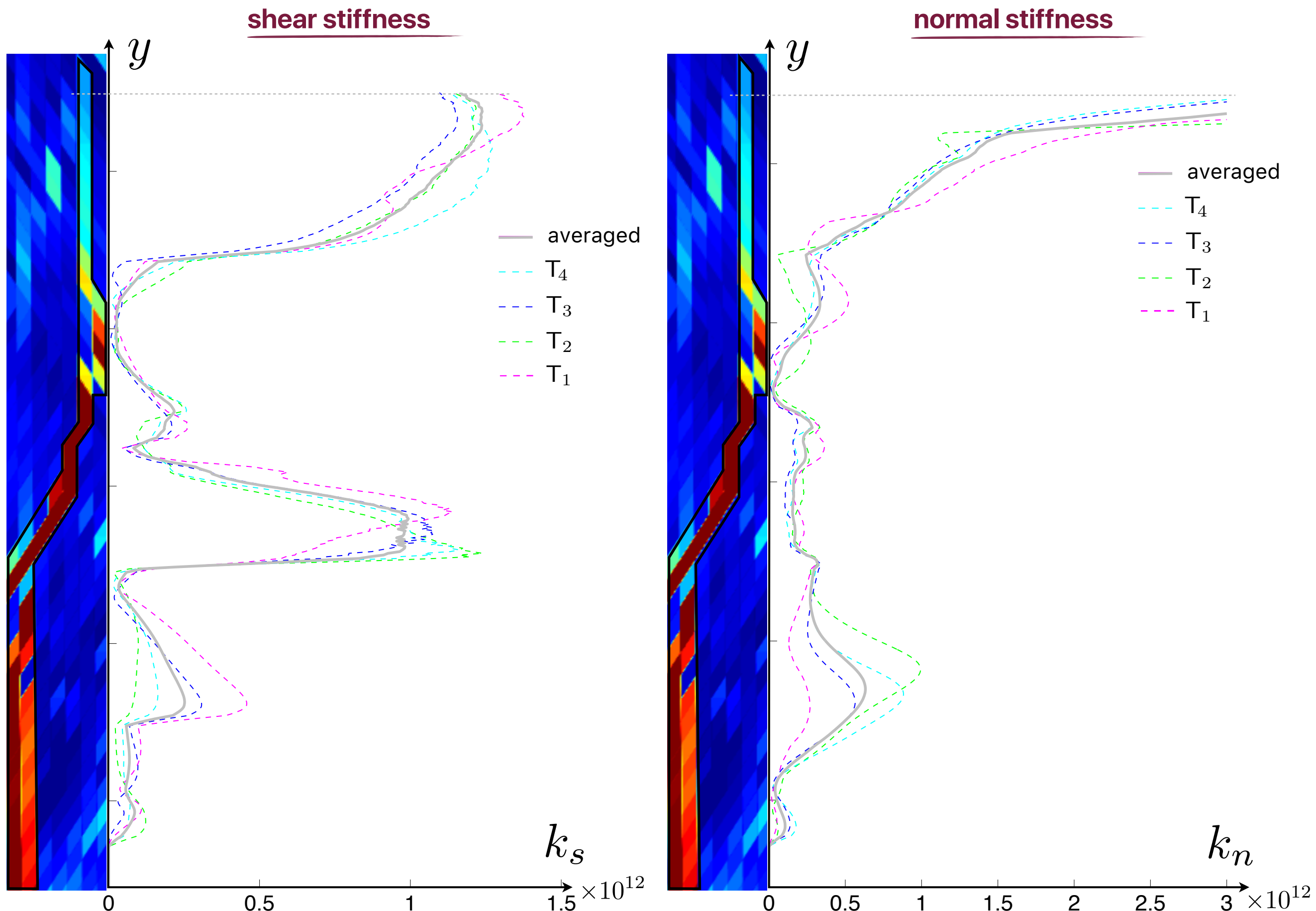
Contact law@ fracture interface



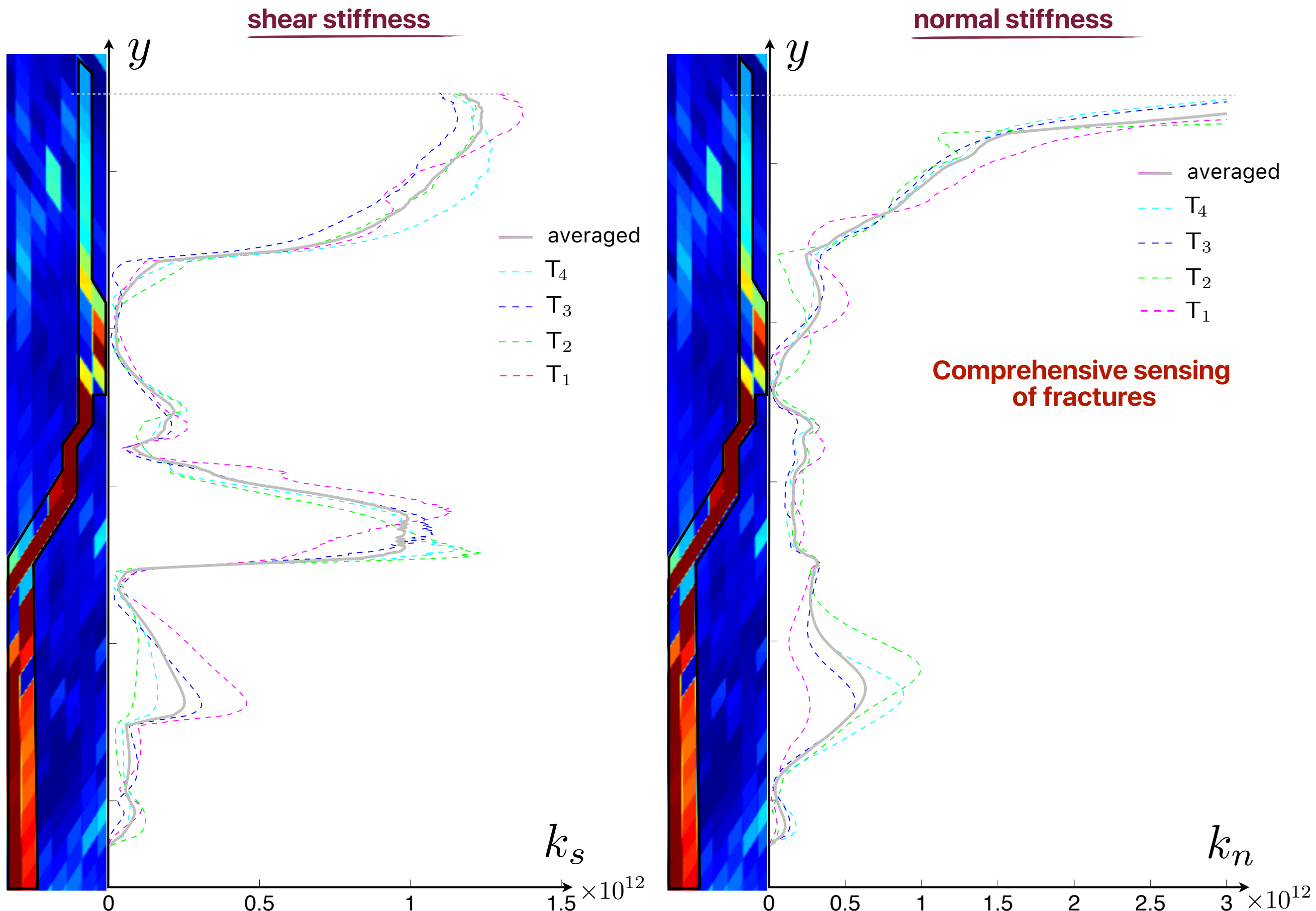
Contact law@ fracture interface



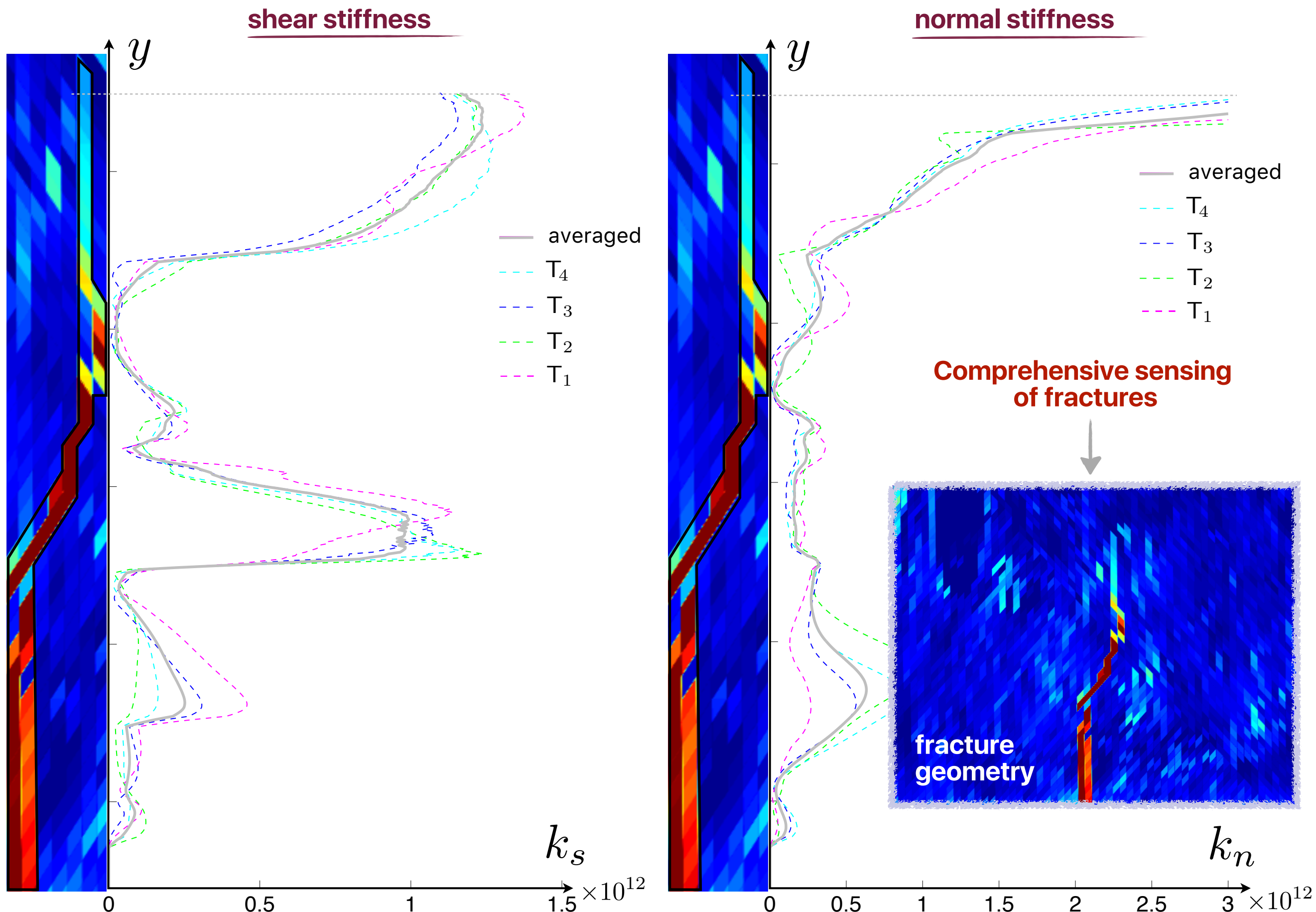
Interfacial Stiffness mixed-mode



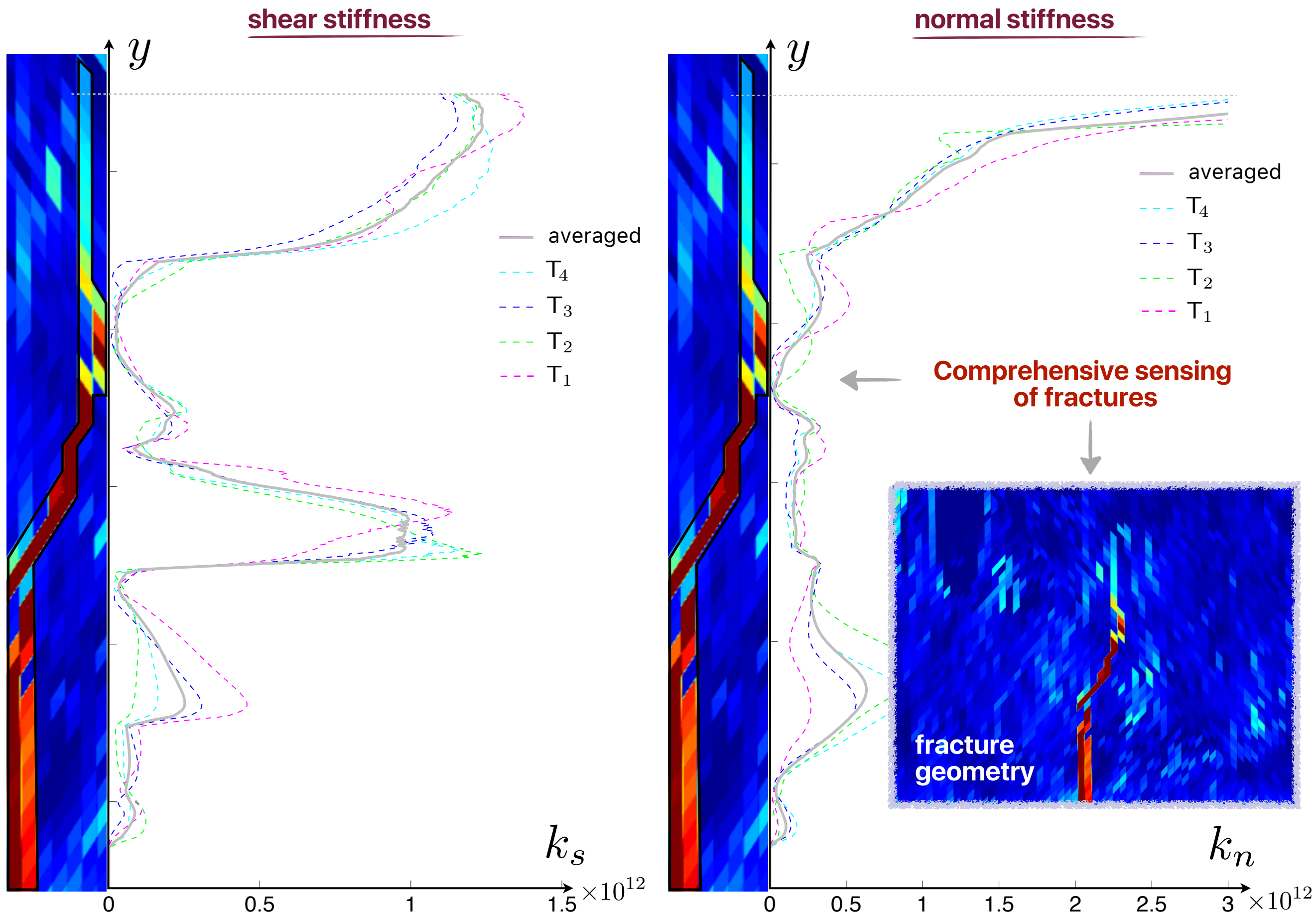
Interfacial Stiffness mixed-mode



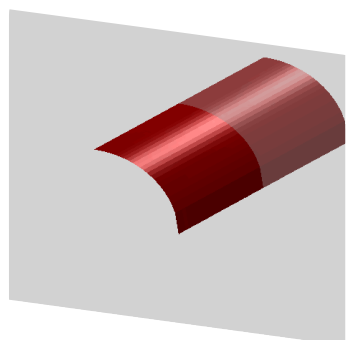
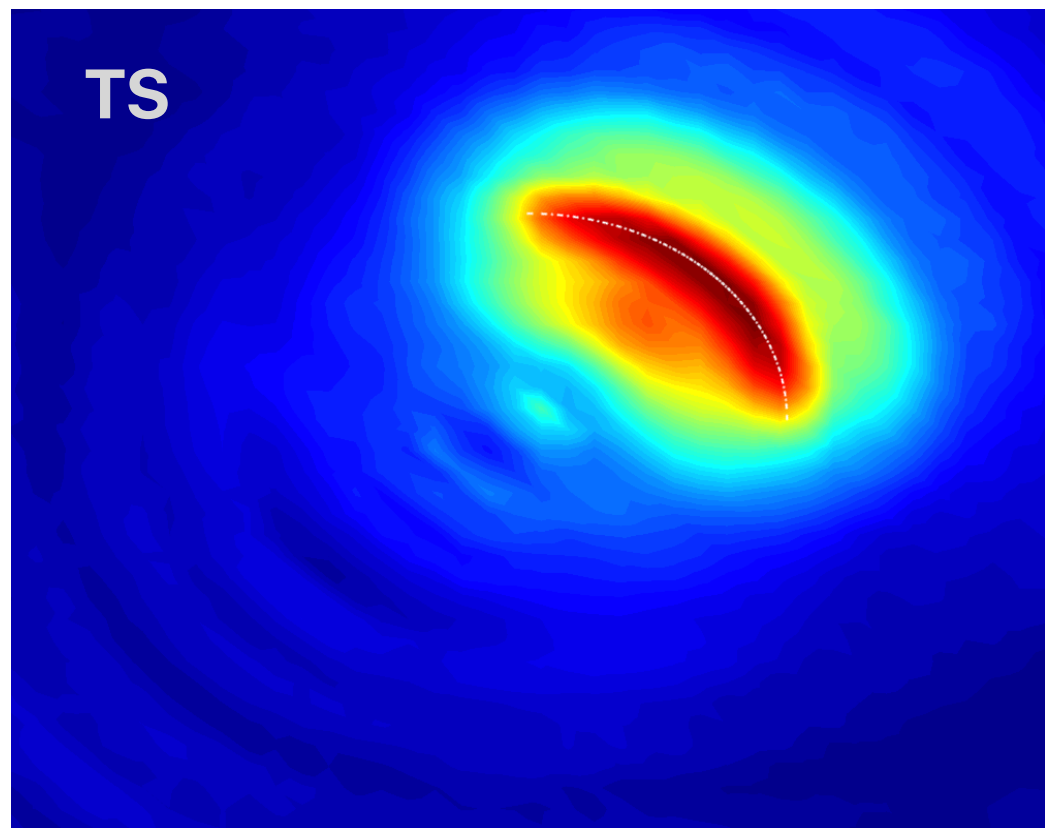
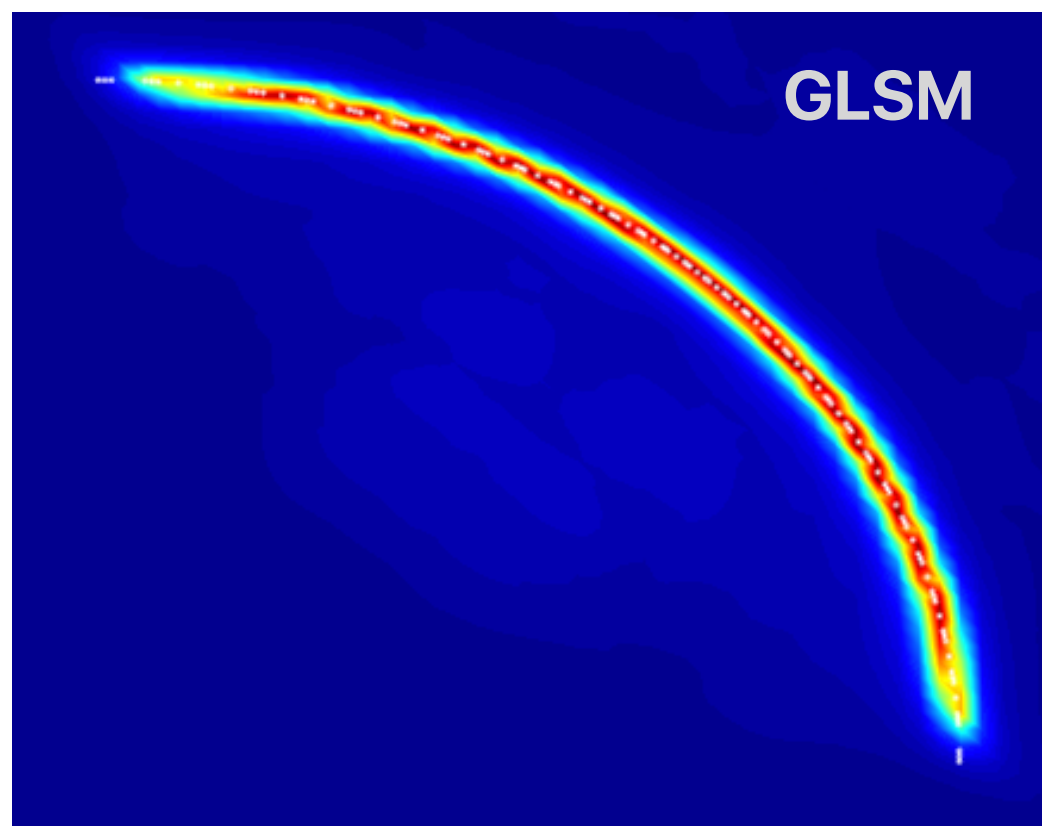
Interfacial Stiffness mixed-mode



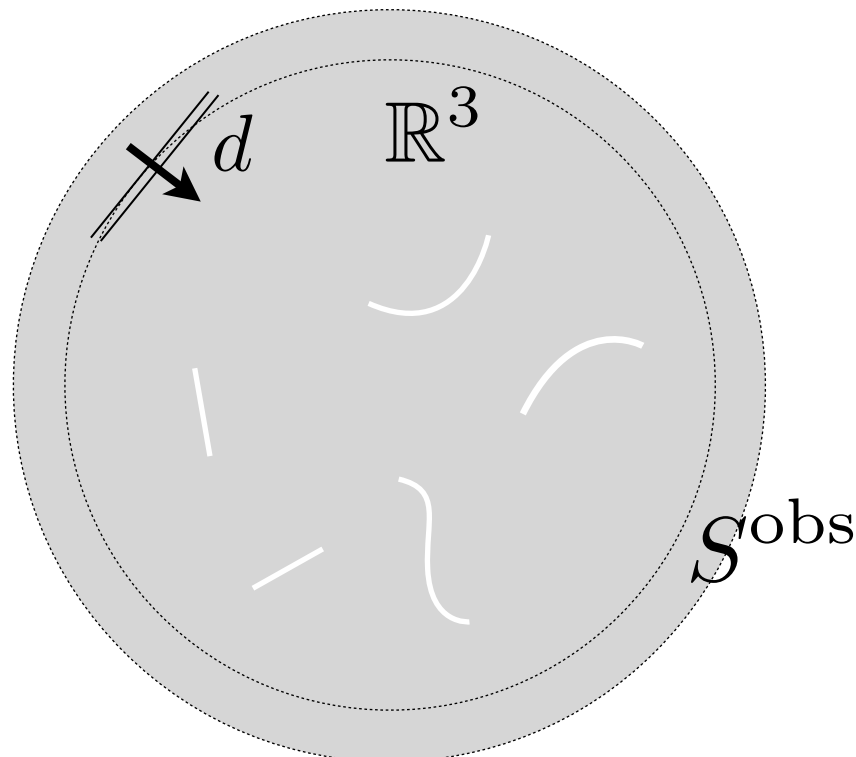
Interfacial Stiffness mixed-mode



Analytical developments toward a robust 3D imaging platform



Generalized Linear Sampling Method



1998-

Colton, Kirsch, Kress, Monk, Arens, Guzina,
Nintcheu Fata, Madyarov , Bellis, Bonnet, ...

Obstacles

2003-

Cakoni, Haddar, Boukari, Kress, Ritter, Potthast,
Monch, Park, Bourgeois, ...

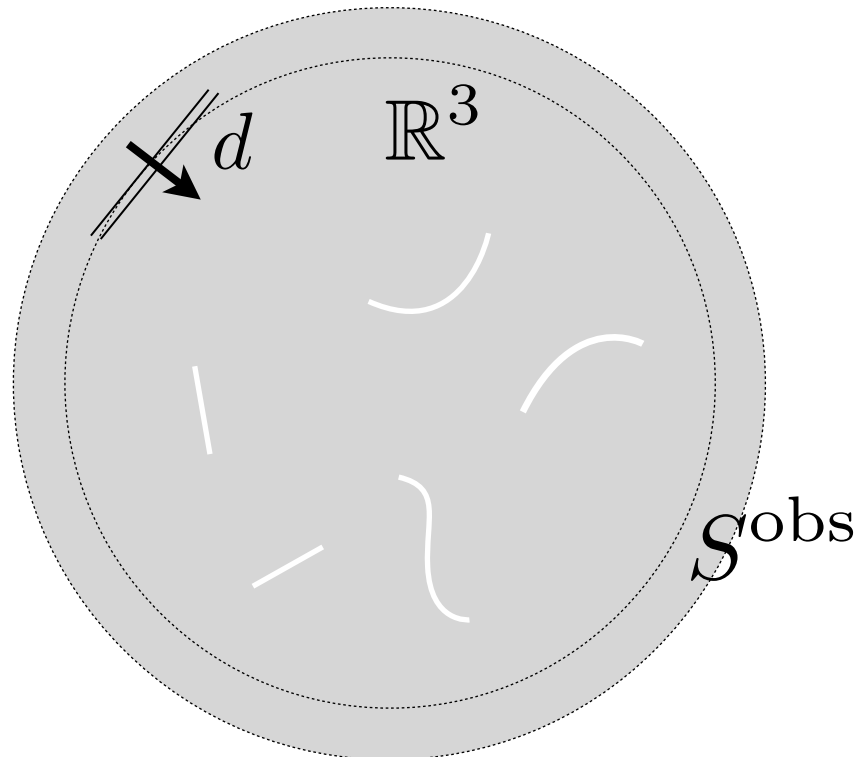
Cracks

2014-

Haddar, Audibert, Cakoni, ...

GLSM

Generalized Linear Sampling Method



1998-

Colton, Kirsch, Kress, Monk, Arens, Guzina,
Nintcheu Fata, Madyarov , Bellis, Bonnet, ...

Obstacles

2003-

Cakoni, Haddar, Boukari, Kress, Ritter, Potthast,
Monch, Park, Bourgeois, ...

Cracks

2014-

Haddar, Audibert, Cakoni, ...

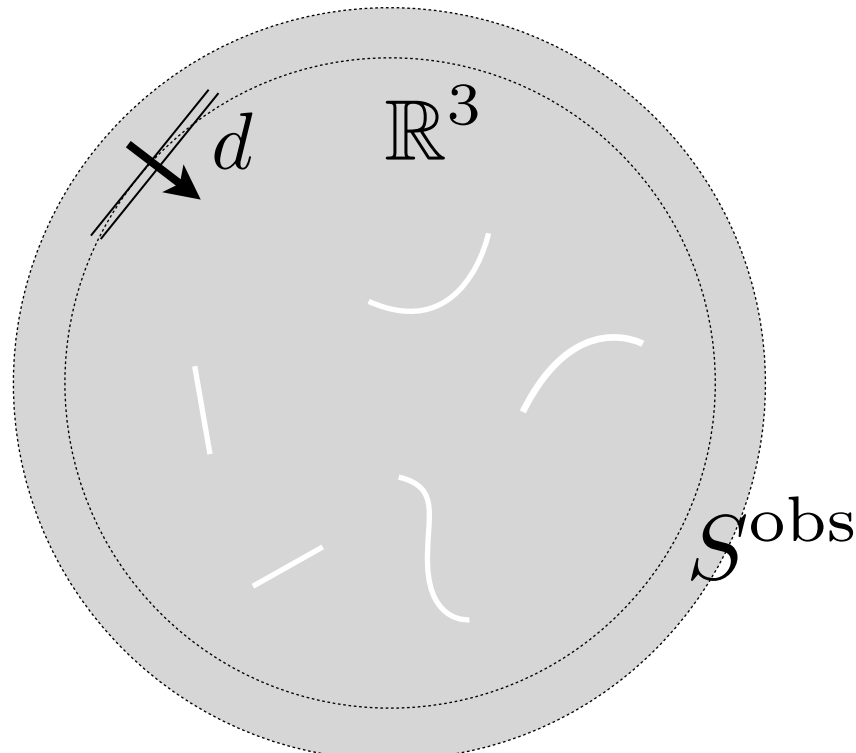
GLSM

Far field pattern

$$\hat{\boldsymbol{\xi}} = \frac{\boldsymbol{\xi}}{|\boldsymbol{\xi}|}, |\boldsymbol{\xi}| \rightarrow \infty$$

$$\boldsymbol{v}(\boldsymbol{\xi}) = \frac{e^{ik_p |\boldsymbol{\xi}|}}{4\pi |\boldsymbol{\xi}| (\lambda + 2\mu)} \boldsymbol{v}_p^\infty(\hat{\boldsymbol{\xi}}) + \frac{e^{ik_s |\boldsymbol{\xi}|}}{4\pi |\boldsymbol{\xi}| \mu} \boldsymbol{v}_s^\infty(\hat{\boldsymbol{\xi}})$$

Generalized Linear Sampling Method



1998-

Colton, Kirsch, Kress, Monk, Arens, Guzina,
Nintcheu Fata, Madyarov , Bellis, Bonnet, ...

Obstacles

2003-

Cakoni, Haddar, Boukari, Kress, Ritter, Potthast,
Monch, Park, Bourgeois, ...

Cracks

2014-

Haddar, Audibert, Cakoni, ...

GLSM

Far field pattern

$$\hat{\xi} = \frac{\xi}{|\xi|}, |\xi| \rightarrow \infty$$

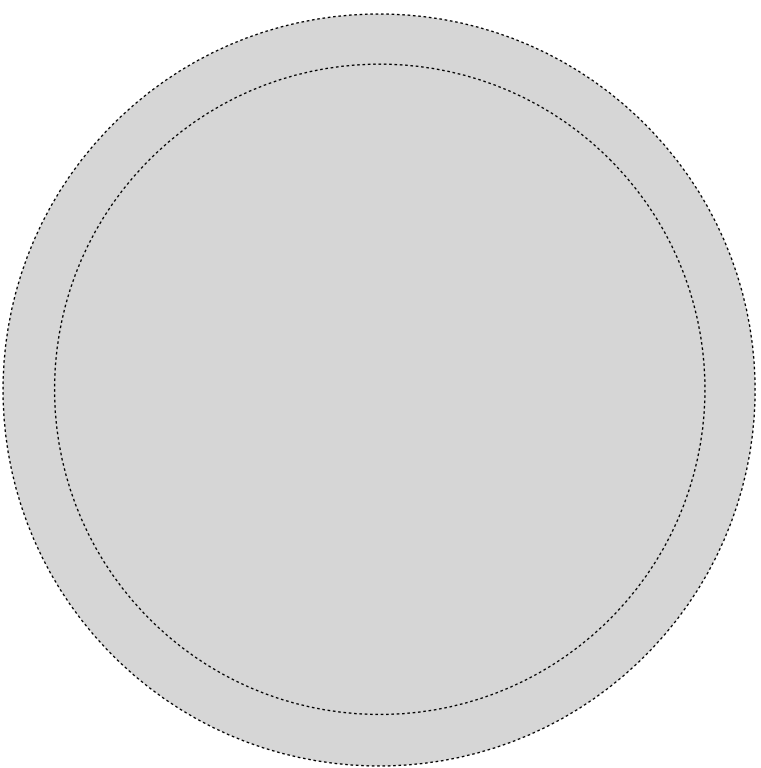
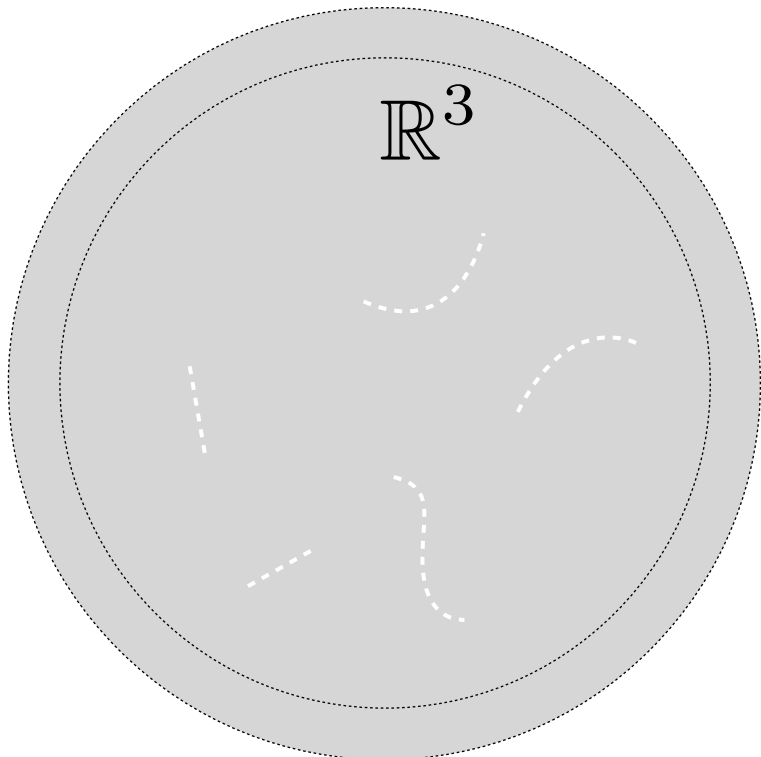
$$\mathbf{v}(\xi) = \frac{e^{ik_p|\xi|}}{4\pi|\xi|(\lambda + 2\mu)} \mathbf{v}_p^\infty(\hat{\xi}) + \frac{e^{ik_s|\xi|}}{4\pi|\xi|\mu} \mathbf{v}_s^\infty(\hat{\xi})$$

Far field operator

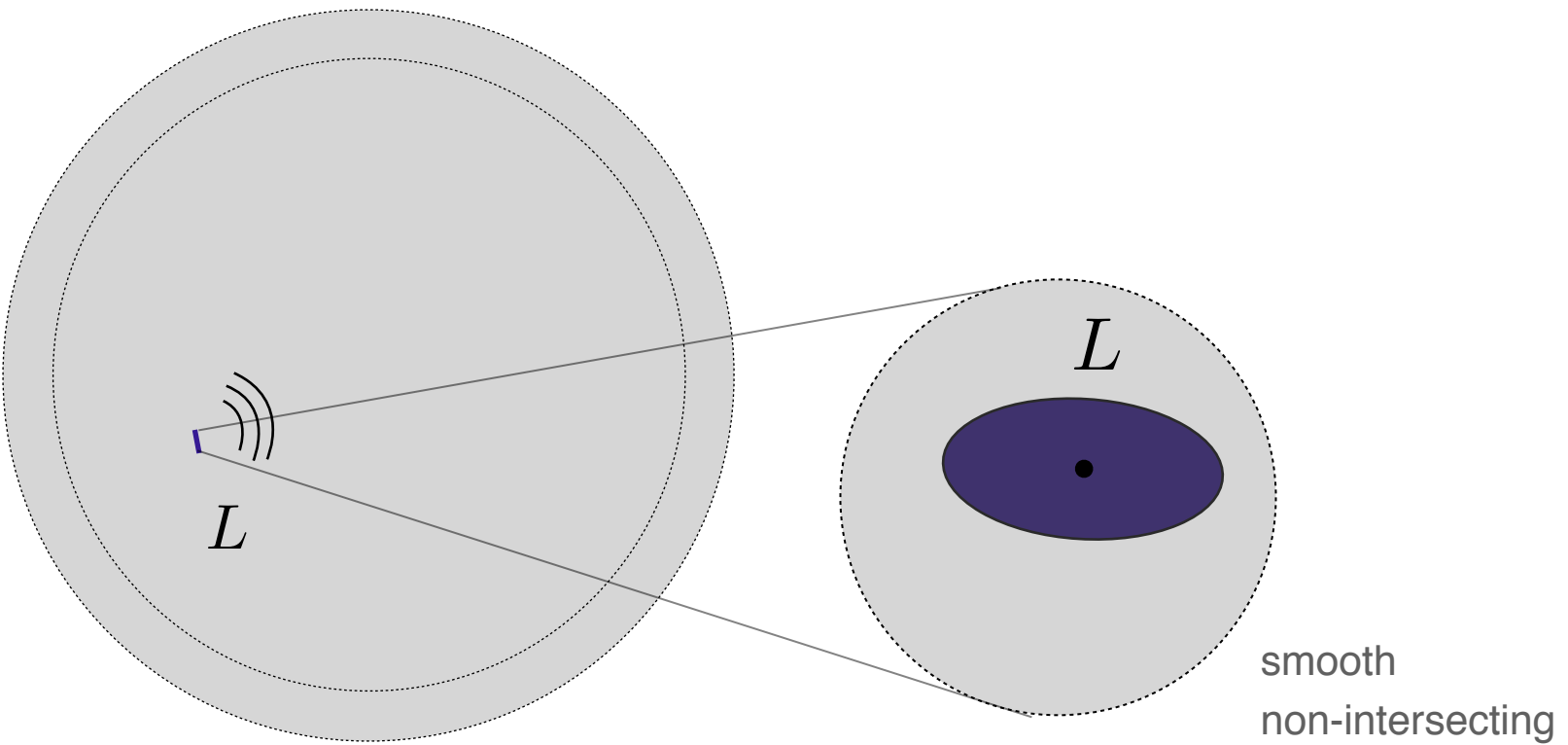
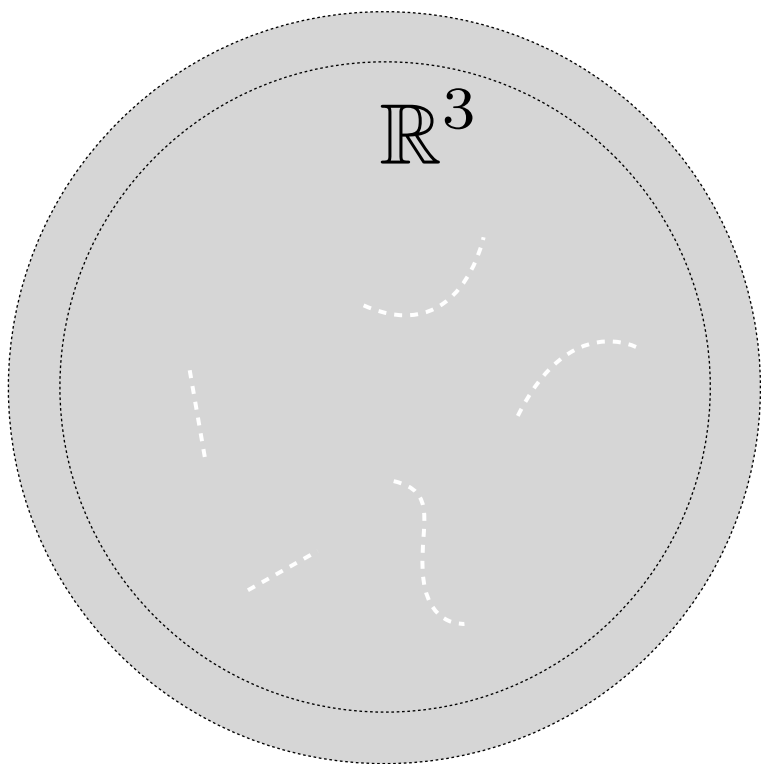
$$\mathbf{v}^\infty := F(\mathbf{g}) := \int_{\Omega_d} \mathbf{g}(d) \cdot \mathbf{W}^\infty(d, \hat{\xi}) dS_d$$

($\mathbf{v}_p^\infty, \mathbf{v}_s^\infty$) ($\mathbf{g}_p, \mathbf{g}_s$) unit sphere measurements

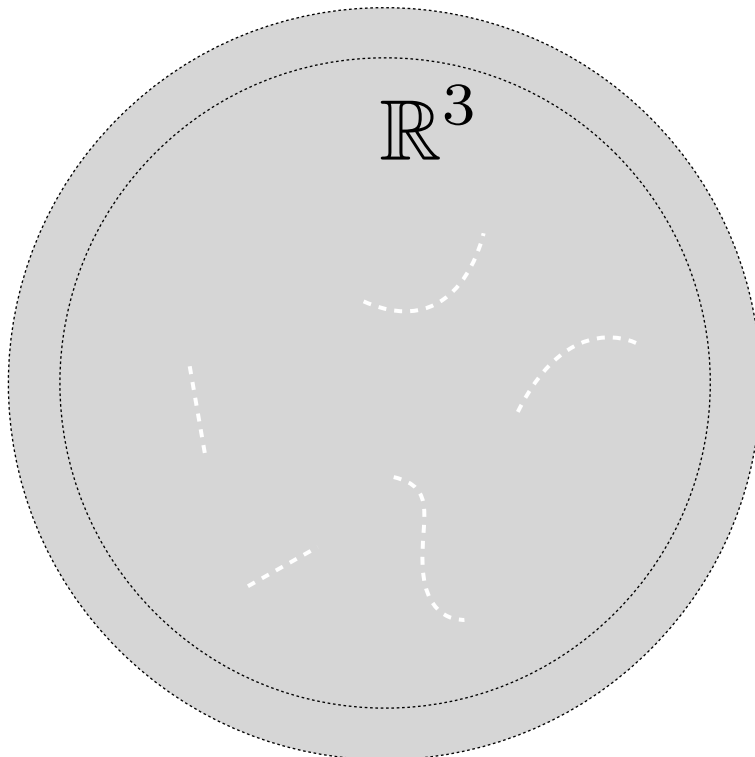
GLSM IDEA



GLSM IDEA



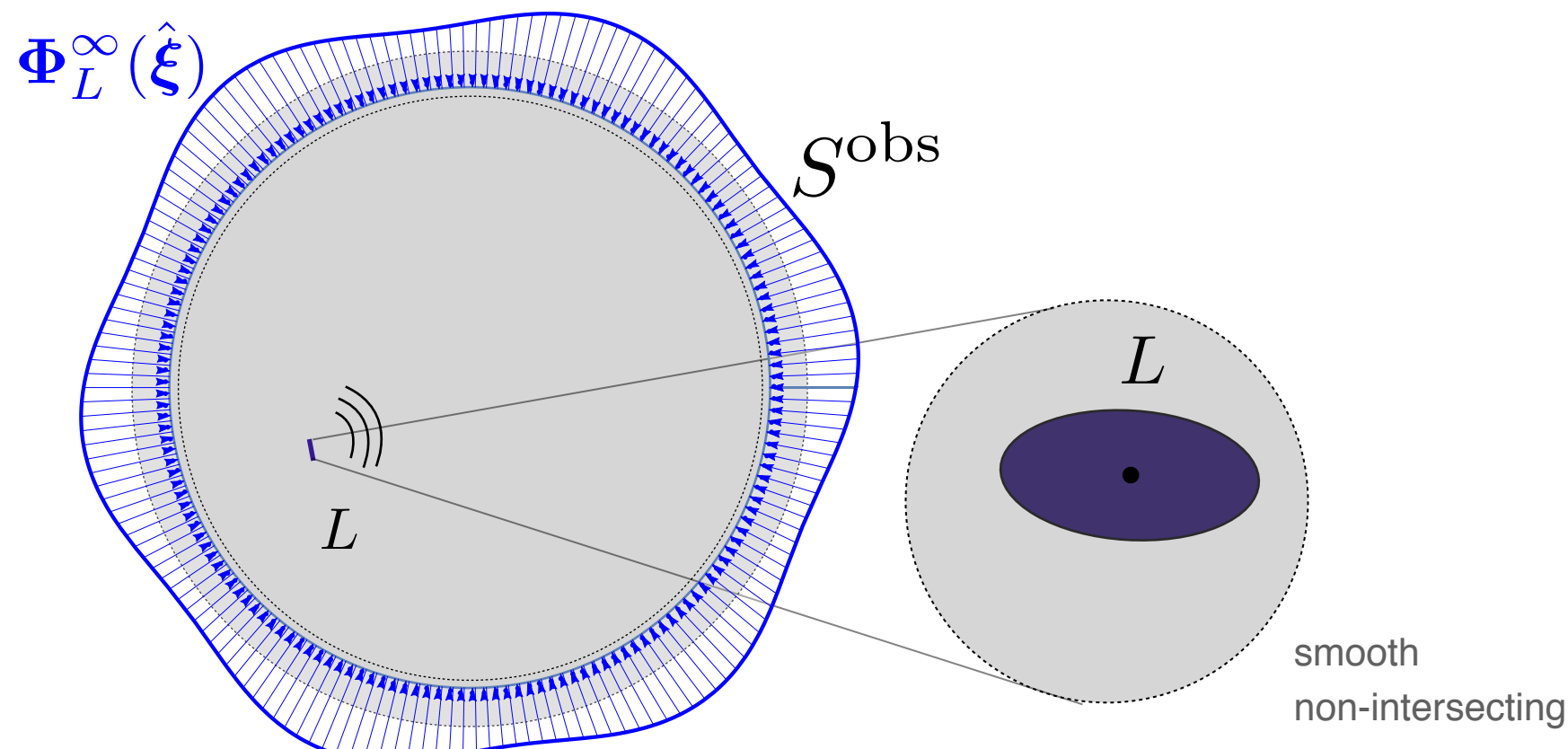
GLSM IDEA



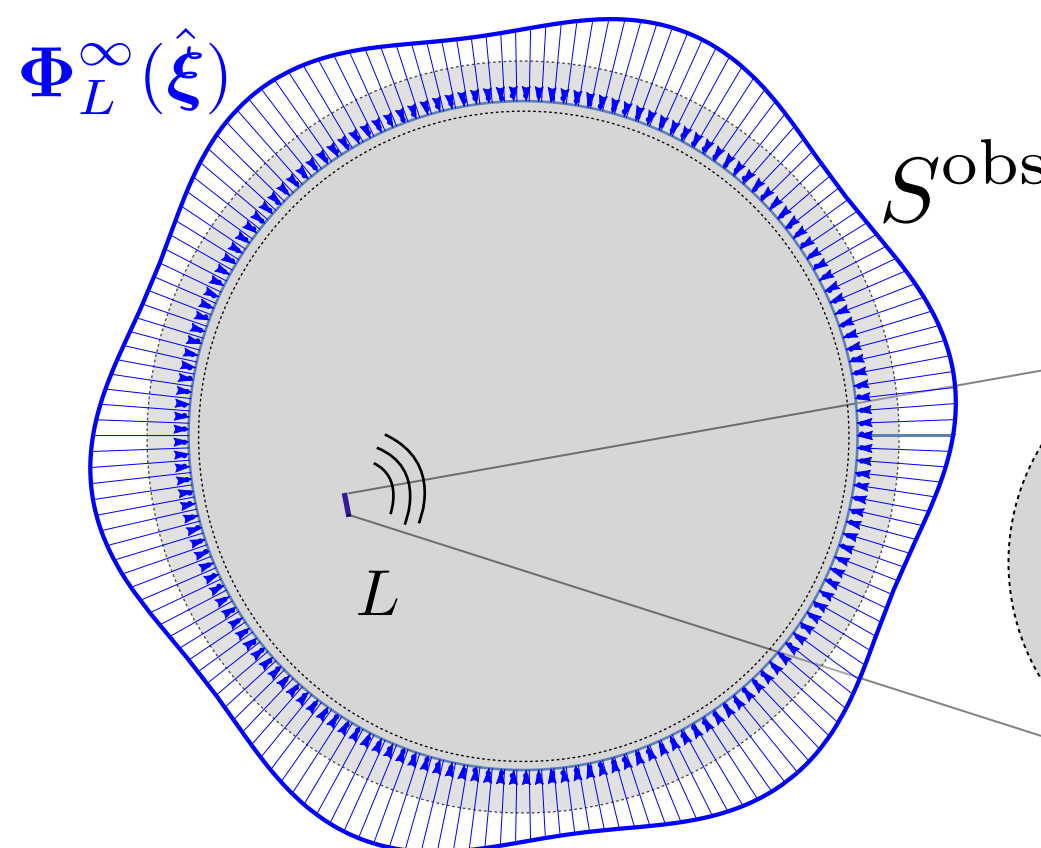
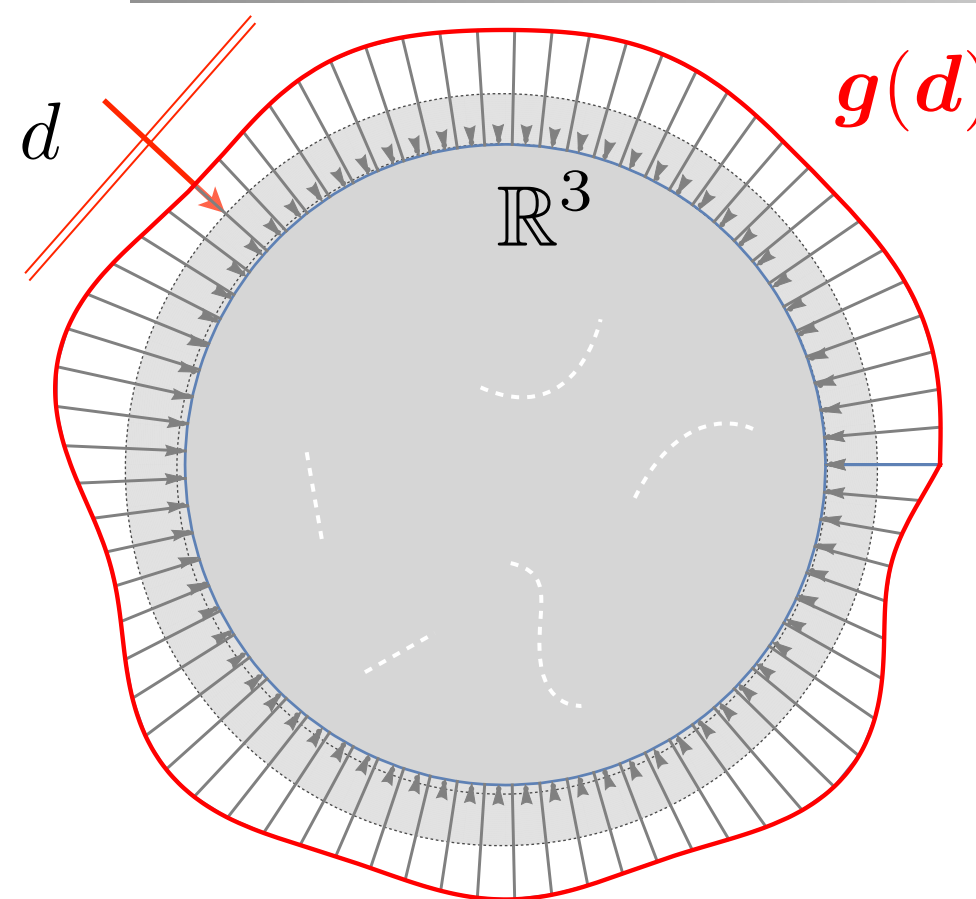
$$\textcolor{red}{a} \in \tilde{H}^{\frac{1}{2}}(L)$$

A small 3D surface plot showing a wavy, orange-yellow surface over a circular domain labeled L . A curved arrow points from the text P patten to the first term of the equation, and another curved arrow points from the text S patten to the second term.

$$\Phi_L^\infty[\textcolor{red}{a}](\hat{\xi}) = - \left(ik_p \hat{\xi} \int_L \{ \lambda(\textcolor{red}{a} \cdot \mathbf{n}) + 2\mu(\mathbf{n} \cdot \hat{\xi})(\textcolor{red}{a} \cdot \hat{\xi}) \} e^{-ik_p \hat{\xi} \cdot \mathbf{y}} dS_y, \right. \\ \left. ik_s \hat{\xi} \times \int_L \{ \mu(\textcolor{red}{a} \times \hat{\xi})(\mathbf{n} \cdot \hat{\xi}) + \mu(\mathbf{n} \times \hat{\xi})(\textcolor{red}{a} \cdot \hat{\xi}) \} e^{-ik_s \hat{\xi} \cdot \mathbf{y}} dS_y \right)$$



GLSM IDEA



$$\Phi_L^\infty[\mathbf{a}](\hat{\boldsymbol{\xi}}) =$$

$$-\left(ik_p \hat{\boldsymbol{\xi}} \int_L \{ \lambda(\mathbf{a} \cdot \mathbf{n}) + 2\mu(\mathbf{n} \cdot \hat{\boldsymbol{\xi}})(\mathbf{a} \cdot \hat{\boldsymbol{\xi}}) \} e^{-ik_p \hat{\boldsymbol{\xi}} \cdot \mathbf{y}} dS_y, \right. \\ \left. ik_s \hat{\boldsymbol{\xi}} \times \int_L \{ \mu(\mathbf{a} \times \hat{\boldsymbol{\xi}})(\mathbf{n} \cdot \hat{\boldsymbol{\xi}}) + \mu(\mathbf{n} \times \hat{\boldsymbol{\xi}})(\mathbf{a} \cdot \hat{\boldsymbol{\xi}}) \} e^{-ik_s \hat{\boldsymbol{\xi}} \cdot \mathbf{y}} dS_y \right)$$

P patten

S patten

IDEA

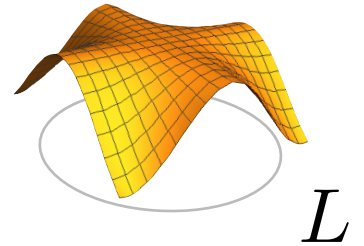
$$\Phi_L^\infty(\hat{\boldsymbol{\xi}}) = \int_{\Omega_d} \mathbf{g}(d) \cdot \mathbf{W}^\infty(d, \hat{\boldsymbol{\xi}}) dS_d$$

experiments

synthetic rearrangement
of the sources

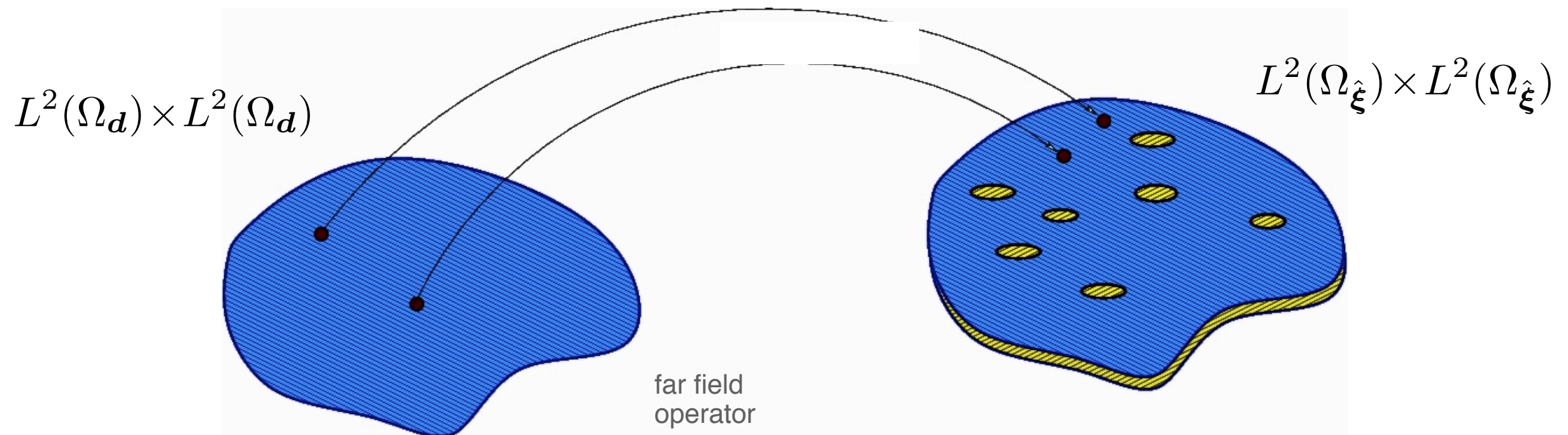
$$F\mathbf{g} = \Phi_L^\infty(\hat{\boldsymbol{\xi}})$$

smooth
non-intersecting



III-posedness

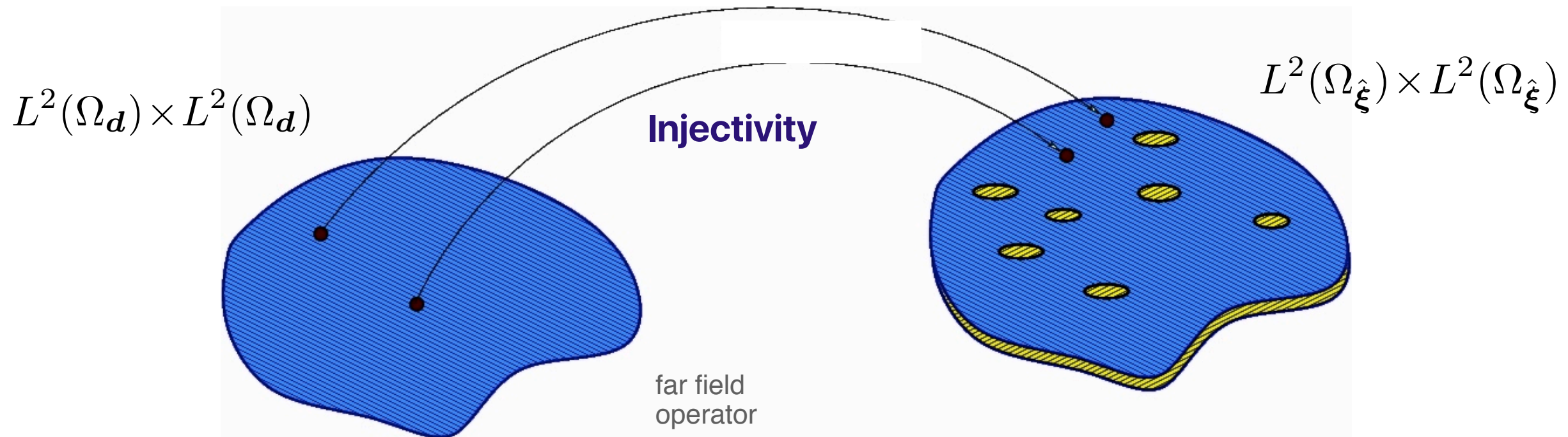
$$F \mathbf{g} = \Phi_L^\infty(\hat{\boldsymbol{\xi}})$$



$$F: L^2(\Omega_d) \times L^2(\Omega_d) \rightarrow L^2(\Omega_{\hat{\boldsymbol{\xi}}}) \times L^2(\Omega_{\hat{\boldsymbol{\xi}}})$$

III-posedness

$$F\mathbf{g} = \Phi_L^\infty(\hat{\xi})$$



$$F: L^2(\Omega_d) \times L^2(\Omega_d) \rightarrow L^2(\Omega_{\hat{\xi}}) \times L^2(\Omega_{\hat{\xi}})$$

Hadamard (1923)

Uniqueness

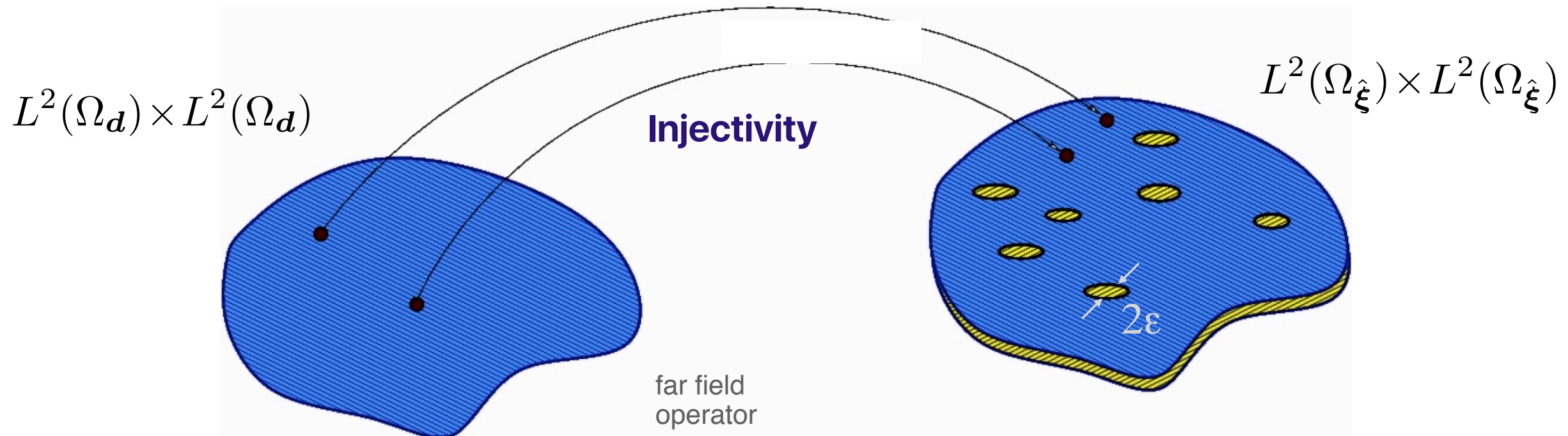
$$F\mathbf{g} = \mathbf{0} \Rightarrow \mathbf{g} = \mathbf{0}$$

injective



III-posedness

$$F\mathbf{g} = \Phi_L^\infty(\hat{\xi})$$



$$F: L^2(\Omega_d) \times L^2(\Omega_d) \rightarrow L^2(\Omega_{\hat{\xi}}) \times L^2(\Omega_{\hat{\xi}})$$

Hadamard (1923)

Uniqueness

$$F\mathbf{g} = \mathbf{0} \Rightarrow \mathbf{g} = \mathbf{0}$$

injective

Existence

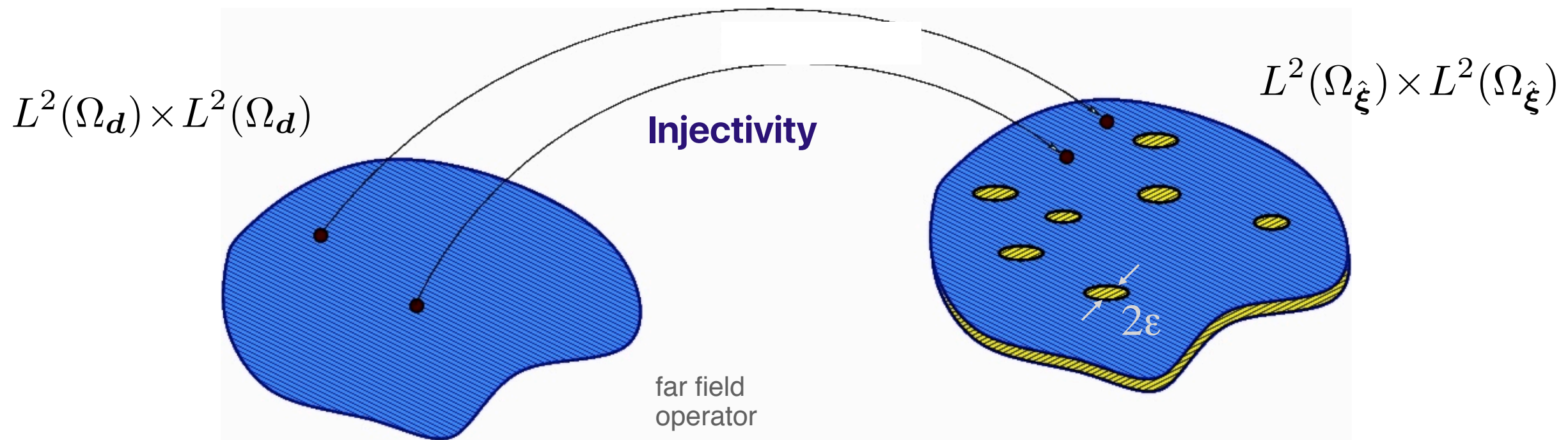
$$\forall \varepsilon > 0, \quad \exists \mathbf{g}^\varepsilon: \|F\mathbf{g}^\varepsilon - \Phi_L^\infty\|_{L^2(\Omega_{\hat{\xi}})} < \varepsilon$$

dense range



III-posedness

$$F\mathbf{g} = \Phi_L^\infty(\hat{\xi})$$



$$F: L^2(\Omega_d) \times L^2(\Omega_d) \rightarrow L^2(\Omega_{\hat{\xi}}) \times L^2(\Omega_{\hat{\xi}})$$

Hadamard (1923)



Uniqueness

$$F\mathbf{g} = \mathbf{0} \Rightarrow \mathbf{g} = \mathbf{0}$$

injective

Existence

$$\forall \varepsilon > 0, \quad \exists \mathbf{g}^\varepsilon: \|F\mathbf{g}^\varepsilon - \Phi_L^\infty\|_{L^2(\Omega_{\hat{\xi}})} < \varepsilon$$

dense range

Stability

$$\exists C > 0: \|\mathbf{g}\|_{L^2(\Omega_d)} \leq C \|\Phi_L^\infty\|_{L^2(\Omega_{\hat{\xi}})}$$

compact operator of infinite dimension \rightarrow no stability

Stability

$$F\mathbf{g} = \Phi_L^\infty(\hat{\xi})$$

1D Backwards heat equation

Fourier Coefficients of the input

$$\|T_0\|_{L^2(\ell)}^2 = \frac{\pi}{2} \sum_{n=1}^{\infty} T_n^{\text{fin}} e^{2n^2\tau}$$

norm of solution

1D Backwards heat equation

Fourier Coefficients of the input

$$\|T_0\|_{L^2(\ell)}^2 = \frac{\pi}{2} \sum_{n=1}^{\infty} T_n^{\text{fin}} e^{2n^2\tau}$$

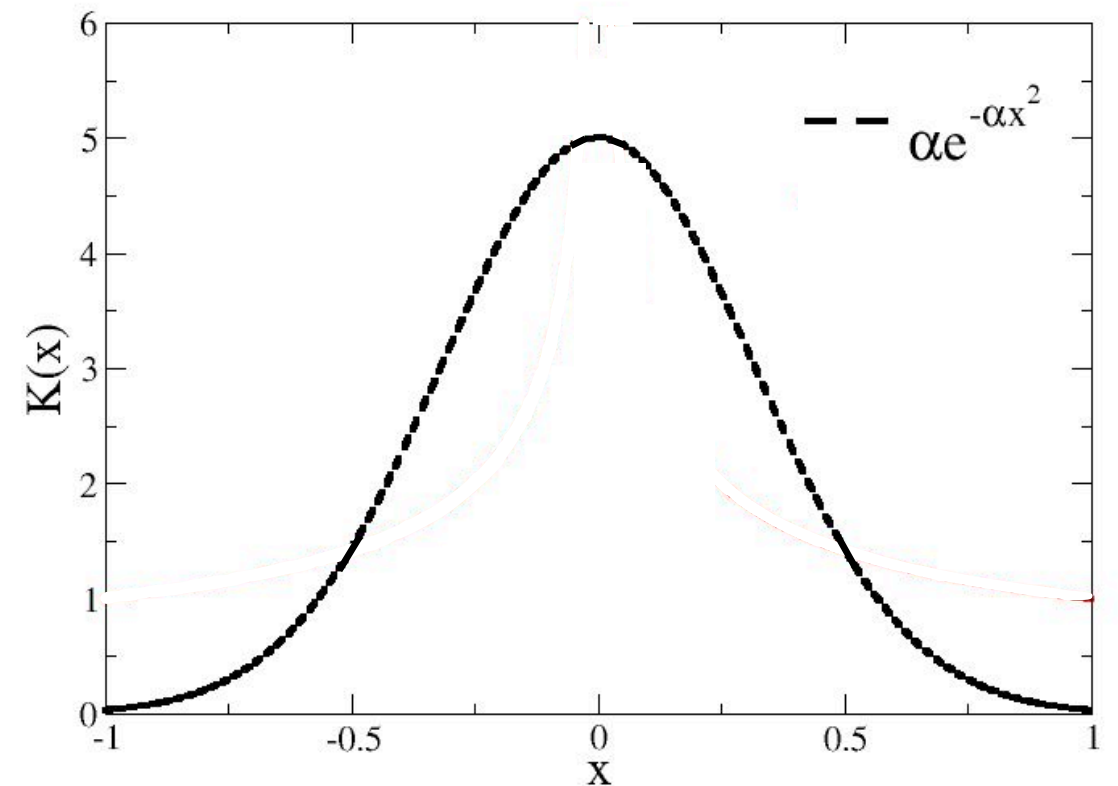
norm of solution

Heat conduction is irreversible

Stability

$$F \mathbf{g} = \Phi_L^\infty(\hat{\xi})$$

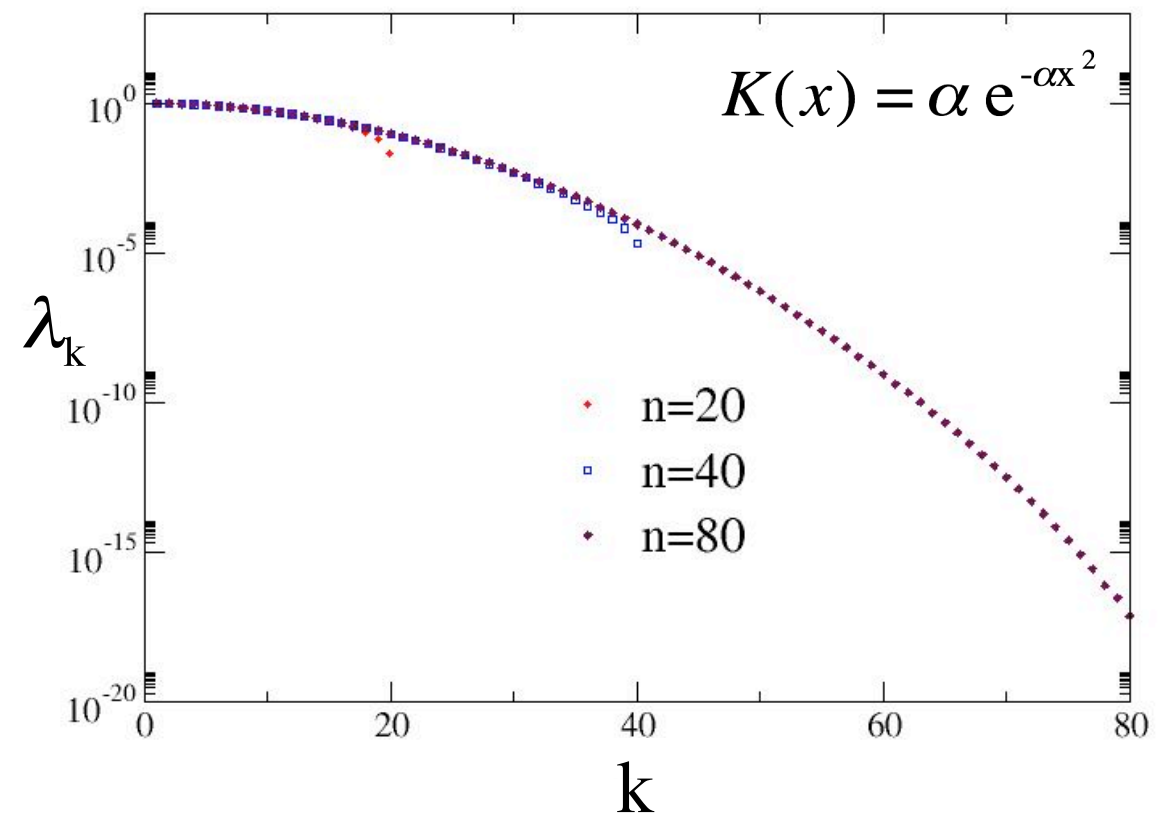
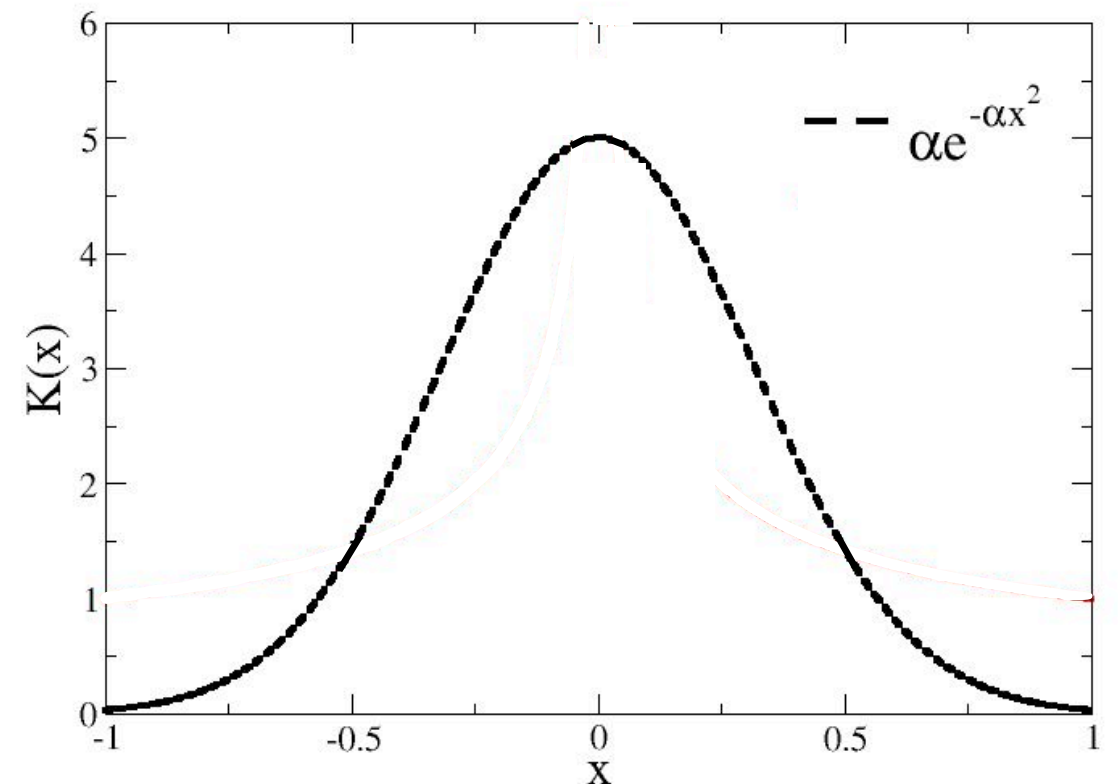
$$\int_{-1}^1 K(\xi - x) \cdot g(x) dx = u(\xi)$$



Stability

$$F \mathbf{g} = \Phi_L^\infty(\hat{\xi})$$

$$\int_{-1}^1 K(\xi - x) \cdot g(x) dx = u(\xi)$$



Stability

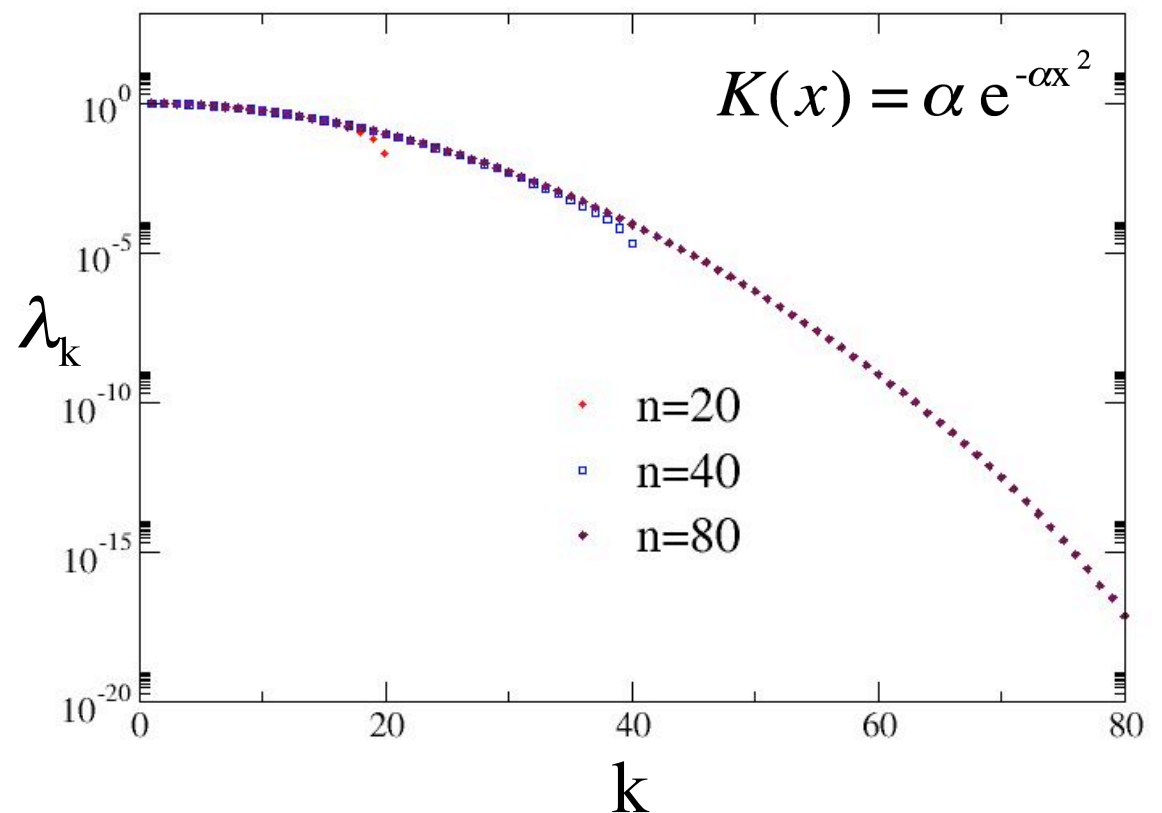
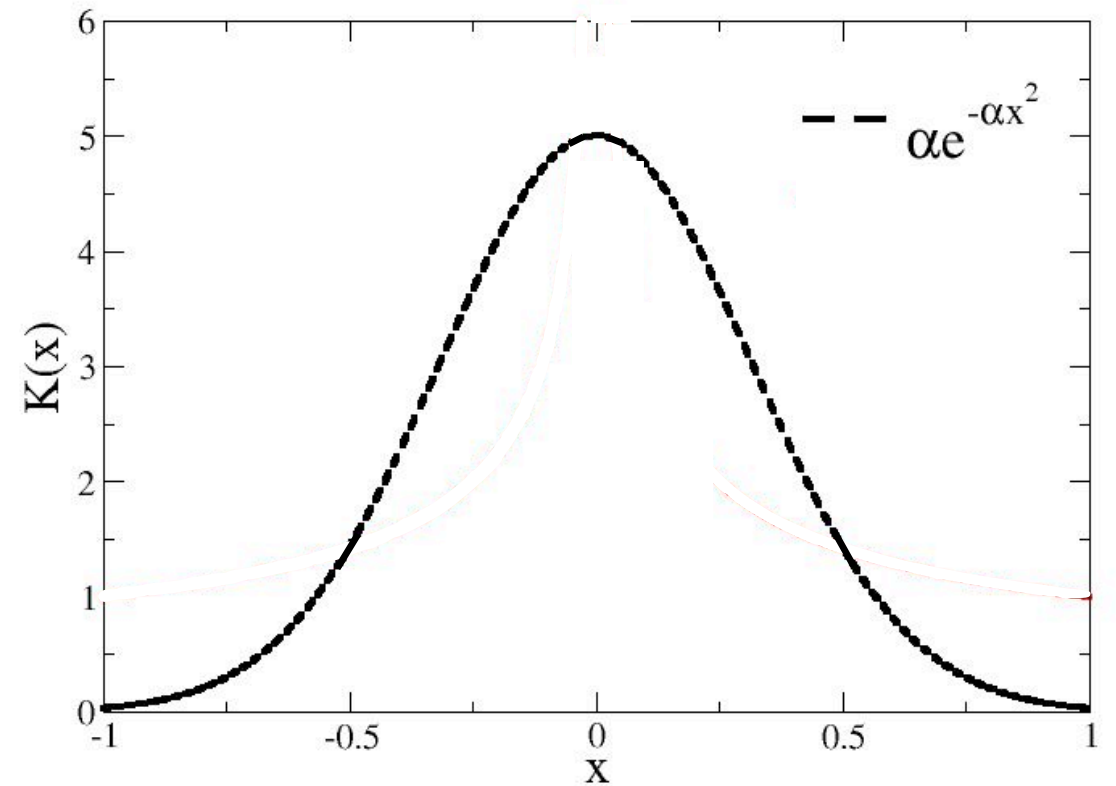
$$F\mathbf{g} = \Phi_L^\infty(\hat{\xi})$$

$$\int_{-1}^1 K(\xi - x) \cdot g(x) dx = u(\xi)$$



Tikhonov regularization

$$\min_{\mathbf{g} \in L^2(\Omega_d)} \left\{ \| F\mathbf{g} - \Phi_L^\infty \|_{L^2(\Omega_{\hat{\xi}})} + \alpha \| \mathbf{g} \|_{L^2(\Omega_d)} \right\}$$



Stability

$$F\mathbf{g} = \Phi_L^\infty(\hat{\xi})$$

$$\int_{-1}^1 K(\xi - x) \cdot g(x) dx = u(\xi)$$



Tikhonov regularization

$$\min_{\mathbf{g} \in L^2(\Omega_d)} \left\{ \| F\mathbf{g} - \Phi_L^\infty \|_{L^2(\Omega_{\hat{\xi}})} + \alpha \| \mathbf{g} \|_{L^2(\Omega_d)} \right\}$$

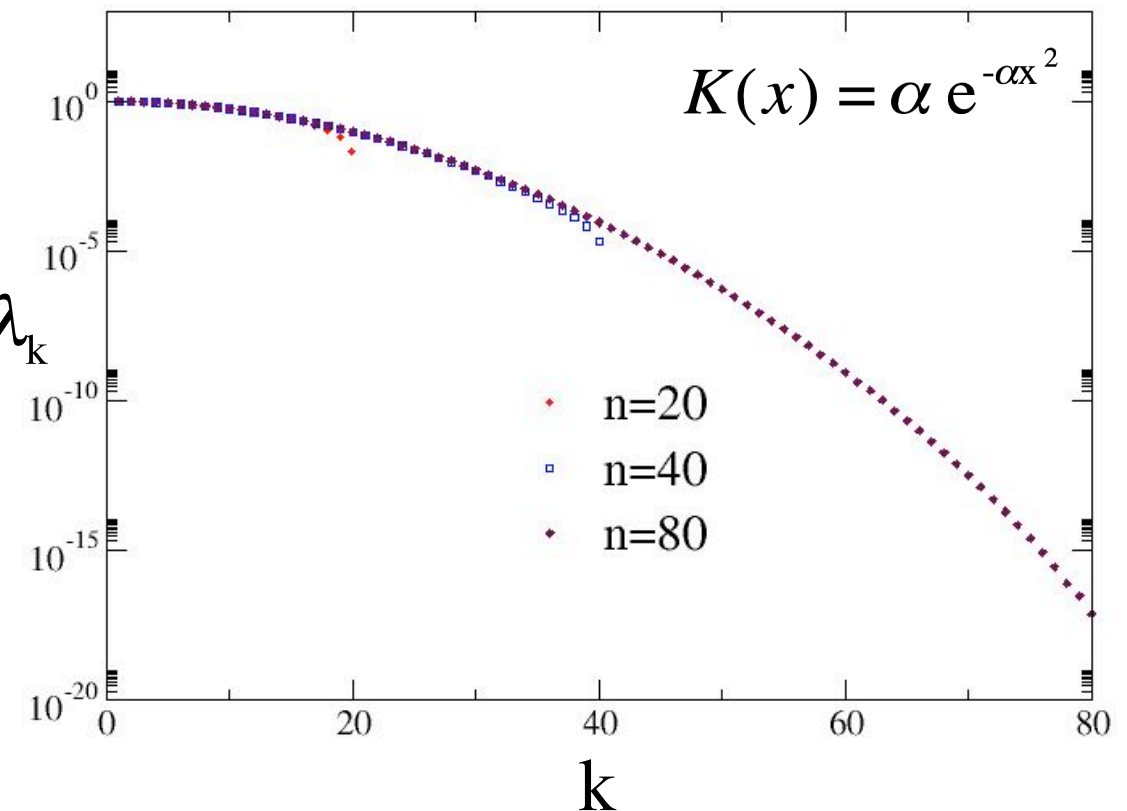
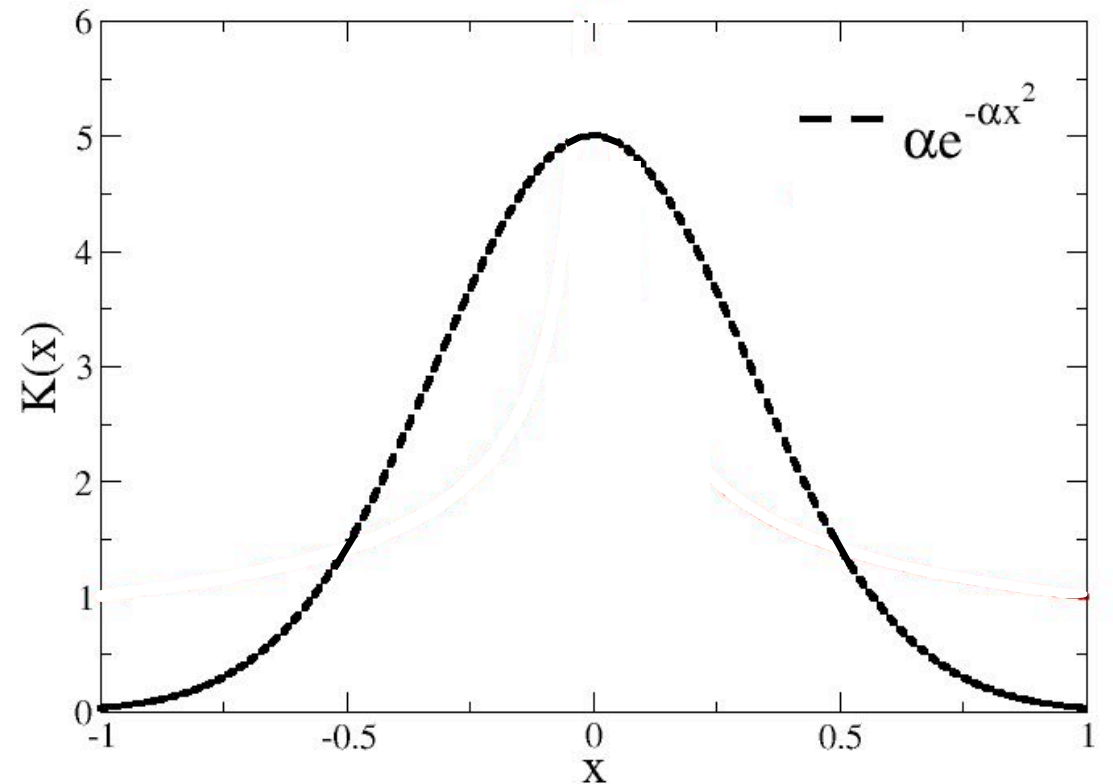


Morozov discrepancy principle

$$\min_{\mathbf{g}^\alpha} \left\{ \| \mathbf{g}^\alpha \|_{L^2(\Omega_d)} : \| F\mathbf{g}^\alpha - \Phi_L^\infty \|_{L^2(\Omega_{\hat{\xi}})} \leq \delta \right\}$$

↑
measurement
noise

$$\lim_{\delta \rightarrow 0} \| \mathbf{g}^\delta \|_{L^2(\Omega_d)} = \infty$$



Problem

$$F\mathbf{g} = \Phi_L^\infty(\hat{\xi})$$

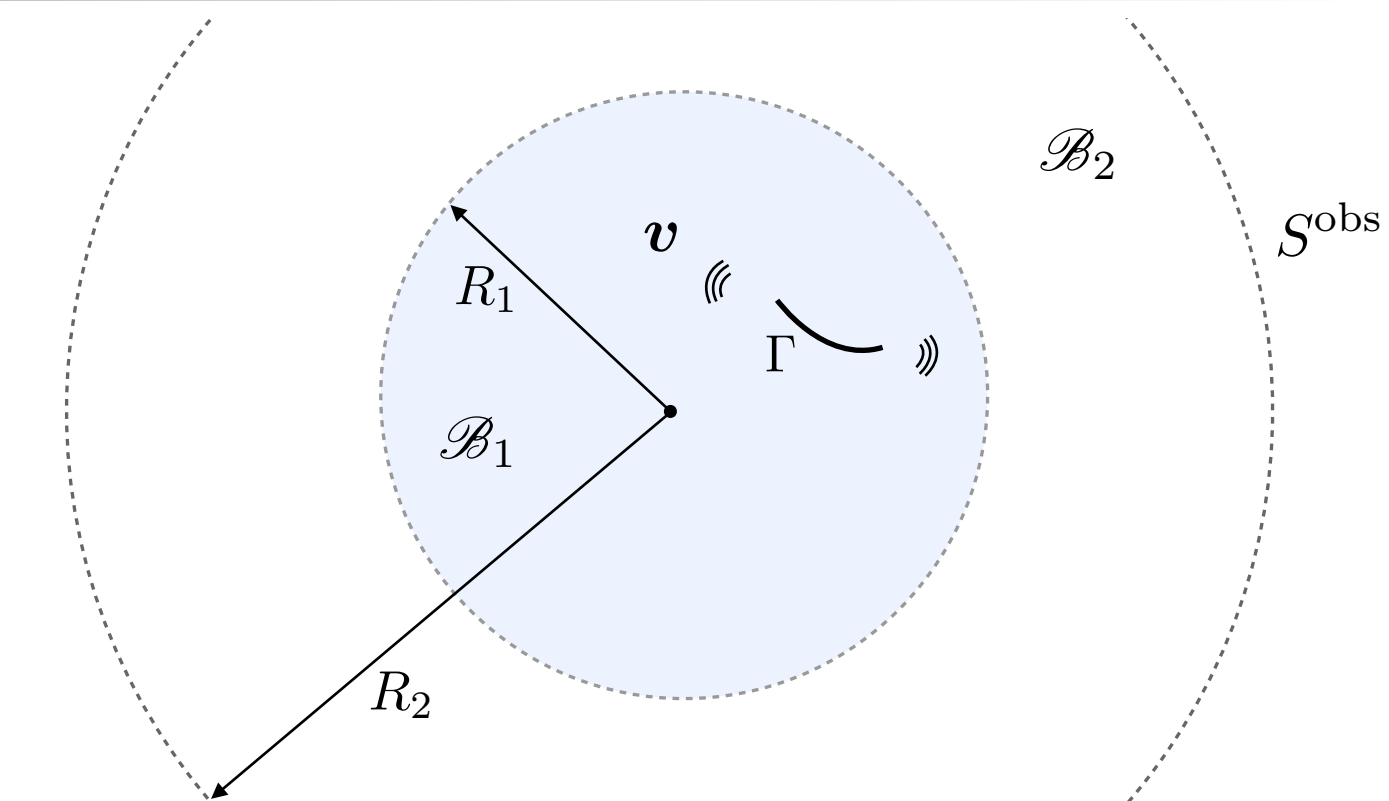
scattered field \mathbb{R}^3

$$\nabla \cdot (C : \nabla \mathbf{v})(\xi) + \rho \omega^2 \mathbf{v}(\xi) = 0, \quad \text{away from } \Gamma$$

$$\mathbf{n} \cdot C : \nabla \mathbf{v} = \mathbf{K}(\xi) \llbracket \mathbf{v} \rrbracket^{\text{COD}} - \mathbf{t}^f, \quad \Gamma \text{ interface}$$

Kupradze - Sommerfeld

$$R_2 \rightarrow \infty$$



Problem

$$F \mathbf{g} = \Phi_L^\infty(\hat{\xi})$$

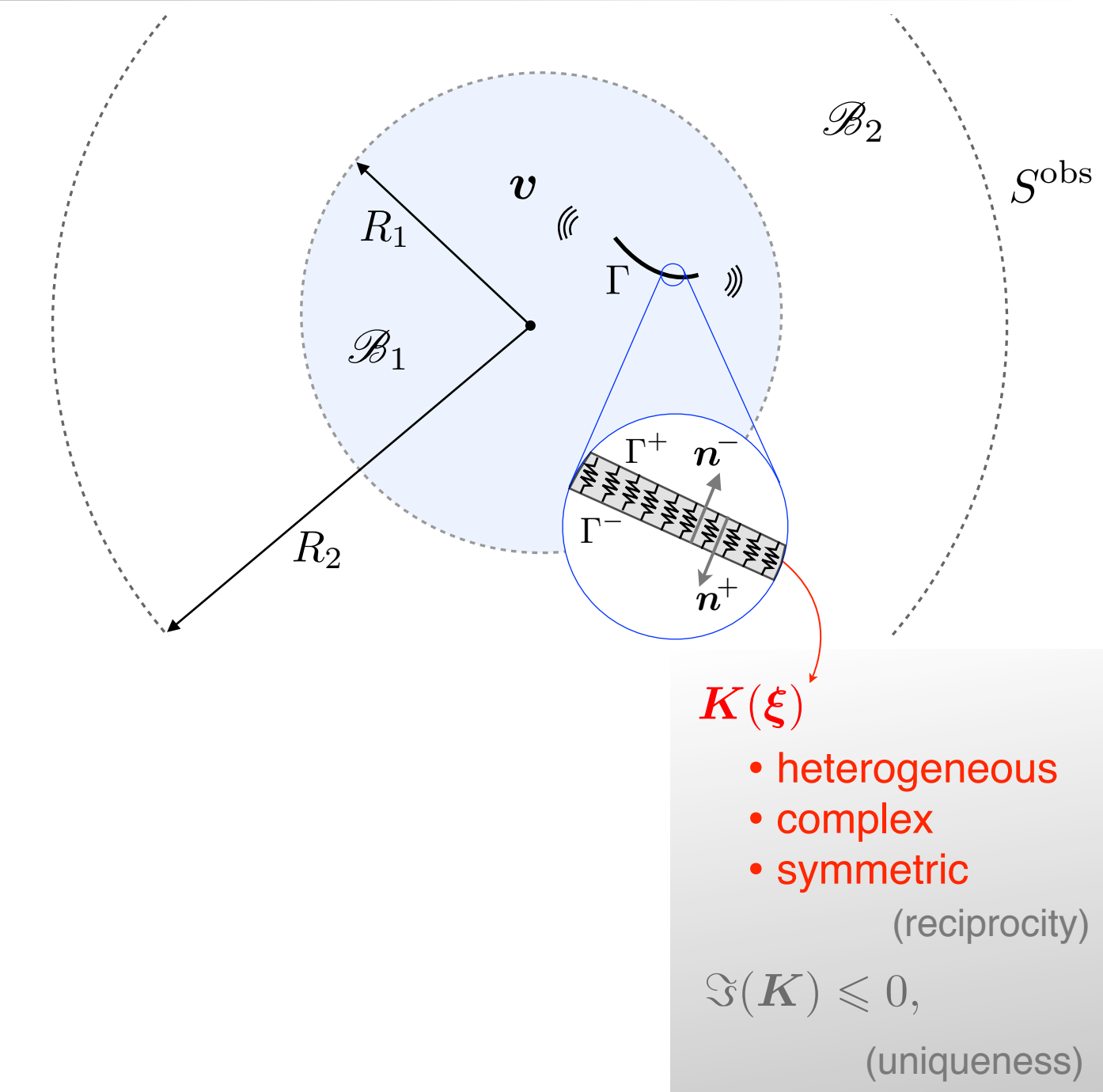
scattered field \mathbb{R}^3

$$\nabla \cdot (C : \nabla \mathbf{v})(\xi) + \rho \omega^2 \mathbf{v}(\xi) = 0, \quad \text{away from } \Gamma$$

$$\mathbf{n} \cdot C : \nabla \mathbf{v} = \mathbf{K}(\xi) \llbracket \mathbf{v} \rrbracket^{\text{COD}} - \mathbf{t}^f, \quad \Gamma \text{ interface}$$

Kupradze - Sommerfeld

$$R_2 \rightarrow \infty$$



Problem

$$F \mathbf{g} = \Phi_L^\infty(\hat{\xi})$$

scattered field \mathbb{R}^3

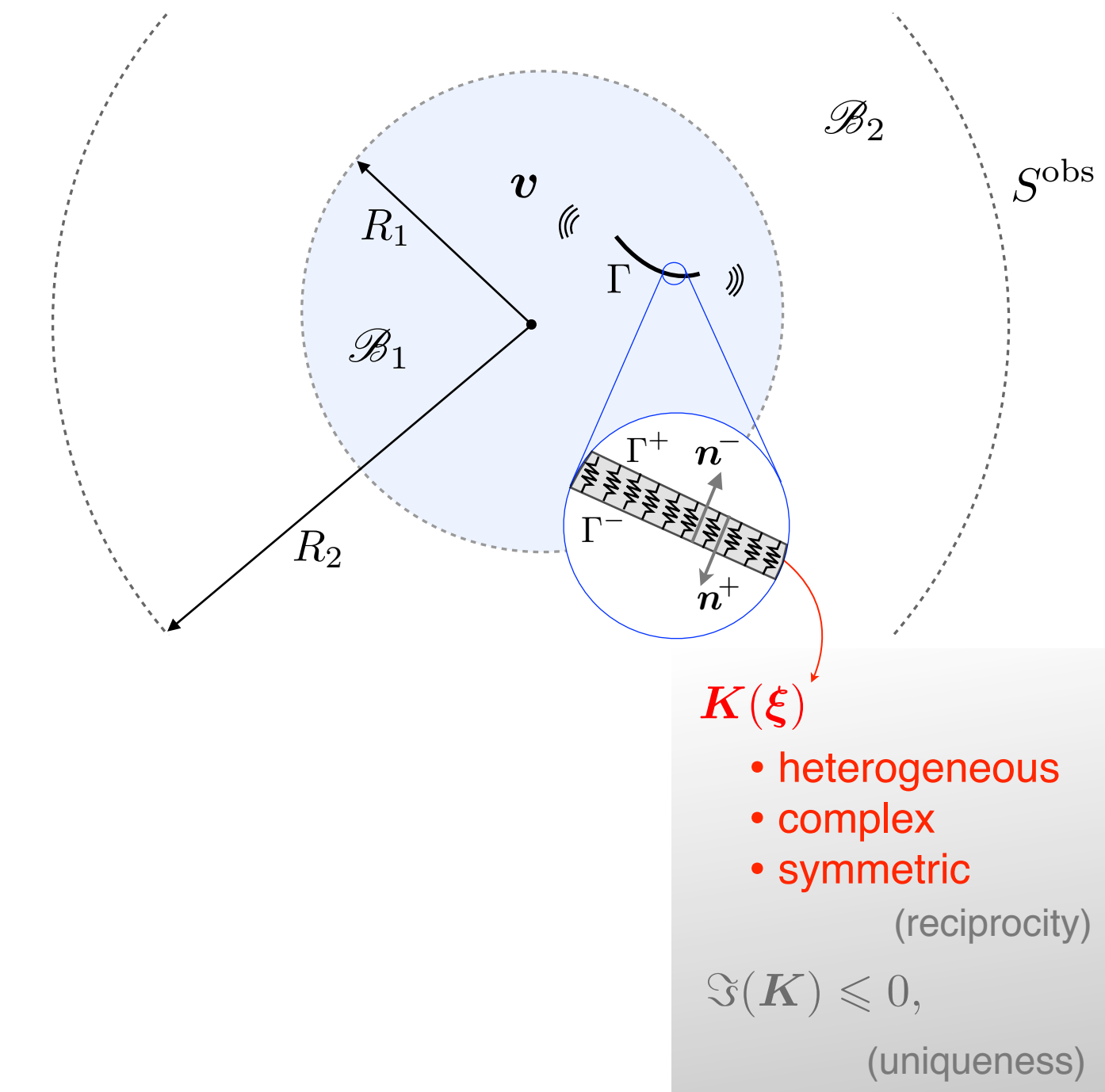
$$\nabla \cdot (C : \nabla \mathbf{v})(\xi) + \rho \omega^2 \mathbf{v}(\xi) = 0, \quad \text{away from } \Gamma$$

$$\mathbf{n} \cdot C : \nabla \mathbf{v} = \mathbf{K}(\xi) \llbracket \mathbf{v} \rrbracket^{\text{COD}} - \mathbf{t}^f, \quad \Gamma \text{ interface}$$

Kupradze - Sommerfeld

dimensional platform $\rho, c = \sqrt{\frac{\mu}{\rho}}, R_1$

$$R_2 \rightarrow \infty$$



Problem

$$F \mathbf{g} = \Phi_L^\infty(\hat{\xi})$$

scattered field \mathbb{R}^3

$$\nabla \cdot (C : \nabla v)(\xi) + \rho \omega^2 v(\xi) = 0, \quad \text{away from } \Gamma$$

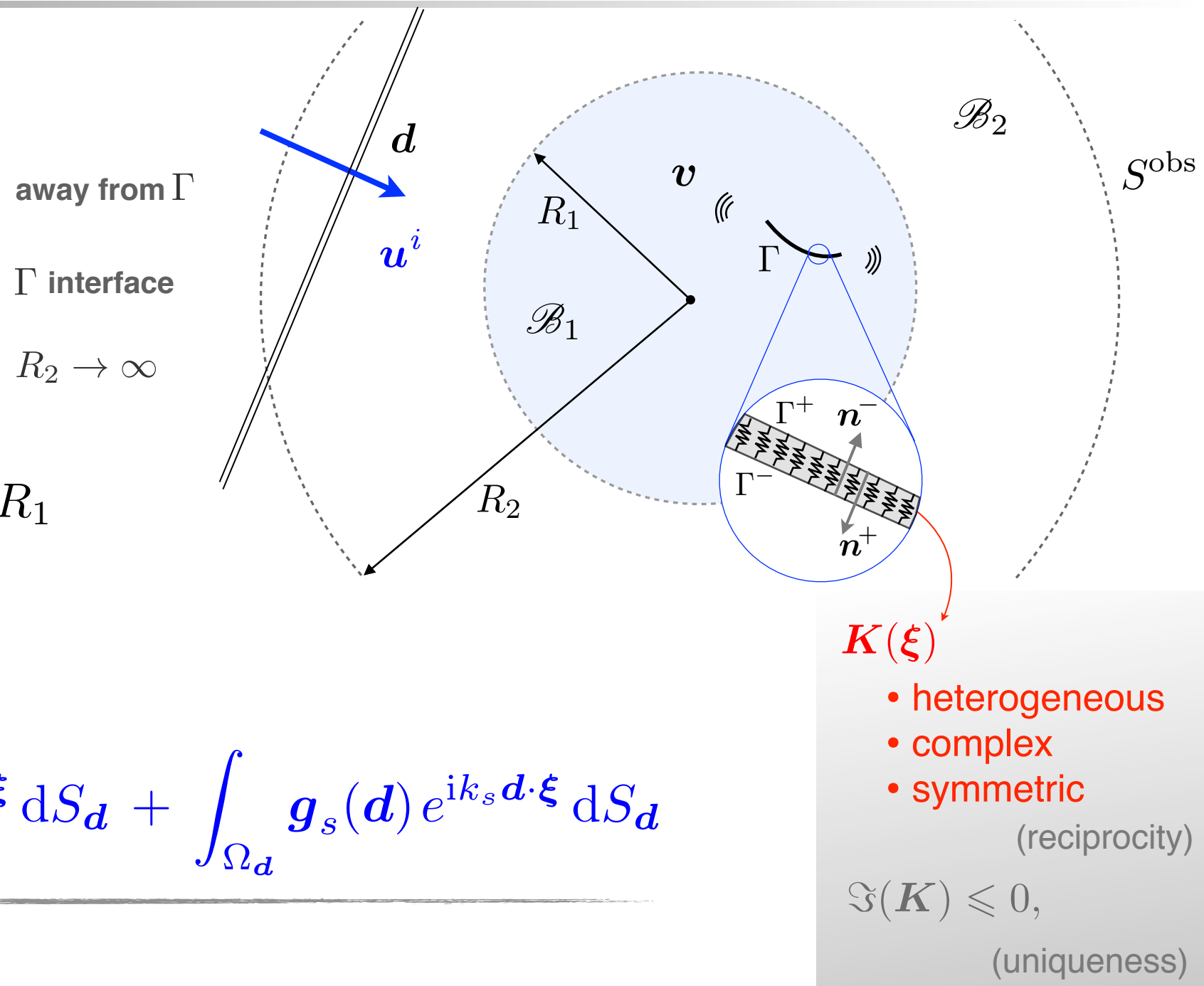
$$n \cdot C : \nabla v = K(\xi) \llbracket v \rrbracket^{\text{COD}} - t^f, \quad \Gamma \text{ interface}$$

Kupradze - Sommerfeld

dimensional platform $\rho, c = \sqrt{\frac{\mu}{\rho}}, R_1$

elastic Herglotz wave function

$$u^i(\xi) = \int_{\Omega_d} g_p(d) e^{ik_p d \cdot \xi} dS_d + \int_{\Omega_d} g_s(d) e^{ik_s d \cdot \xi} dS_d$$



Problem

$$F\mathbf{g} = \Phi_L^\infty(\hat{\xi})$$

scattered field \mathbb{R}^3

$$\nabla \cdot (C : \nabla \mathbf{v})(\xi) + \rho \omega^2 \mathbf{v}(\xi) = 0, \quad \text{away from } \Gamma$$

$$\mathbf{n} \cdot C : \nabla \mathbf{v} = \mathbf{K}(\xi) [\![\mathbf{v}]\!]^{\text{COD}} - \mathbf{t}^f, \quad \Gamma \text{ interface}$$

Kupradze - Sommerfeld

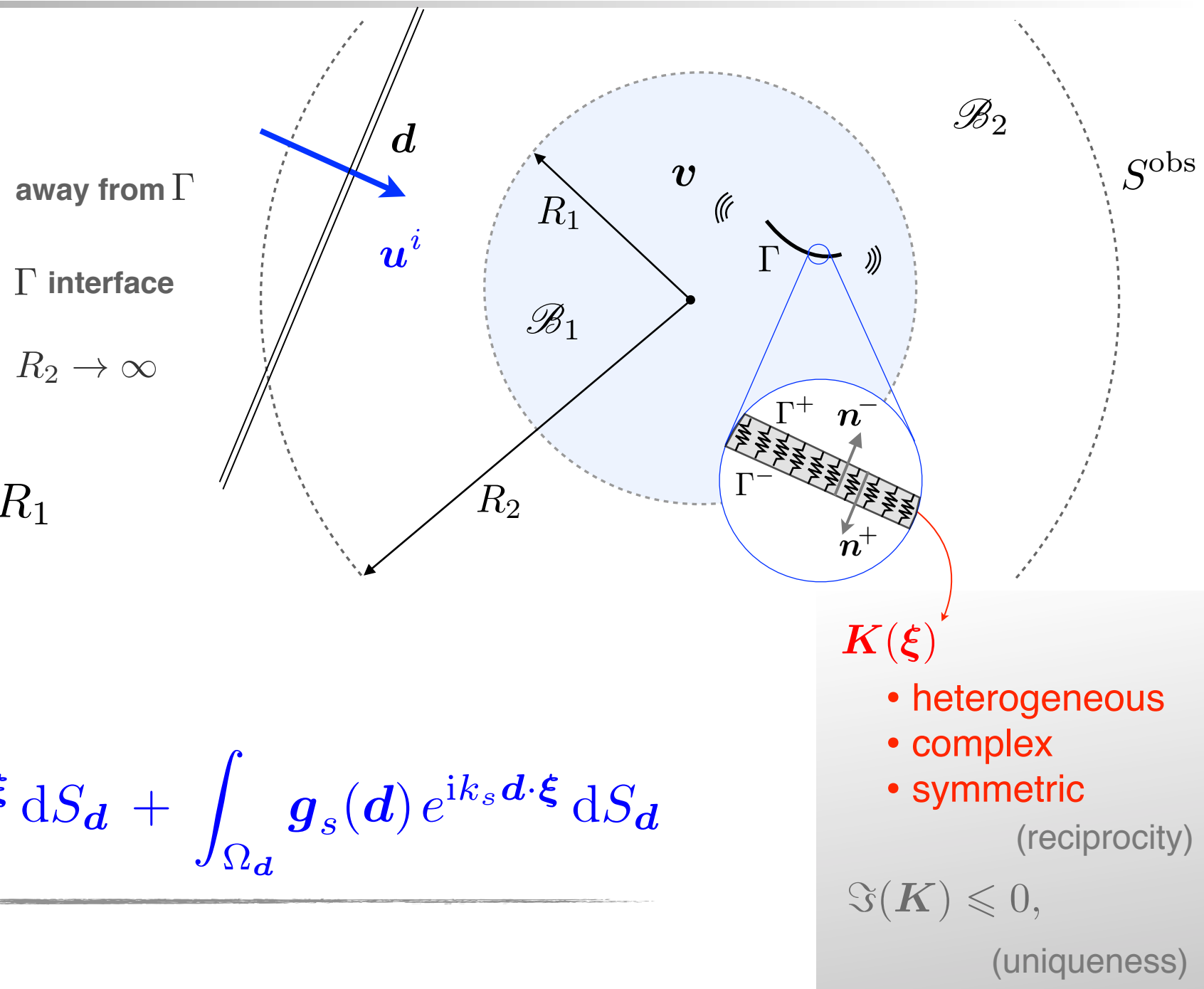
dimensional platform $\rho, c = \sqrt{\frac{\mu}{\rho}}, R_1$

elastic Herglotz wave function

$$\mathbf{u}^i(\xi) = \int_{\Omega_d} \mathbf{g}_p(\mathbf{d}) e^{ik_p \mathbf{d} \cdot \xi} dS_{\mathbf{d}} + \int_{\Omega_d} \mathbf{g}_s(\mathbf{d}) e^{ik_s \mathbf{d} \cdot \xi} dS_{\mathbf{d}}$$

GLSM cost functional

$$J_\alpha^\delta = \alpha (|(F_\sharp^\delta \mathbf{g}, \mathbf{g})| + \delta \|\mathbf{g}\|^2) + \|F^\delta \mathbf{g} - \Phi_L^\infty\|^2$$



Problem

$$F\mathbf{g} = \Phi_L^\infty(\hat{\xi})$$

scattered field \mathbb{R}^3

$$\nabla \cdot (C : \nabla \mathbf{v})(\xi) + \rho \omega^2 \mathbf{v}(\xi) = 0, \quad \text{away from } \Gamma$$

$$\mathbf{n} \cdot C : \nabla \mathbf{v} = \mathbf{K}(\xi) [\![\mathbf{v}]\!]^{\text{COD}} - \mathbf{t}^f, \quad \Gamma \text{ interface}$$

Kupradze - Sommerfeld

dimensional platform $\rho, c = \sqrt{\frac{\mu}{\rho}}, R_1$

elastic Herglotz wave function

$$\mathbf{u}^i(\xi) = \int_{\Omega_d} \mathbf{g}_p(\mathbf{d}) e^{ik_p \mathbf{d} \cdot \xi} dS_{\mathbf{d}} + \int_{\Omega_d} \mathbf{g}_s(\mathbf{d}) e^{ik_s \mathbf{d} \cdot \xi} dS_{\mathbf{d}}$$

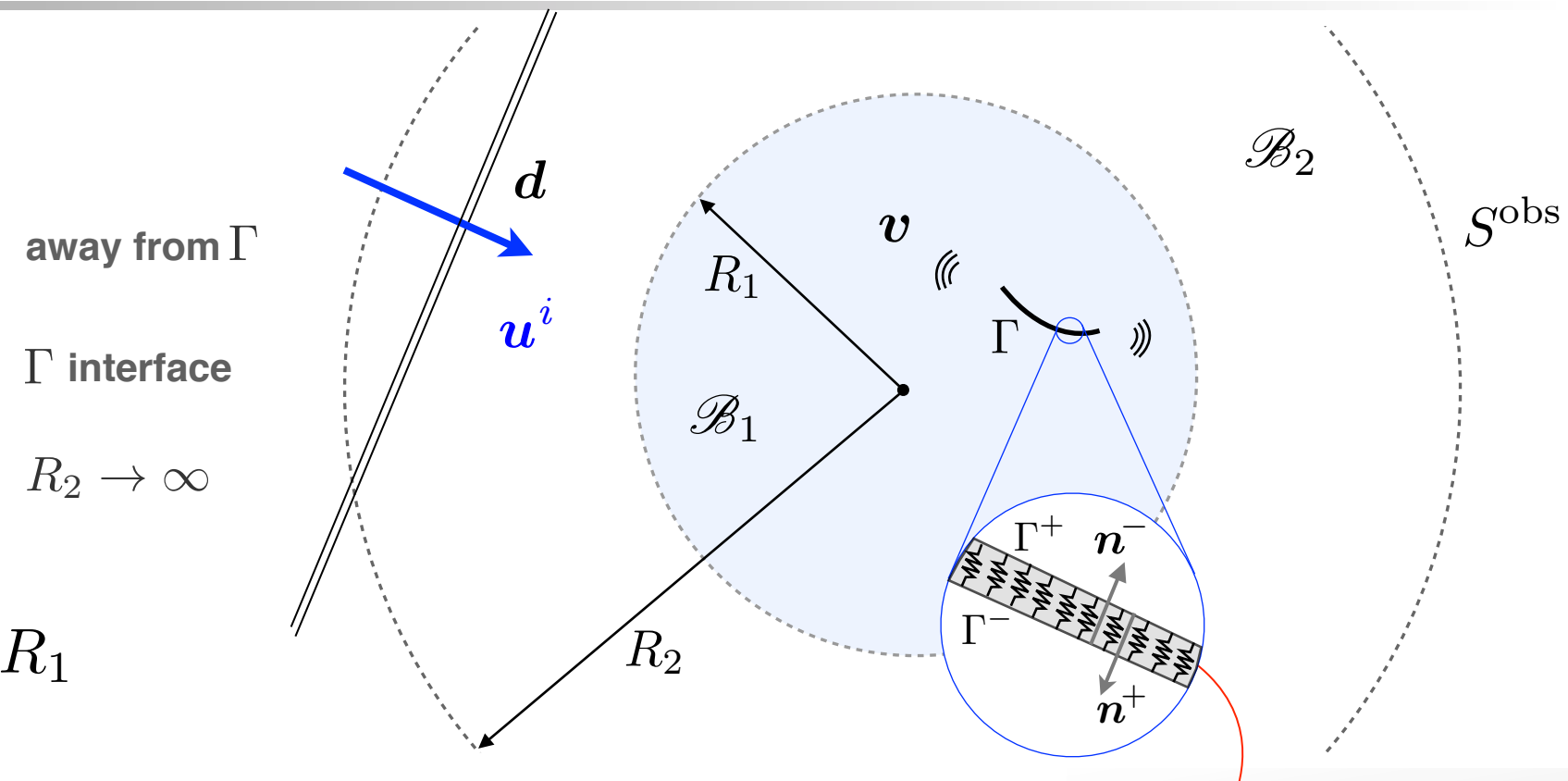
GLSM cost functional

$$J_\alpha^\delta = \alpha (|(F_\sharp^\delta \mathbf{g}, \mathbf{g})| + \delta \|\mathbf{g}\|^2) + \|F^\delta \mathbf{g} - \Phi_L^\infty\|^2$$

noisy operator



$$F_\sharp^\delta = |\Re(F^\delta)| + \Im(F^\delta)$$



- $\mathbf{K}(\xi)$
- heterogeneous
 - complex
 - symmetric
- (reciprocity)

$\Im(\mathbf{K}) \leq 0,$
(uniqueness)

Problem

$$F\mathbf{g} = \Phi_L^\infty(\hat{\xi})$$

scattered field \mathbb{R}^3

$$\nabla \cdot (C : \nabla \mathbf{v})(\xi) + \rho \omega^2 \mathbf{v}(\xi) = 0, \quad \text{away from } \Gamma$$

$$\mathbf{n} \cdot C : \nabla \mathbf{v} = \mathbf{K}(\xi) [\![\mathbf{v}]\!]^{\text{COD}} - \mathbf{t}^f, \quad \Gamma \text{ interface}$$

Kupradze - Sommerfeld

dimensional platform $\rho, c = \sqrt{\frac{\mu}{\rho}}, R_1$

elastic Herglotz wave function

$$\mathbf{u}^i(\xi) = \int_{\Omega_d} \mathbf{g}_p(\mathbf{d}) e^{ik_p \mathbf{d} \cdot \xi} dS_{\mathbf{d}} + \int_{\Omega_d} \mathbf{g}_s(\mathbf{d}) e^{ik_s \mathbf{d} \cdot \xi} dS_{\mathbf{d}}$$

GLSM cost functional

$$J_\alpha^\delta = \alpha (|(F_\sharp^\delta \mathbf{g}, \mathbf{g})| + \delta \|\mathbf{g}\|^2) + \|F^\delta \mathbf{g} - \Phi_L^\infty\|^2$$

KNOWN OPTIMIZED MINIMUM \mathbf{g}

noisy operator



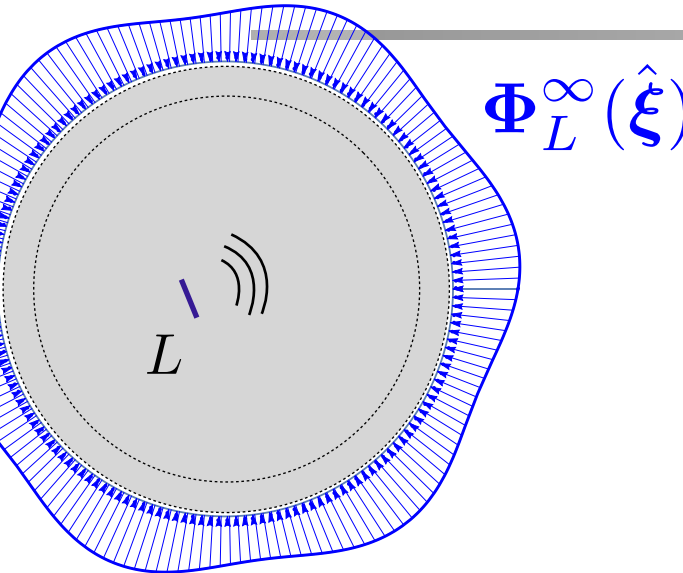
- $\mathbf{K}(\xi)$
- heterogeneous
 - complex
 - symmetric
- (reciprocity)

$\Im(\mathbf{K}) \leq 0,$
(uniqueness)

$$F_\sharp^\delta = |\Re(F^\delta)| + \Im(F^\delta)$$

Main Theorem

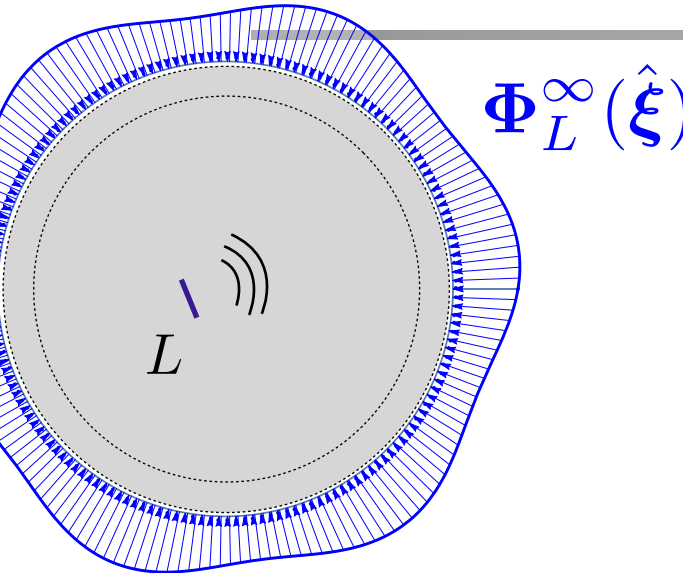
$$F \textcolor{red}{g} = \Phi_L^\infty(\hat{\xi})$$



$$F = \mathcal{H}^* T \mathcal{H}$$

Main Theorem

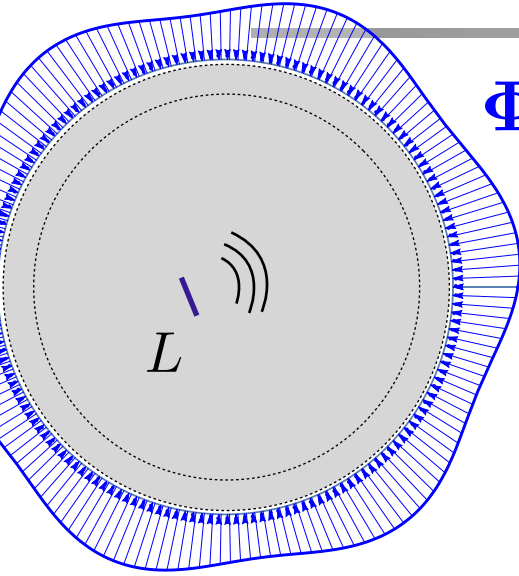
$$F \mathbf{g} = \Phi_L^\infty(\hat{\xi})$$



$$\text{dense range} \quad F = \mathcal{H}^* T \overline{\mathcal{H}} \quad \begin{matrix} \text{coercive} \\ \text{compact} \end{matrix}$$

Main Theorem

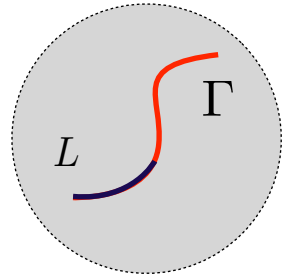
$$F \mathbf{g} = \Phi_L^\infty(\hat{\xi})$$



$$\begin{array}{c} \text{dense} \\ \text{range} \end{array} \swarrow \quad F = \mathcal{H}^* T \overbrace{\mathcal{H}}^{\substack{\text{coercive} \\ \text{compact}}} \quad \searrow$$

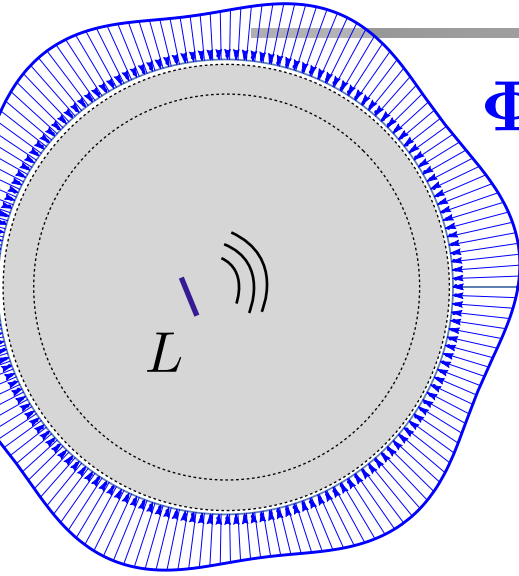
$$L \subset \Gamma \rightarrow \Phi_L^\infty(\hat{\xi}) \in \text{Range}(\mathcal{H}^*)$$

$$L \not\subset \Gamma \rightarrow \Phi_L^\infty(\hat{\xi}) \notin \text{Range}(\mathcal{H}^*)$$



Main Theorem

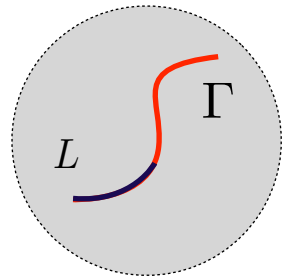
$$F \mathbf{g} = \Phi_L^\infty(\hat{\xi})$$



dense range \nearrow $F = \mathcal{H}^* T \mathcal{H}$ coercive
 \searrow compact

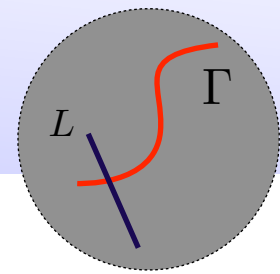
$$L \subset \Gamma \rightarrow \Phi_L^\infty(\hat{\xi}) \in \text{Range}(\mathcal{H}^*)$$

$$L \not\subset \Gamma \rightarrow \Phi_L^\infty(\hat{\xi}) \notin \text{Range}(\mathcal{H}^*)$$



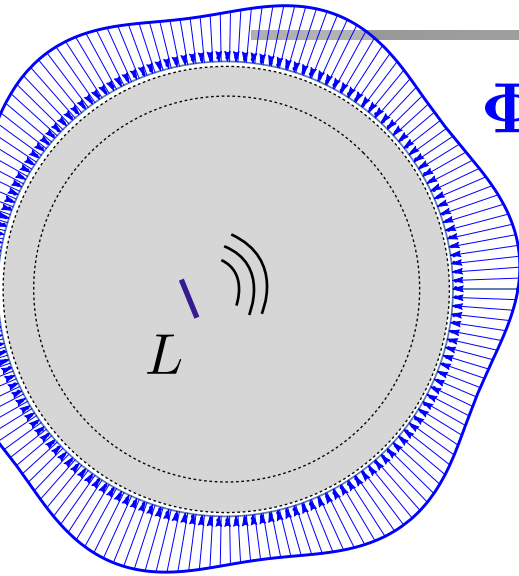
$$\limsup_{\alpha \rightarrow 0} \|\mathcal{H} \mathbf{g}\|_{H^{-\frac{1}{2}}(\Gamma)} < \infty \quad L \subset \Gamma$$

$$\lim_{\alpha \rightarrow 0} \|\mathcal{H} \mathbf{g}\|_{H^{-\frac{1}{2}}(\Gamma)} = \infty \quad L \not\subset \Gamma$$



Main Theorem

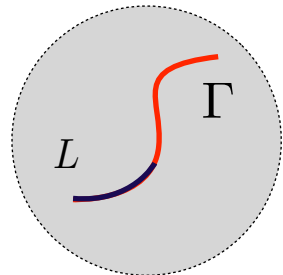
$$F \mathbf{g} = \Phi_L^\infty(\hat{\xi})$$



dense range $\xrightarrow{} F = \mathcal{H}^* T \mathcal{H}$ coercive
 compact

$$L \subset \Gamma \rightarrow \Phi_L^\infty(\hat{\xi}) \in \text{Range}(\mathcal{H}^*)$$

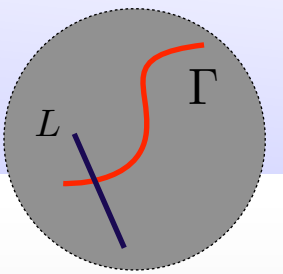
$$L \not\subset \Gamma \rightarrow \Phi_L^\infty(\hat{\xi}) \notin \text{Range}(\mathcal{H}^*)$$



$$\limsup_{\alpha \rightarrow 0} \|\mathcal{H} \mathbf{g}\|_{H^{-\frac{1}{2}}(\Gamma)} < \infty \quad L \subset \Gamma$$

$$\lim_{\alpha \rightarrow 0} \|\mathcal{H} \mathbf{g}\|_{H^{-\frac{1}{2}}(\Gamma)} = \infty \quad L \not\subset \Gamma$$

$$J_\alpha = \|F^\delta \mathbf{g} - \Phi_L^\infty\|^2 + \alpha \|\mathbf{g}\|^2$$



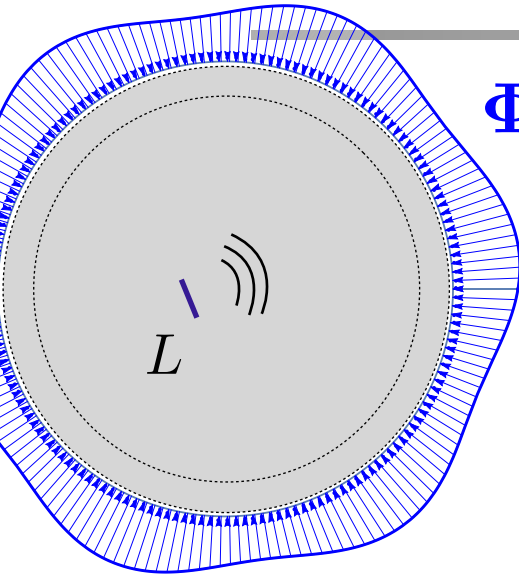
LSM

indicator
functionals

$$\mathcal{I}_{\text{LSM}} = 1 / \|\mathbf{g}\|_{L^2(\Omega_d)}^2$$

Main Theorem

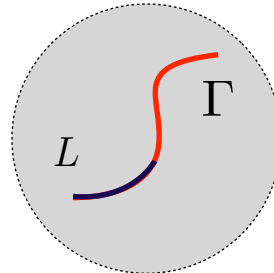
$$F \mathbf{g} = \Phi_L^\infty(\hat{\xi})$$



dense range $\xrightarrow{} F = \mathcal{H}^* T \mathcal{H}$ coercive
 compact

$$L \subset \Gamma \quad \rightarrow \quad \Phi_L^\infty(\hat{\xi}) \in \text{Range}(\mathcal{H}^*)$$

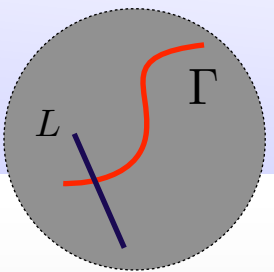
$$L \not\subset \Gamma \quad \rightarrow \quad \Phi_L^\infty(\hat{\xi}) \notin \text{Range}(\mathcal{H}^*)$$



$$\limsup_{\alpha \rightarrow 0} \|\mathcal{H} \mathbf{g}\|_{H^{-\frac{1}{2}}(\Gamma)} < \infty \quad L \subset \Gamma$$

$$\lim_{\alpha \rightarrow 0} \|\mathcal{H} \mathbf{g}\|_{H^{-\frac{1}{2}}(\Gamma)} = \infty \quad L \not\subset \Gamma$$

$$J_\alpha = \|F^\delta \mathbf{g} - \Phi_L^\infty\|^2 + \alpha \|\mathbf{g}\|^2$$



LSM

indicator
functionals

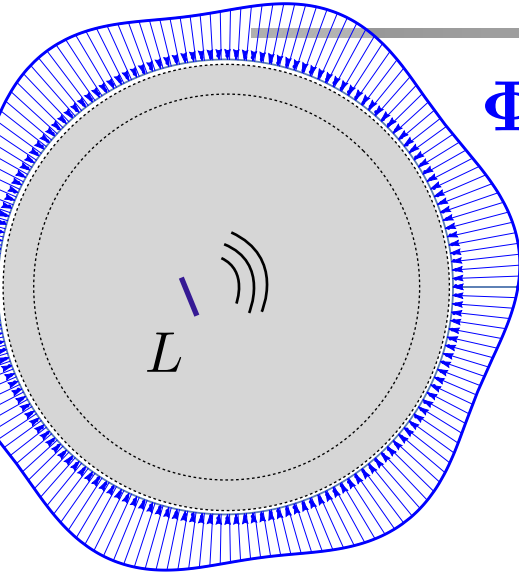
$$\mathcal{I}_{\text{LSM}} = 1/\|\mathbf{g}\|_{L^2(\Omega_d)}^2$$

GLSM

$$\mathcal{I}_{\text{GLSM}} = 1/\sqrt{\delta \|\mathbf{g}\|^2 + |(F_\sharp^\delta \mathbf{g}, \mathbf{g})|}$$

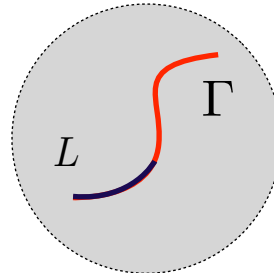
Main Theorem

$$F \mathbf{g} = \Phi_L^\infty(\hat{\xi})$$



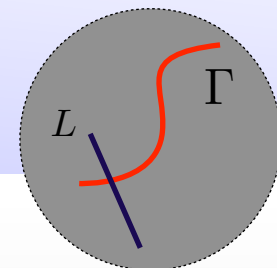
dense range $\xrightarrow{} F = \mathcal{H}^* T \mathcal{H}$ coercive
 $\xrightarrow{} \text{compact}$

$$\begin{aligned} L \subset \Gamma &\rightarrow \Phi_L^\infty(\hat{\xi}) \in \text{Range}(\mathcal{H}^*) \\ L \not\subset \Gamma &\rightarrow \Phi_L^\infty(\hat{\xi}) \notin \text{Range}(\mathcal{H}^*) \end{aligned}$$



$$\limsup_{\alpha \rightarrow 0} \|\mathcal{H} \mathbf{g}\|_{H^{-\frac{1}{2}}(\Gamma)} < \infty \quad L \subset \Gamma$$

$$\lim_{\alpha \rightarrow 0} \|\mathcal{H} \mathbf{g}\|_{H^{-\frac{1}{2}}(\Gamma)} = \infty \quad L \not\subset \Gamma$$



$$J_\alpha = \|F^\delta \mathbf{g} - \Phi_L^\infty\|^2 + \alpha \|\mathbf{g}\|^2$$

LSM

$$\mathcal{I}_{\text{LSM}} = 1/\|\mathbf{g}\|_{L^2(\Omega_d)}^2$$

indicator functionals

$$\begin{aligned} J_\alpha^\delta &= \alpha(|(F_\sharp^\delta \mathbf{g}, \mathbf{g})| + \delta \|\mathbf{g}\|^2) + \\ &\quad \|F^\delta \mathbf{g} - \Phi_L^\infty\|^2 \end{aligned}$$

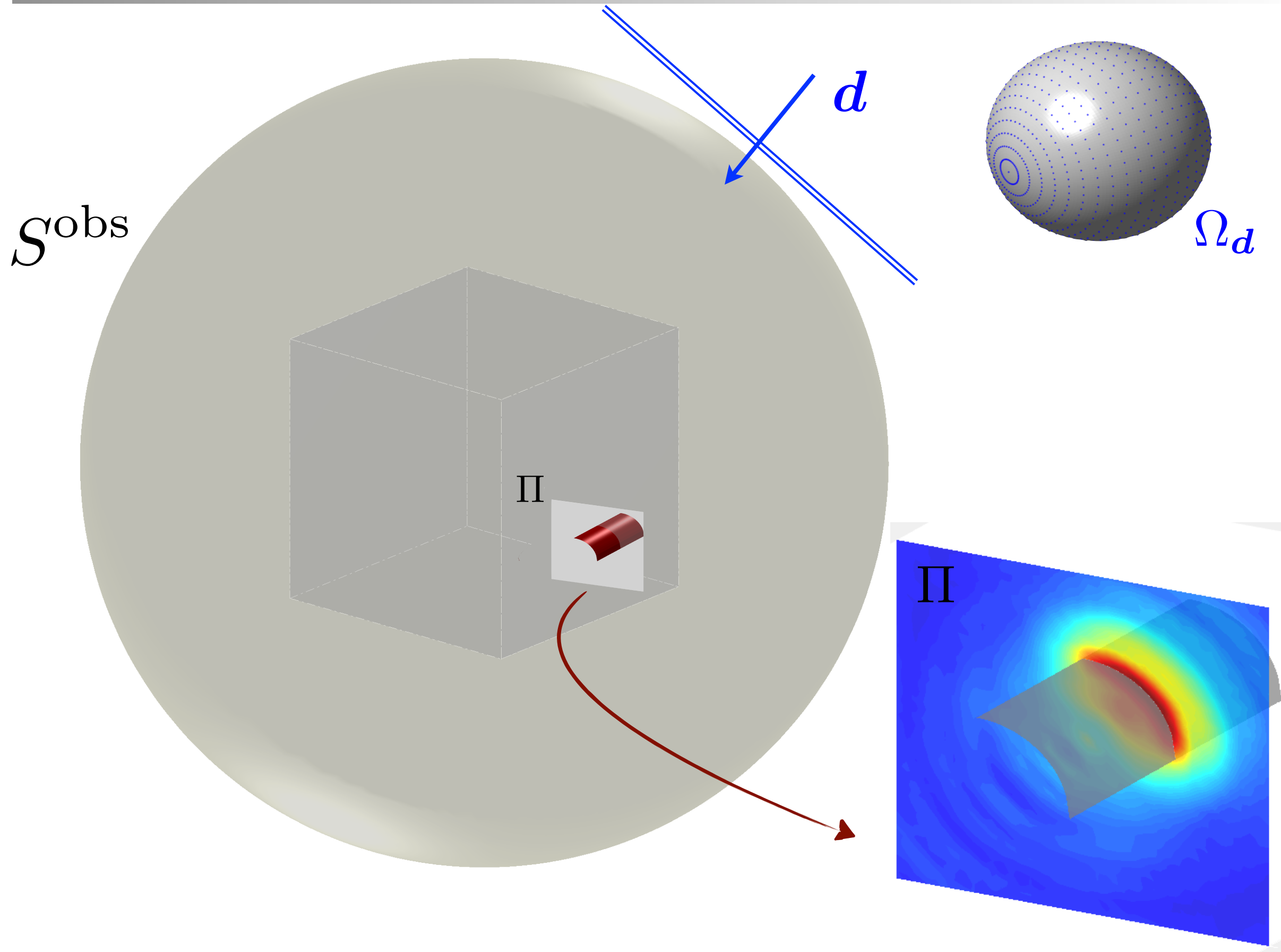
GLSM

$$\mathcal{I}_{\text{GLSM}} = 1/\sqrt{\delta \|\mathbf{g}\|^2 + |(F_\sharp^\delta \mathbf{g}, \mathbf{g})|}$$

GLSM^{opt}

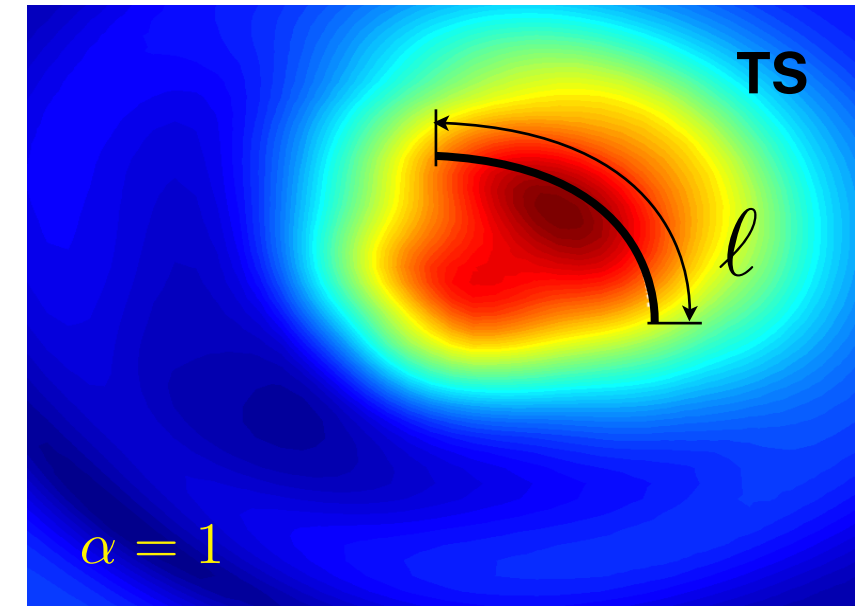
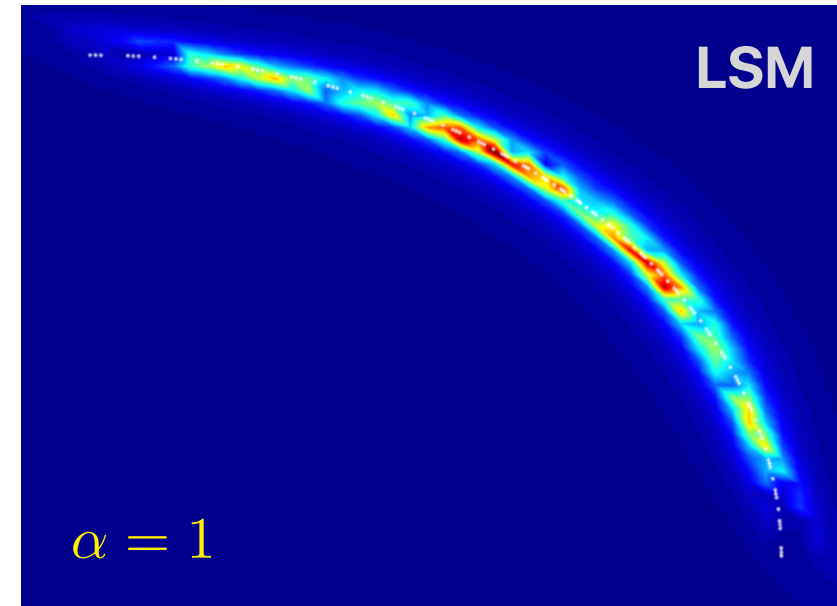
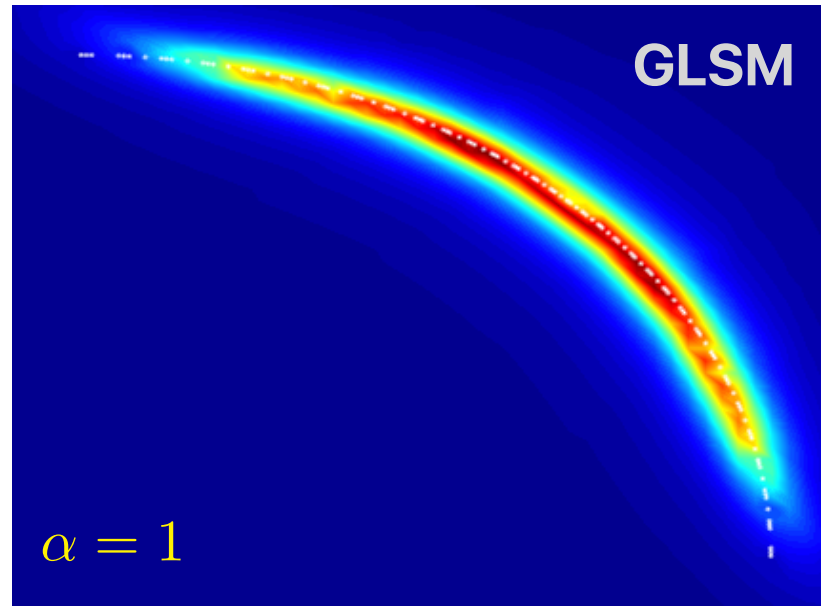
$$\mathcal{I}_{\text{GLSM}} = 1/\sqrt{\delta \|\mathbf{g}\|^2 + |(F_\sharp^\delta \mathbf{g}, \mathbf{g})|}$$

Numerical results



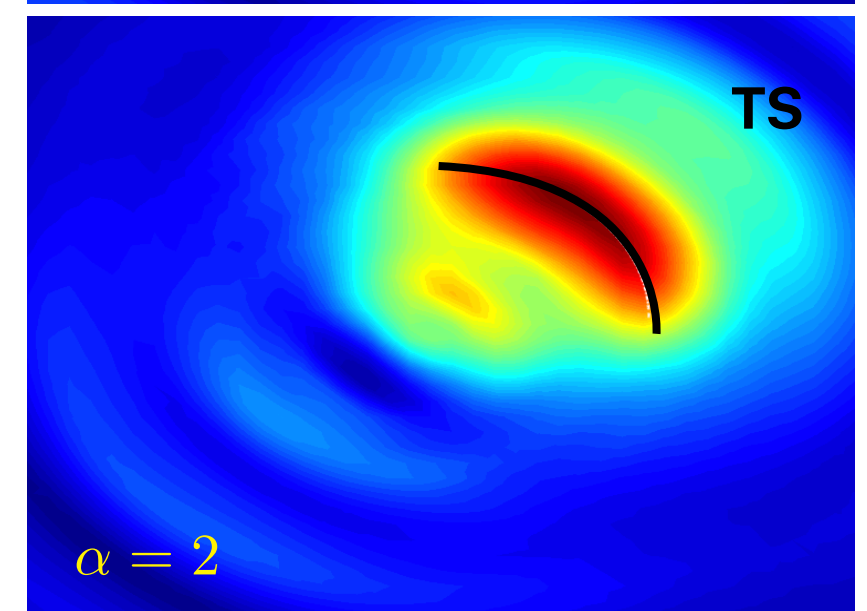
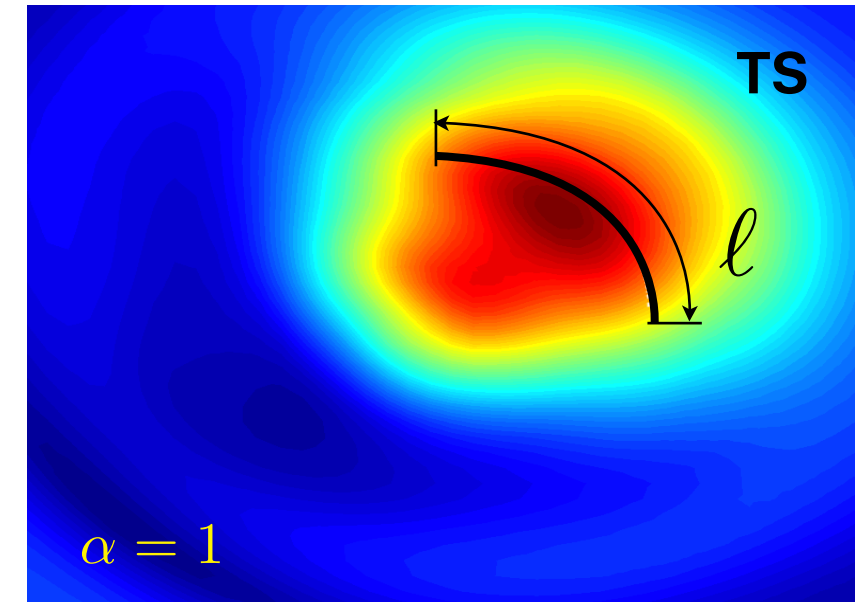
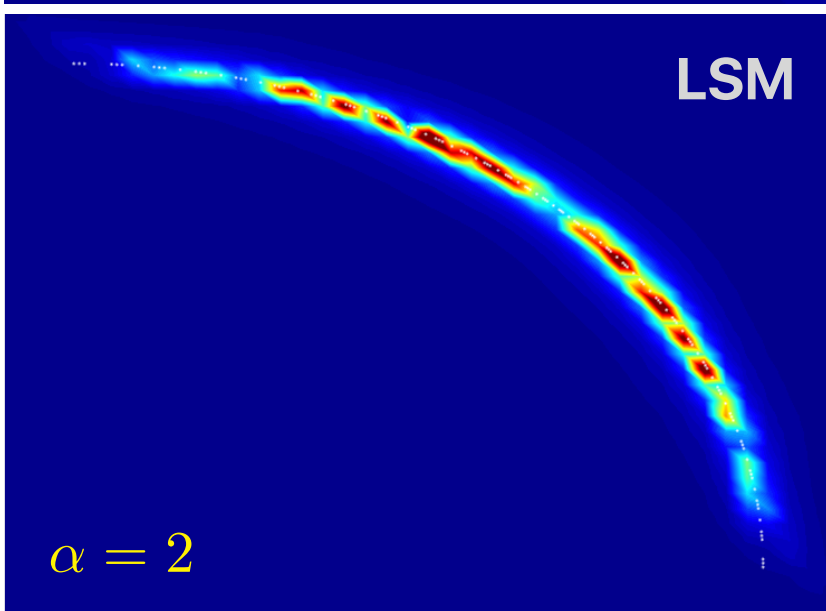
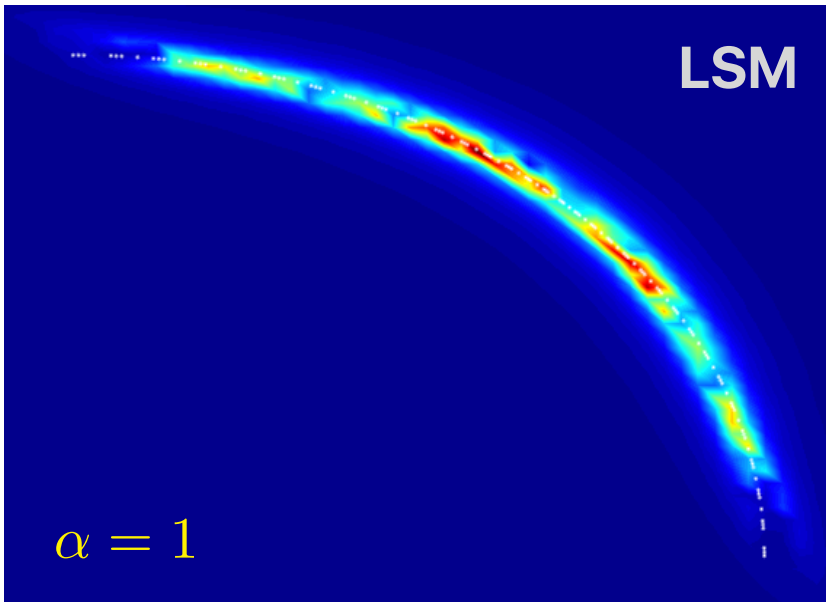
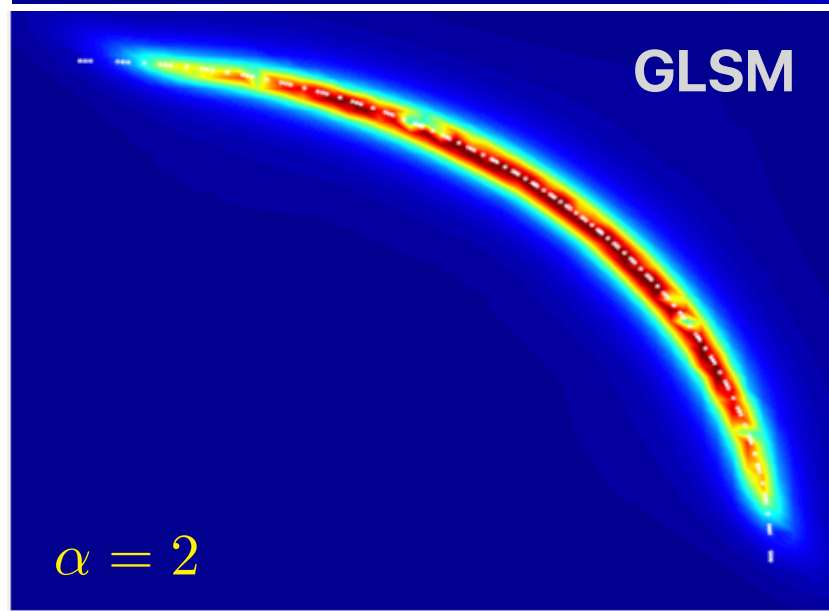
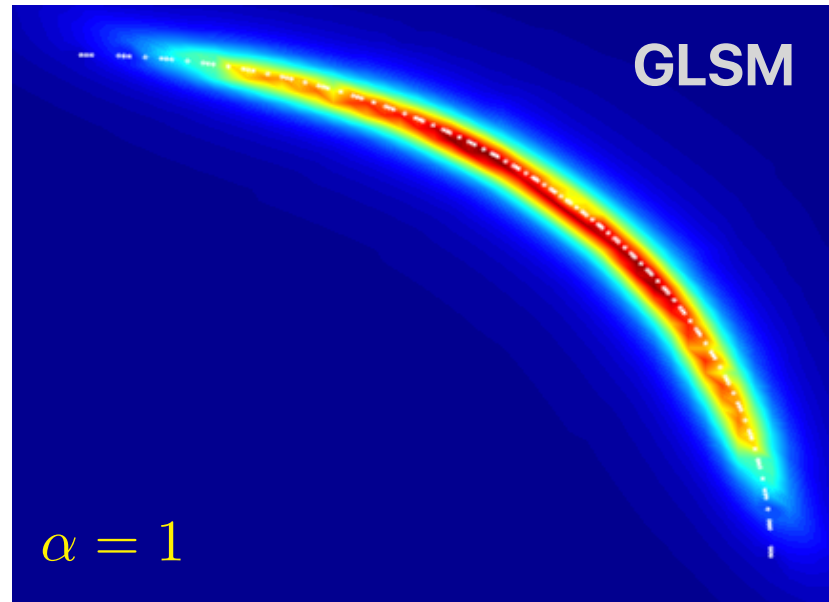
Mid-plane reconstruction

$$\alpha = \ell/\lambda$$



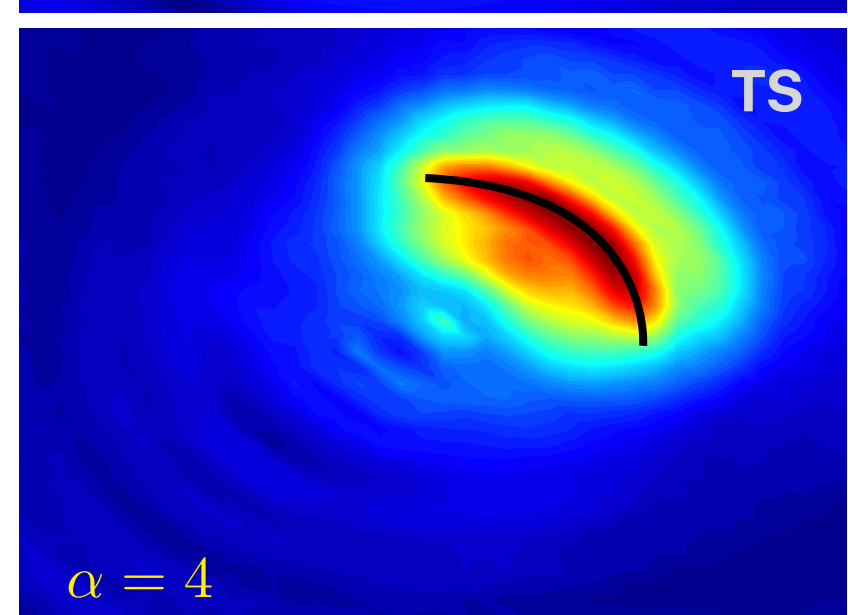
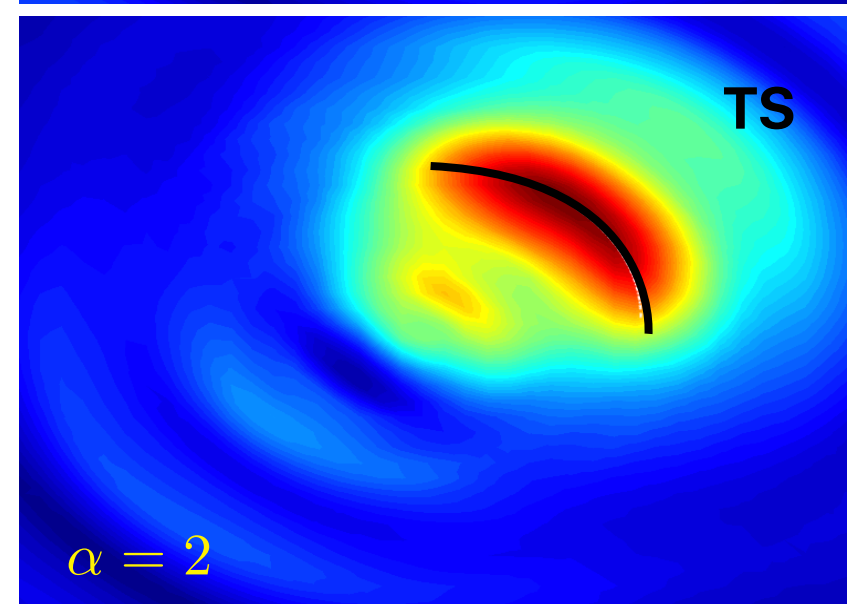
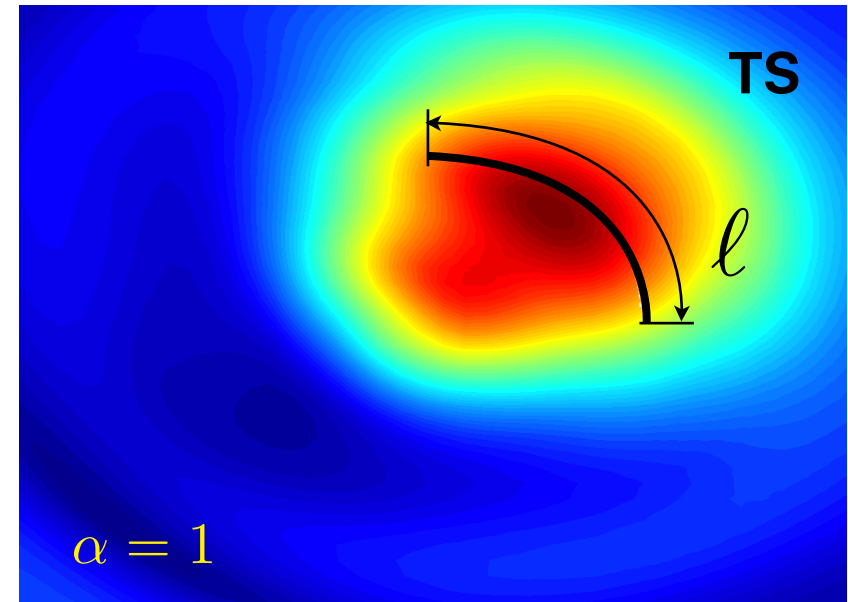
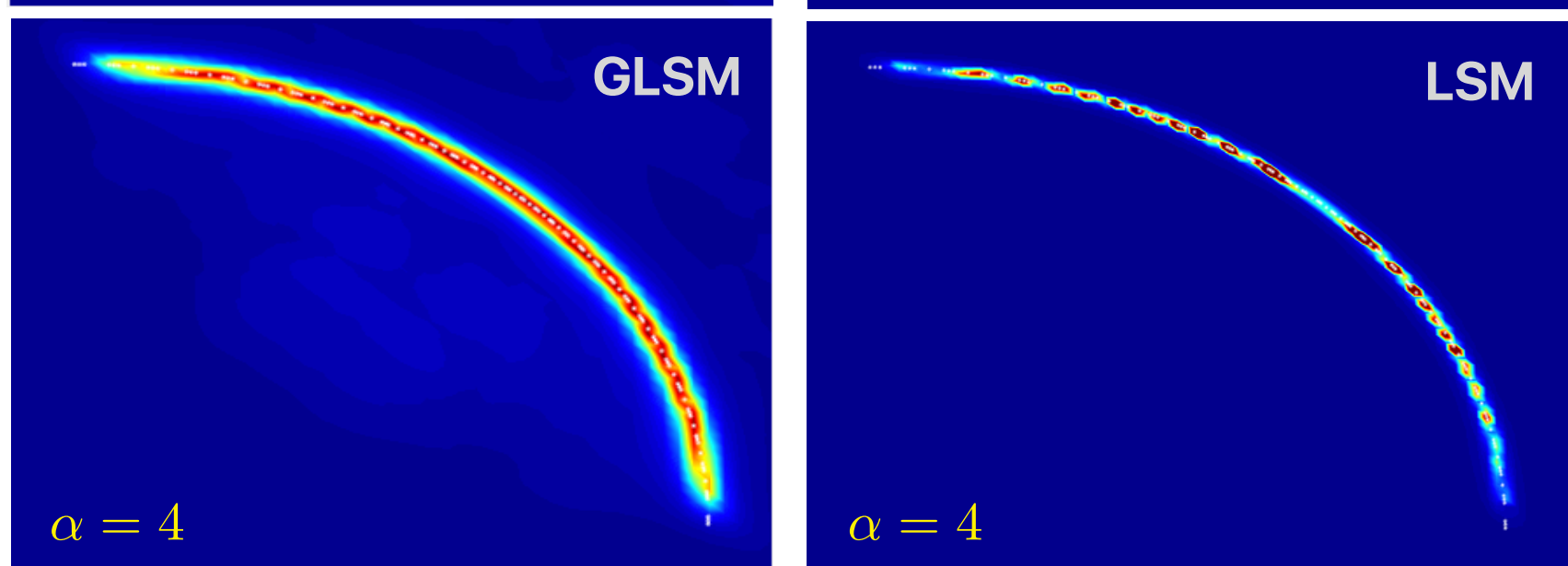
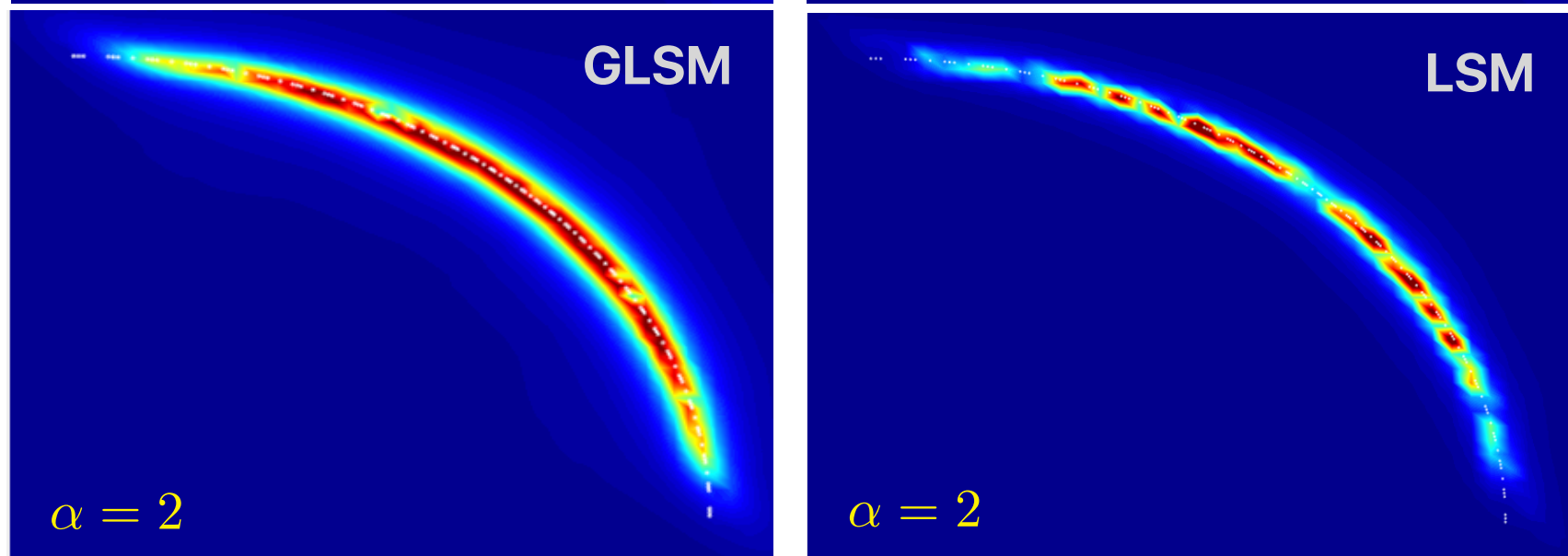
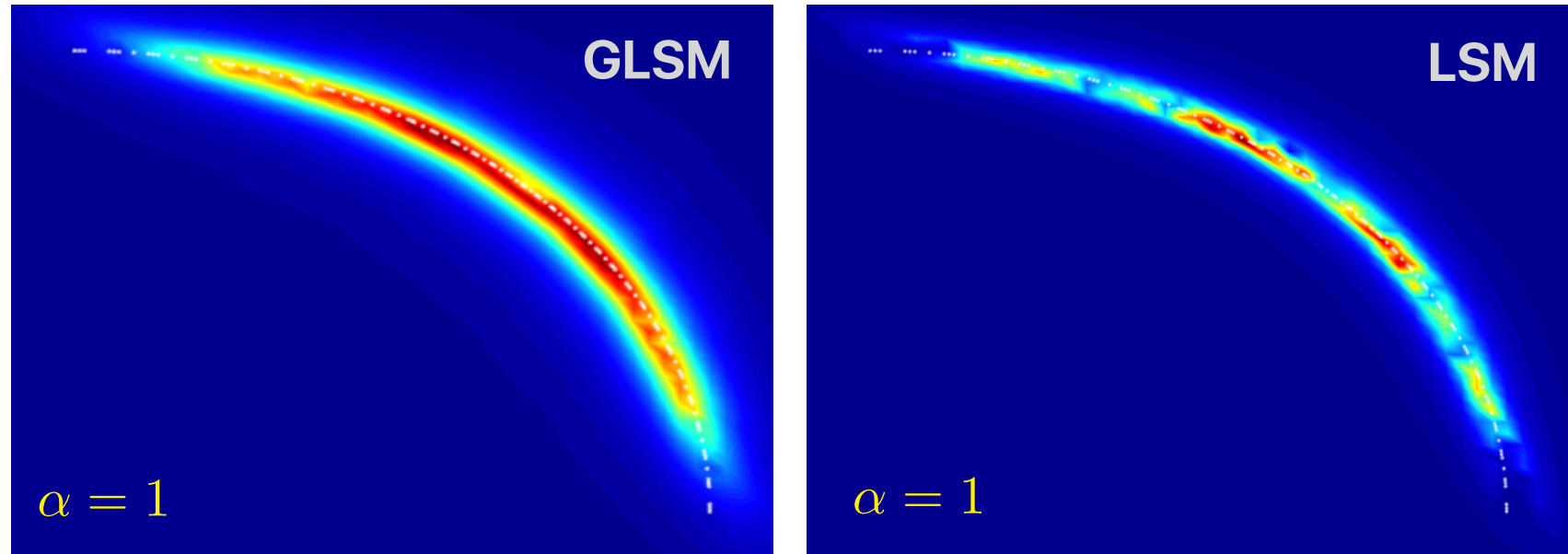
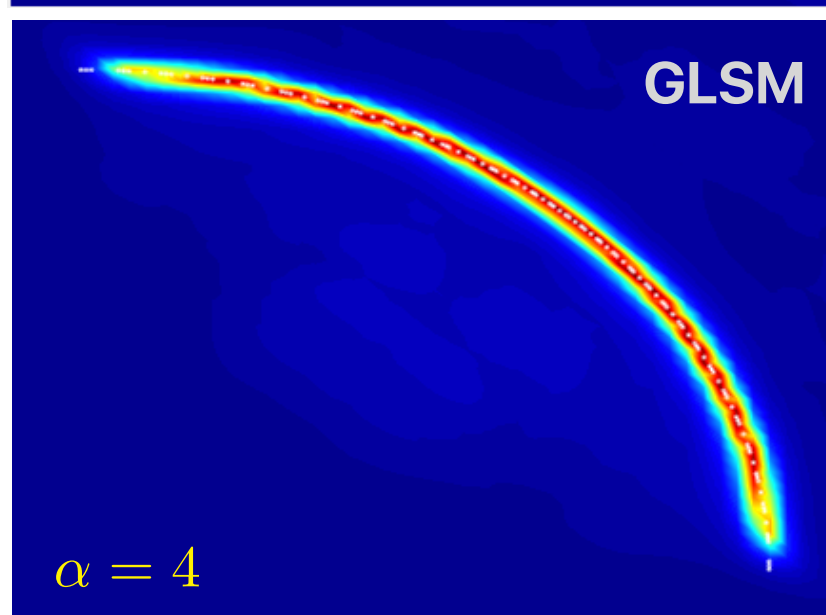
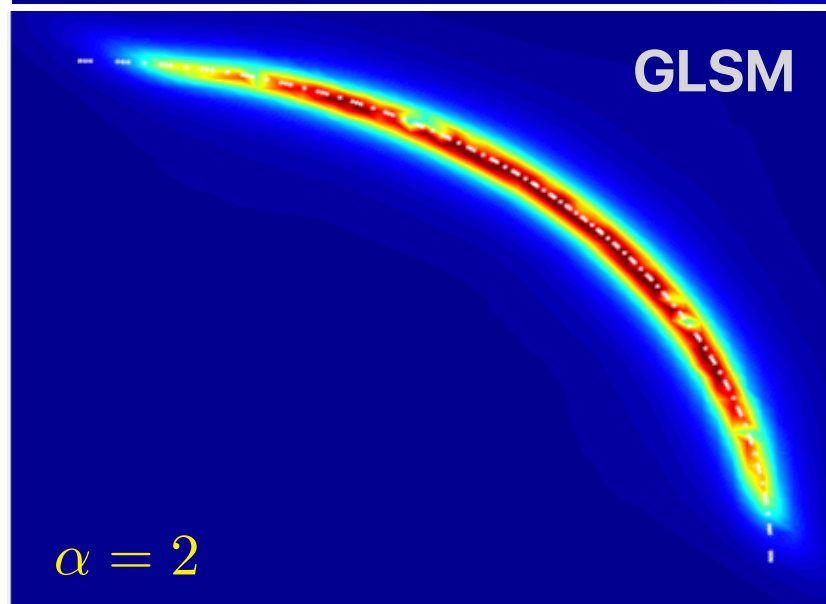
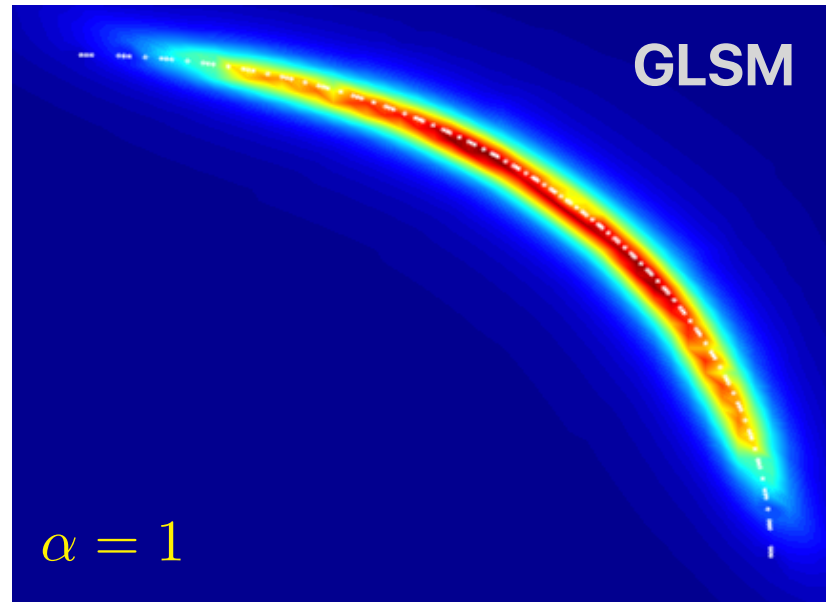
Mid-plane reconstruction

$$\alpha = \ell/\lambda$$



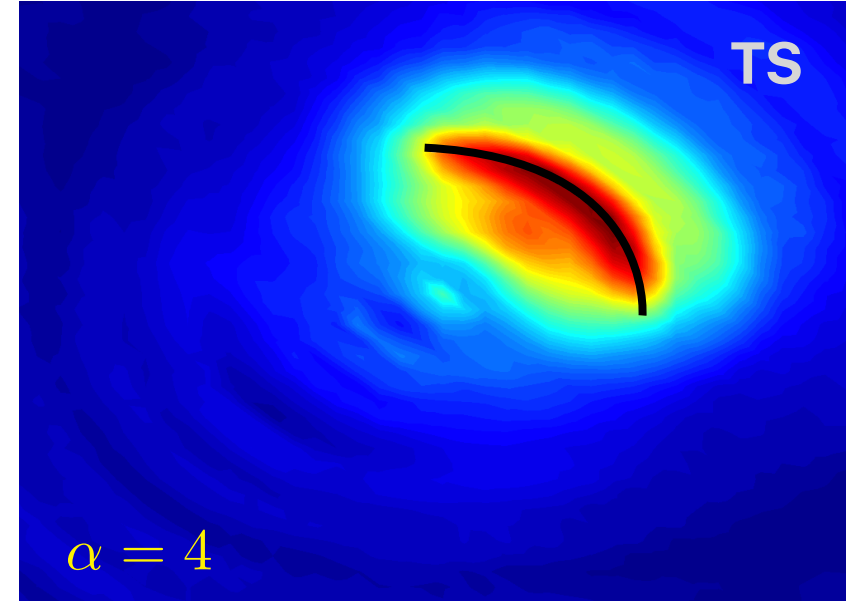
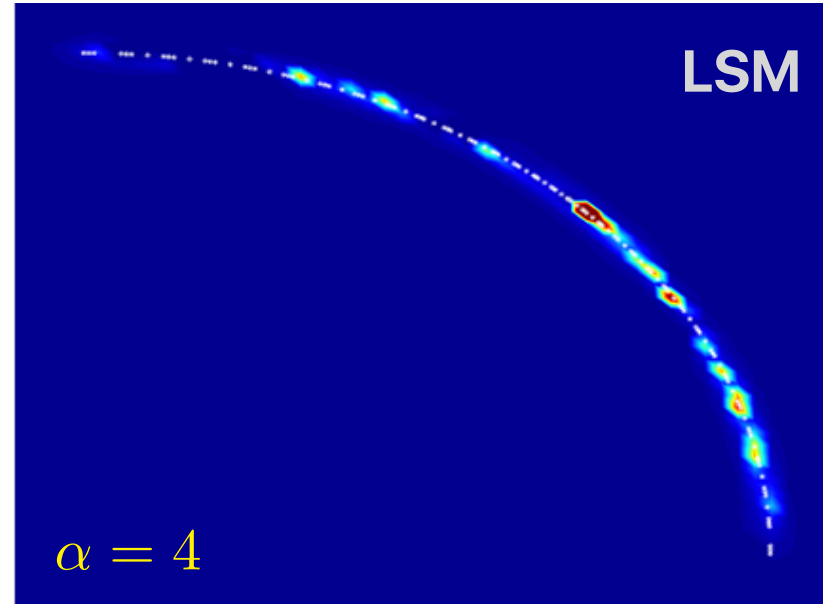
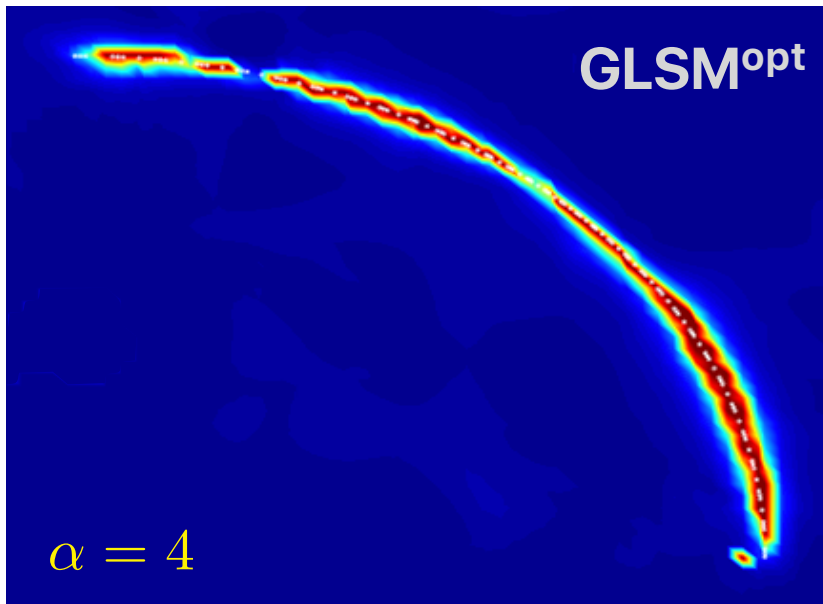
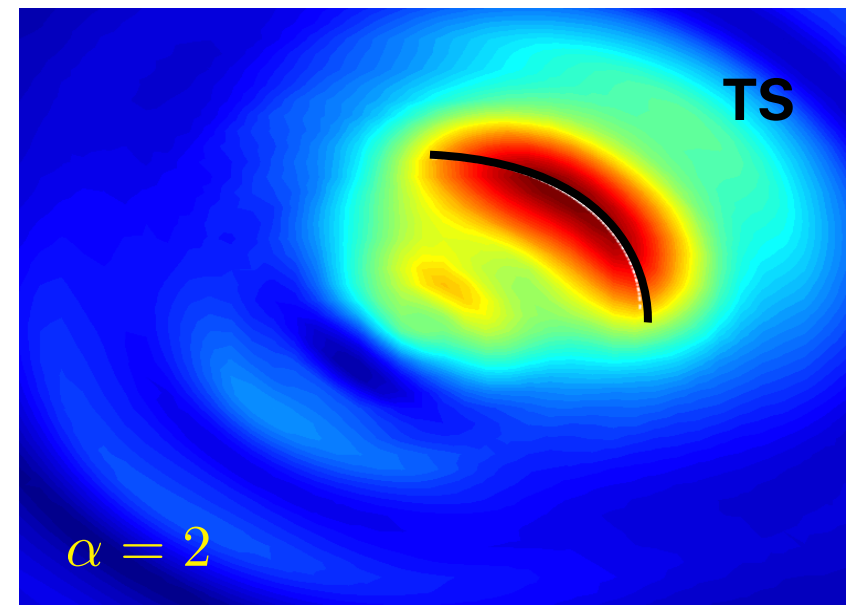
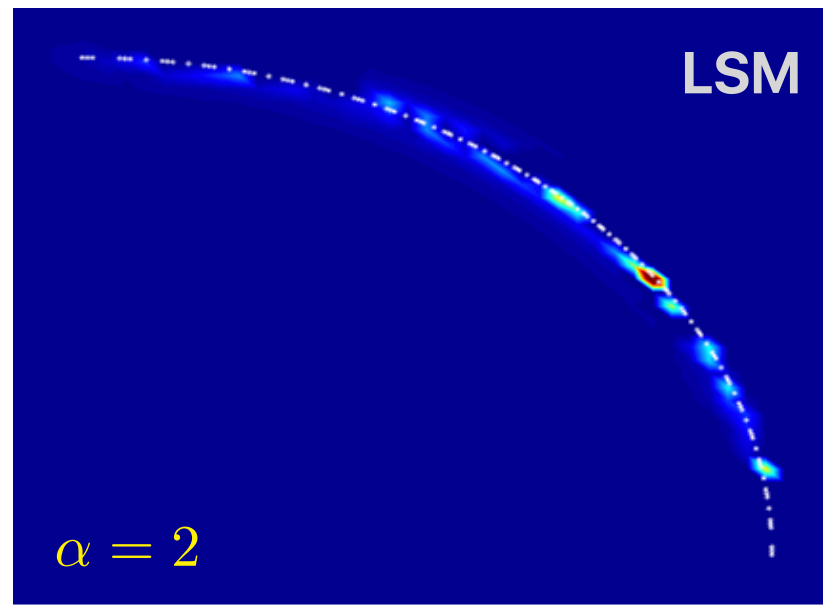
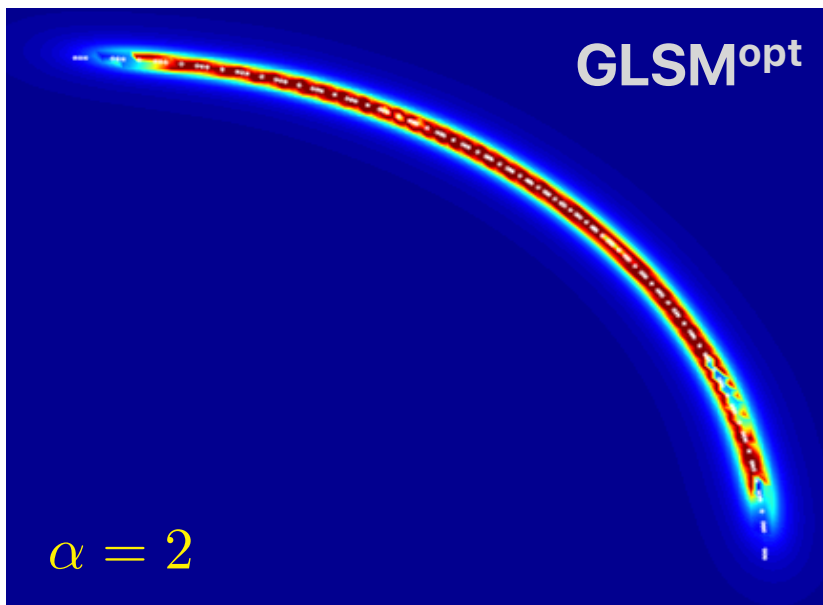
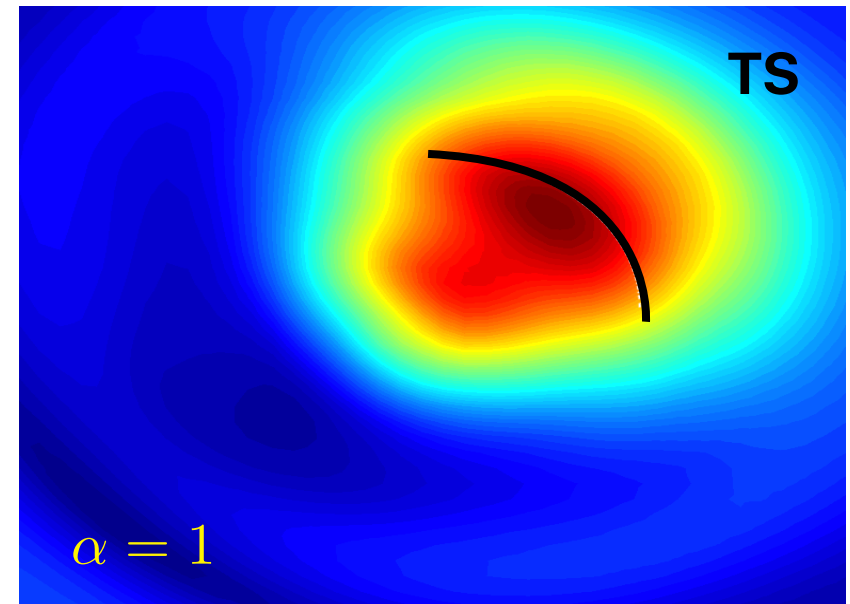
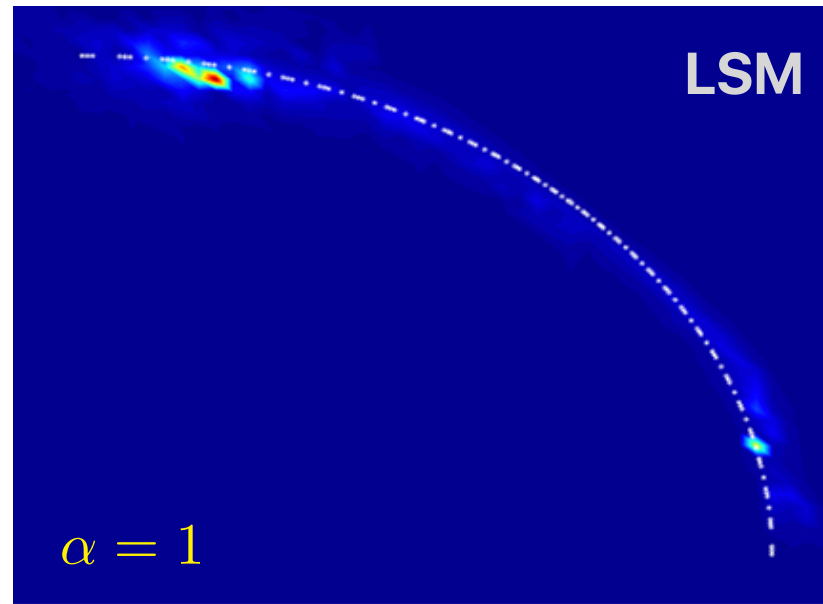
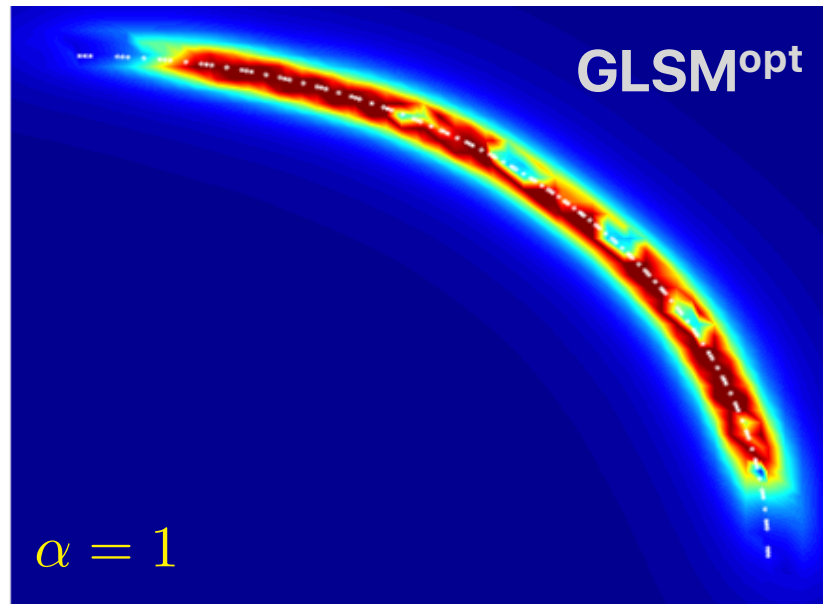
Mid-plane reconstruction

$$\alpha = \ell/\lambda$$

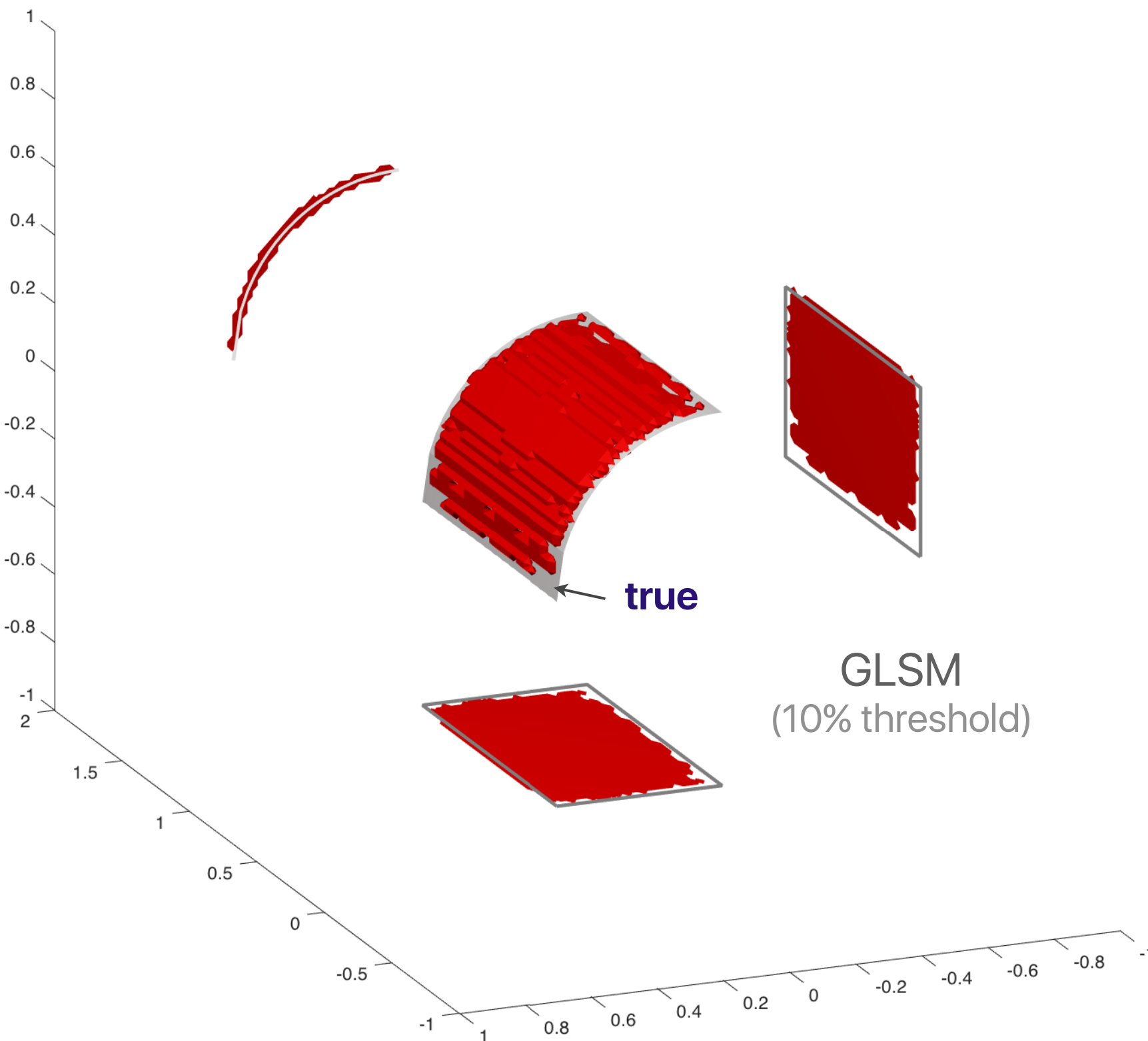
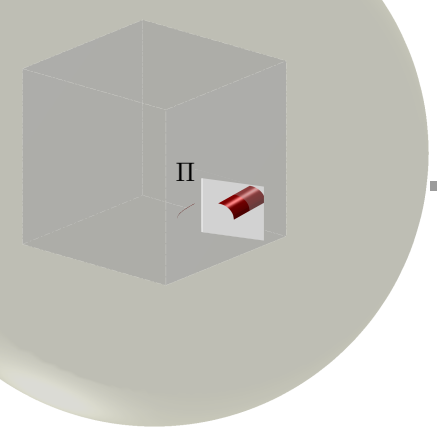


5% noise

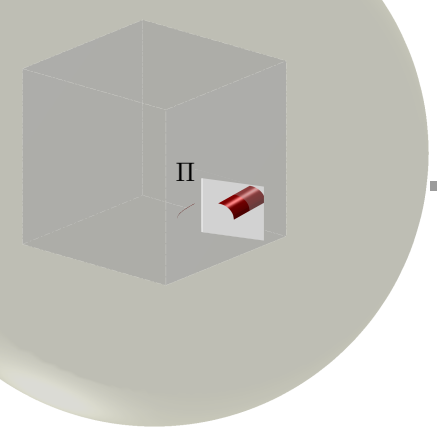
$$\alpha = \ell/\lambda$$



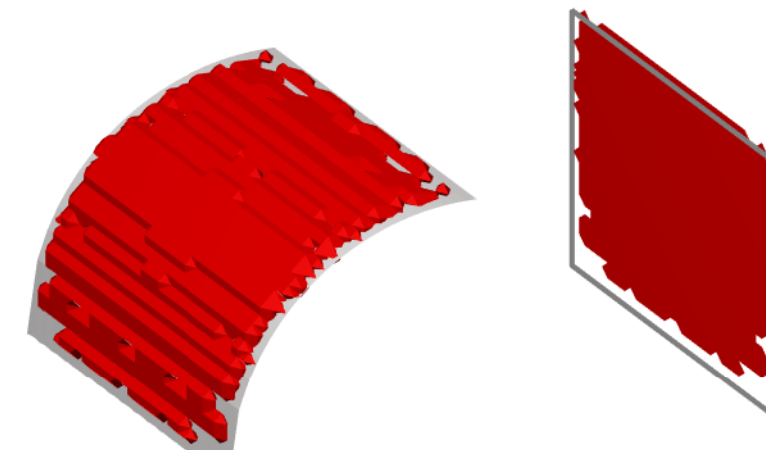
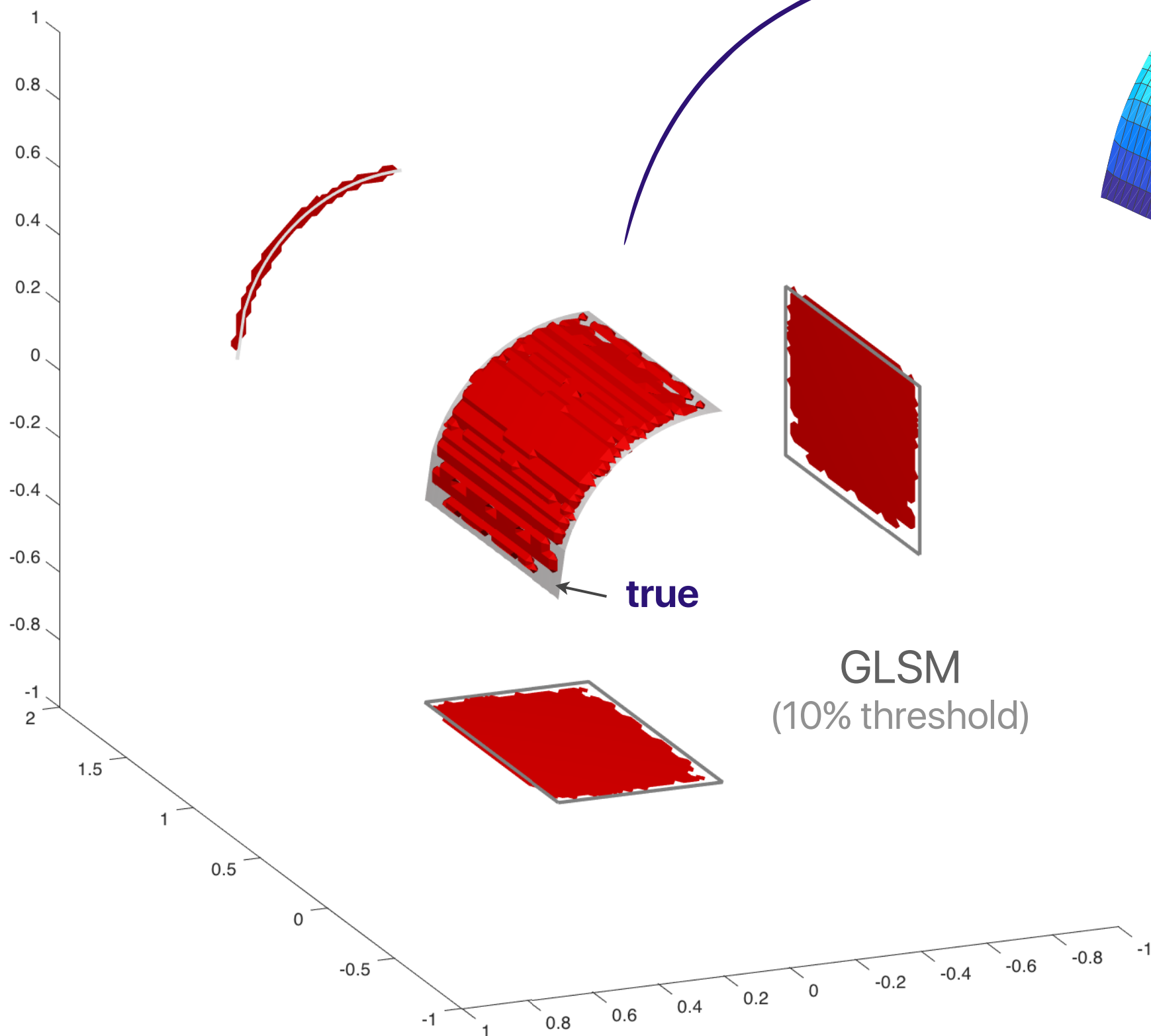
3D Reconstruction



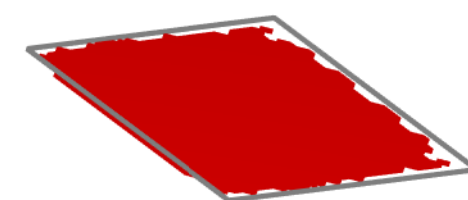
3D Reconstruction



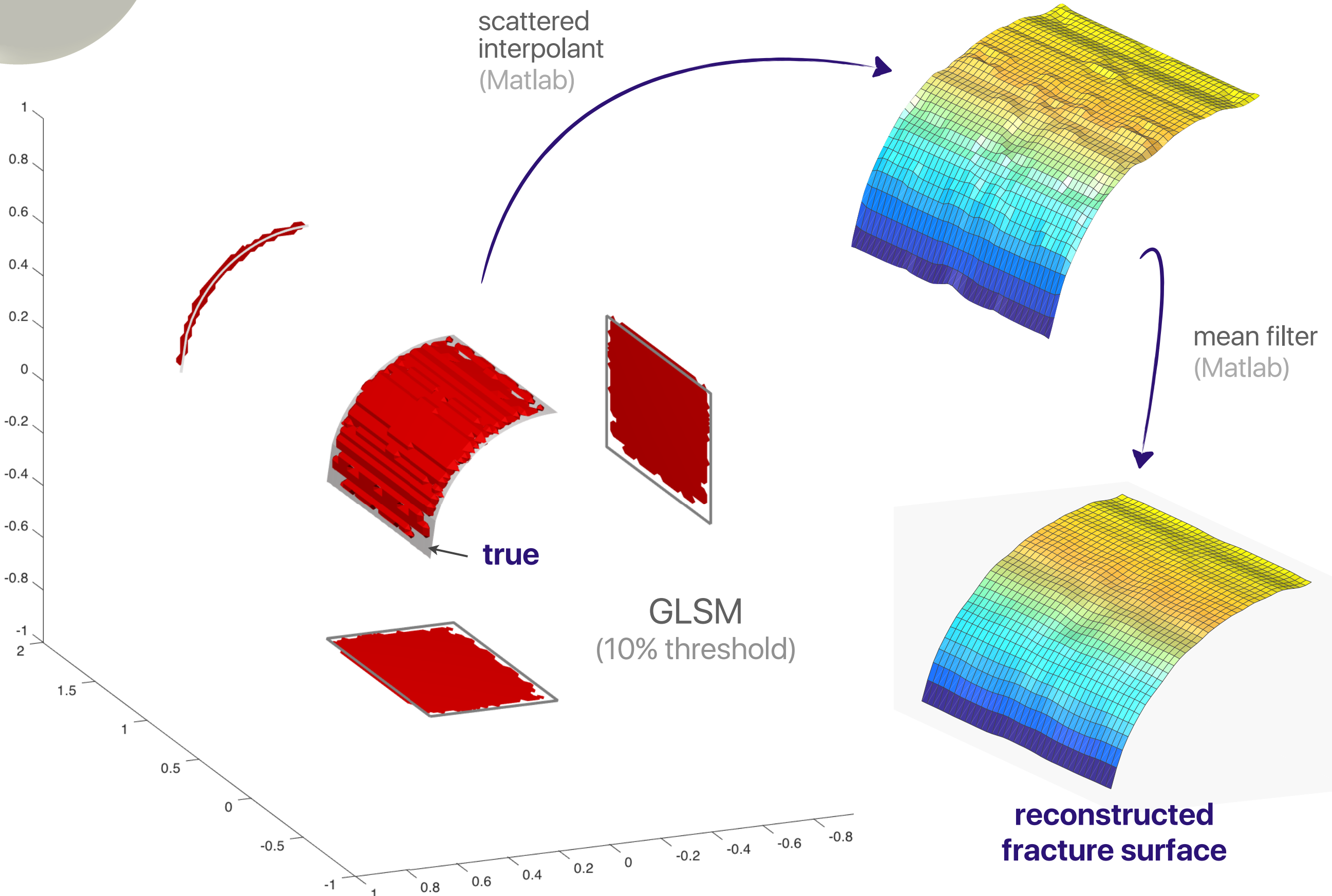
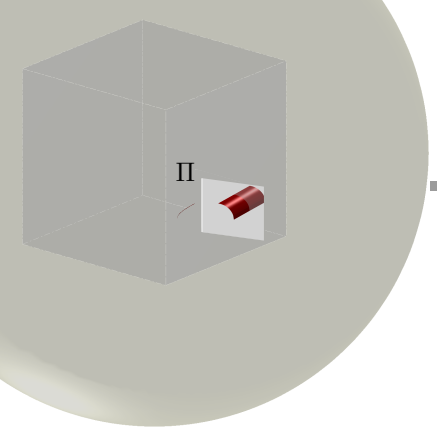
scattered
interpolant
(Matlab)

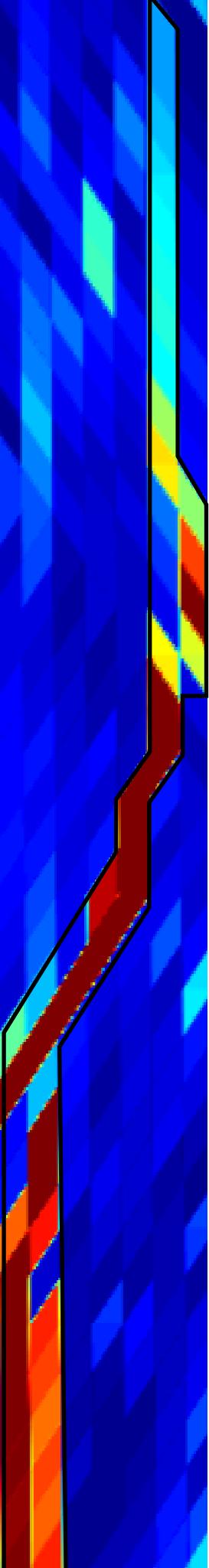


GLSM
(10% threshold)



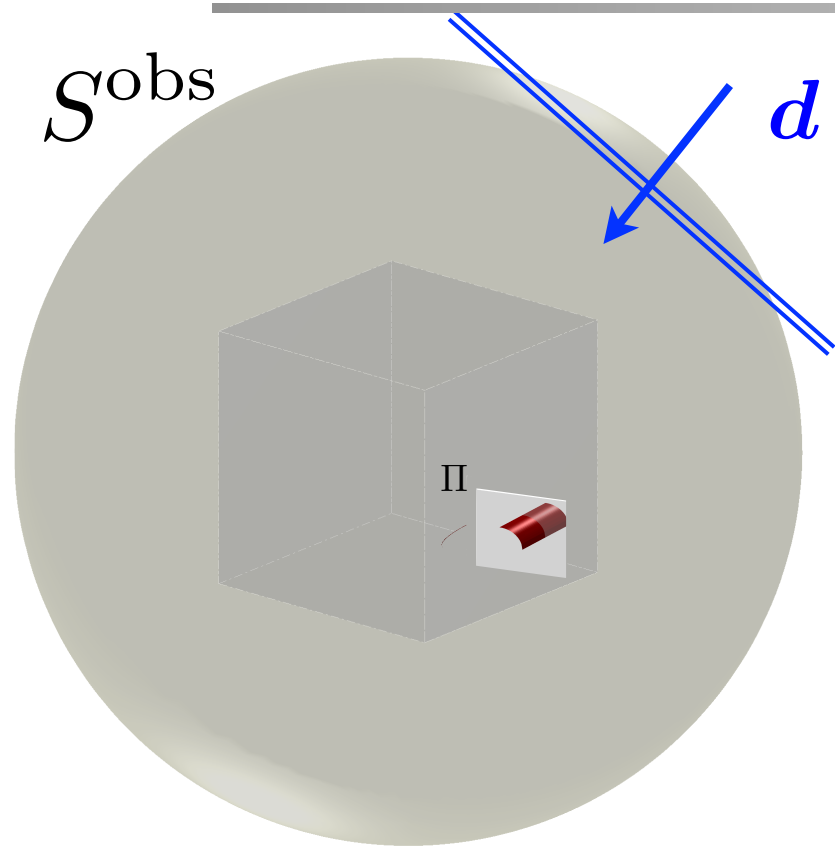
3D Reconstruction



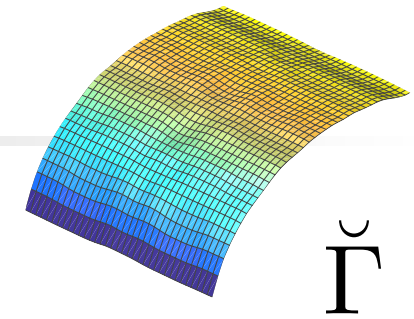


Characterization of the fracture heterogeneous interface

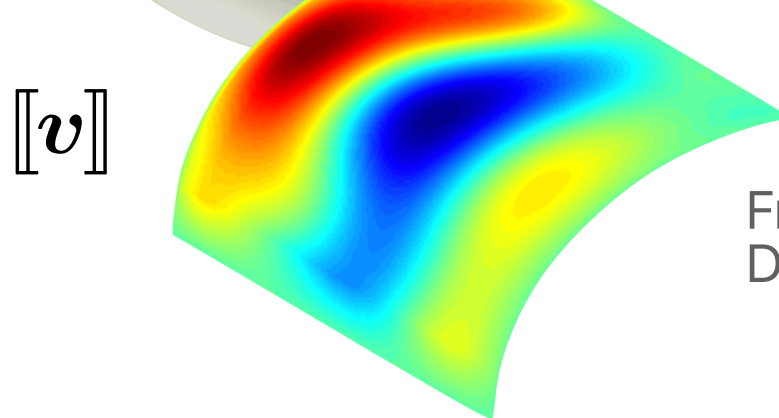
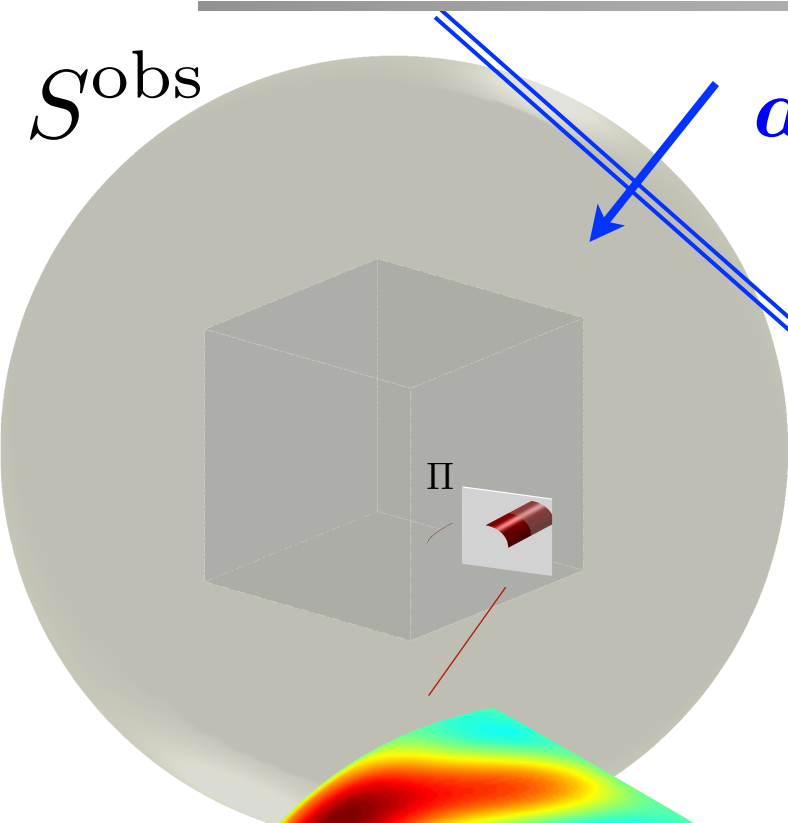
FOD Reconstruction



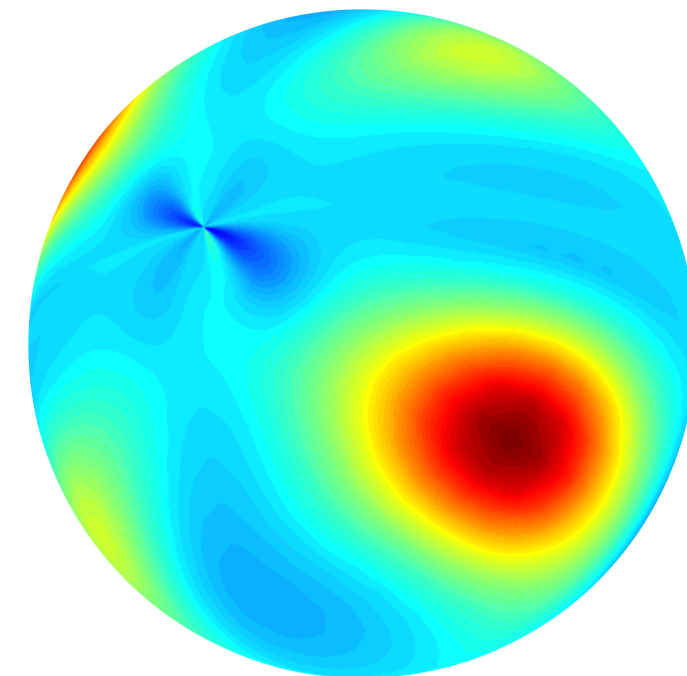
recovered
fracture surface



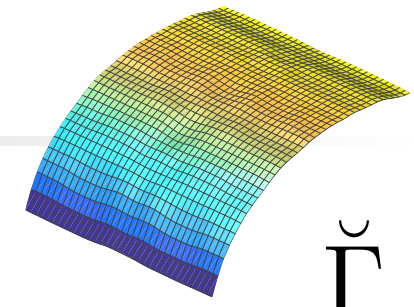
FOD Reconstruction



Fracture Opening
Displacement profile

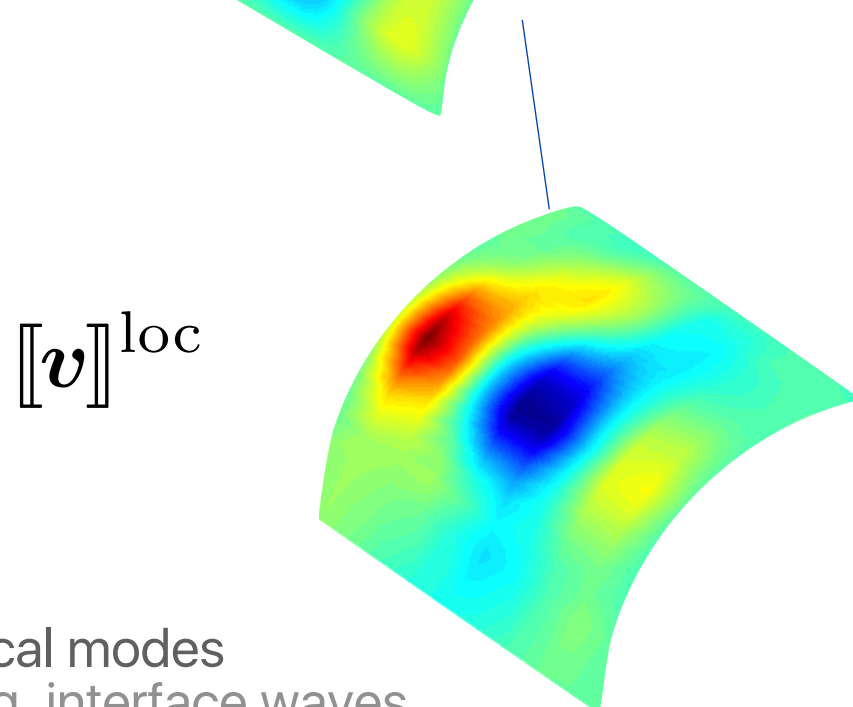
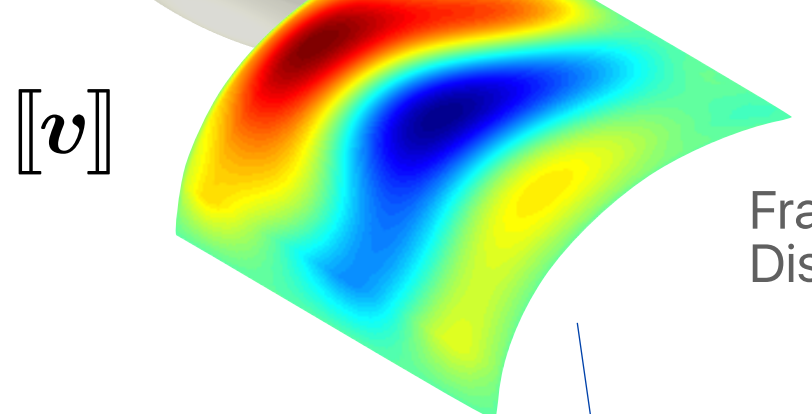
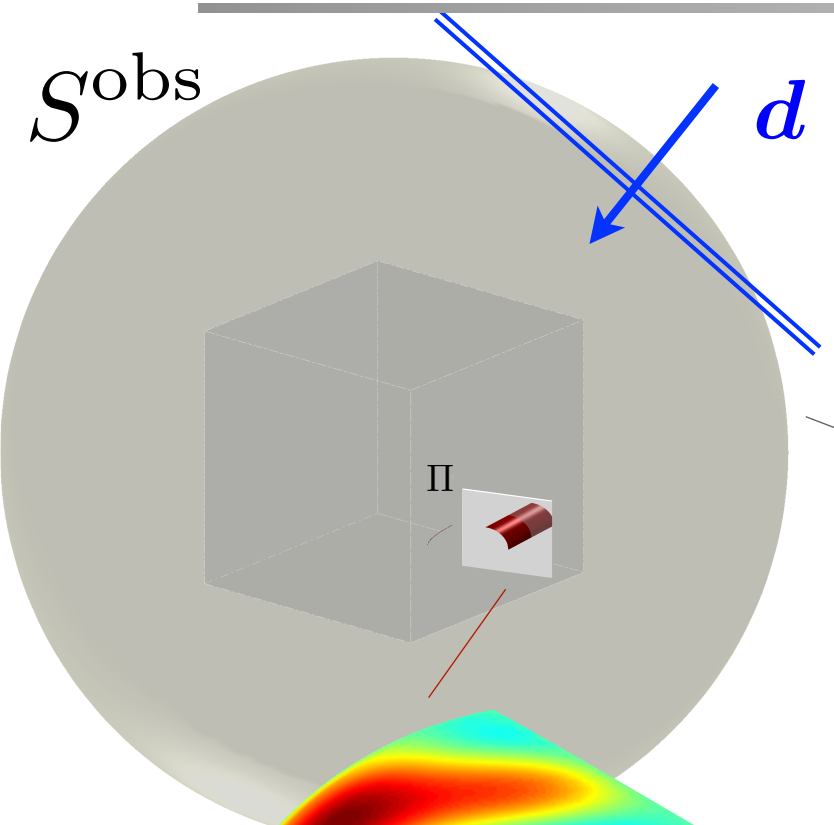


recovered
fracture surface

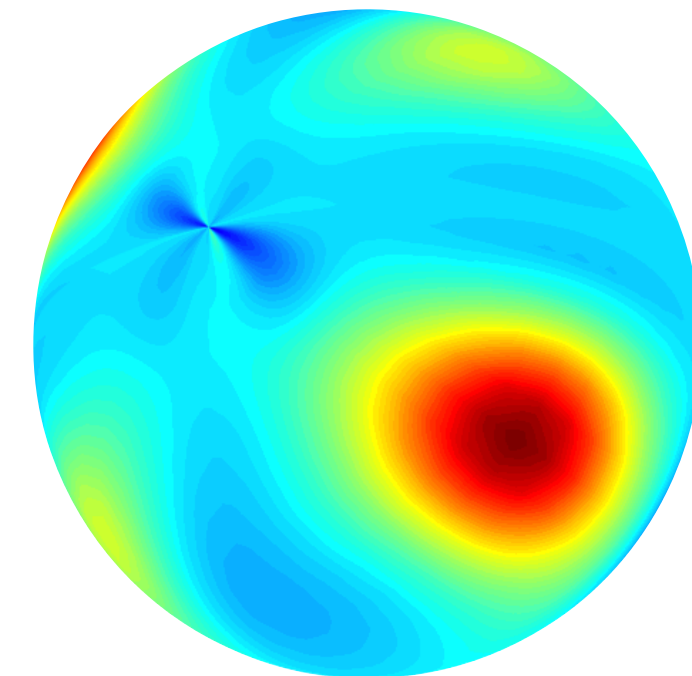


far-field pattern
of the scattered wavefield

FOD Reconstruction

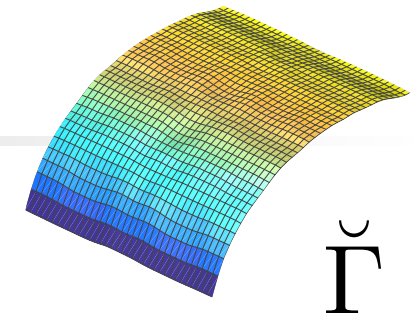


local modes
e.g. interface waves



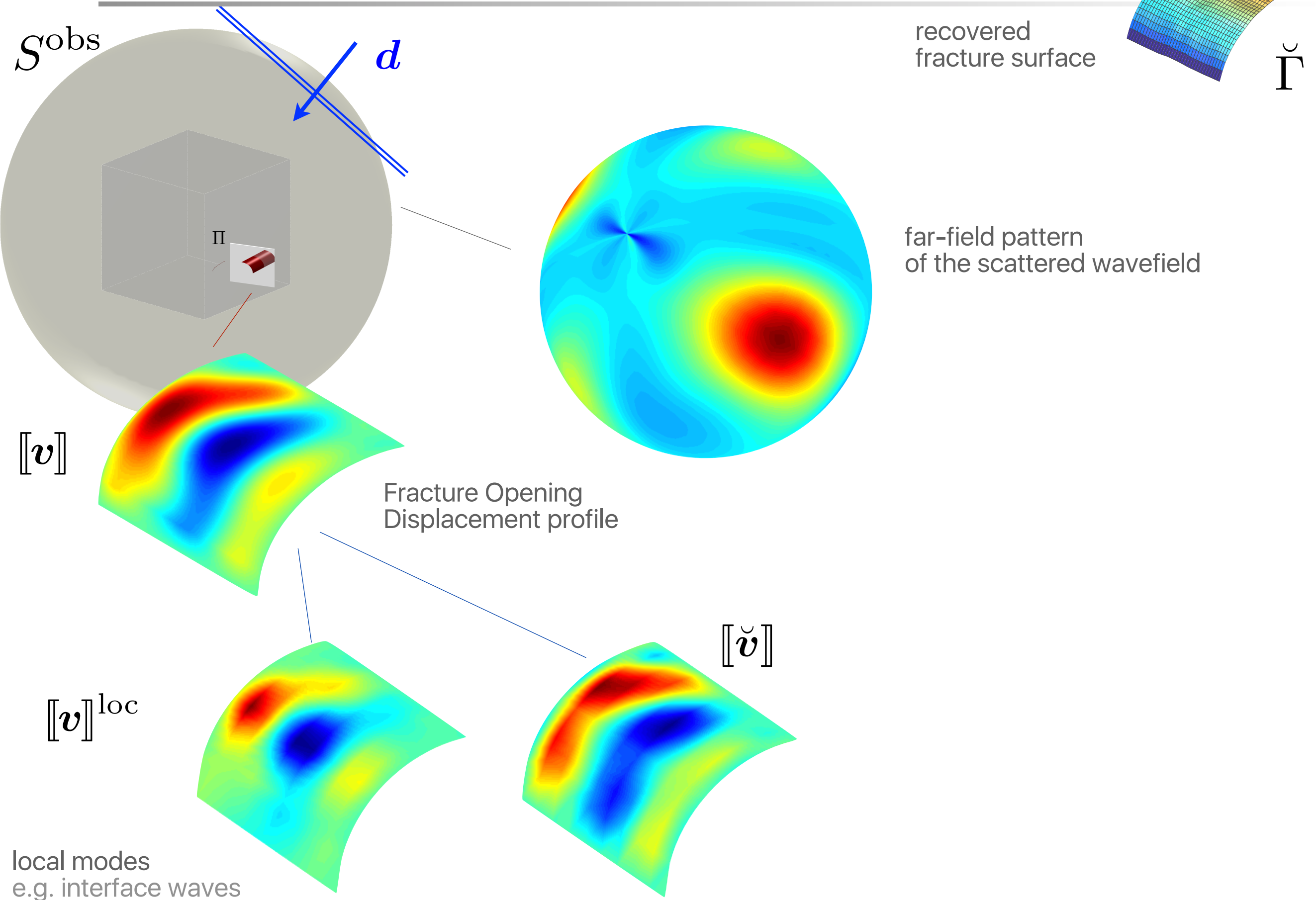
Fracture Opening
Displacement profile

recovered
fracture surface

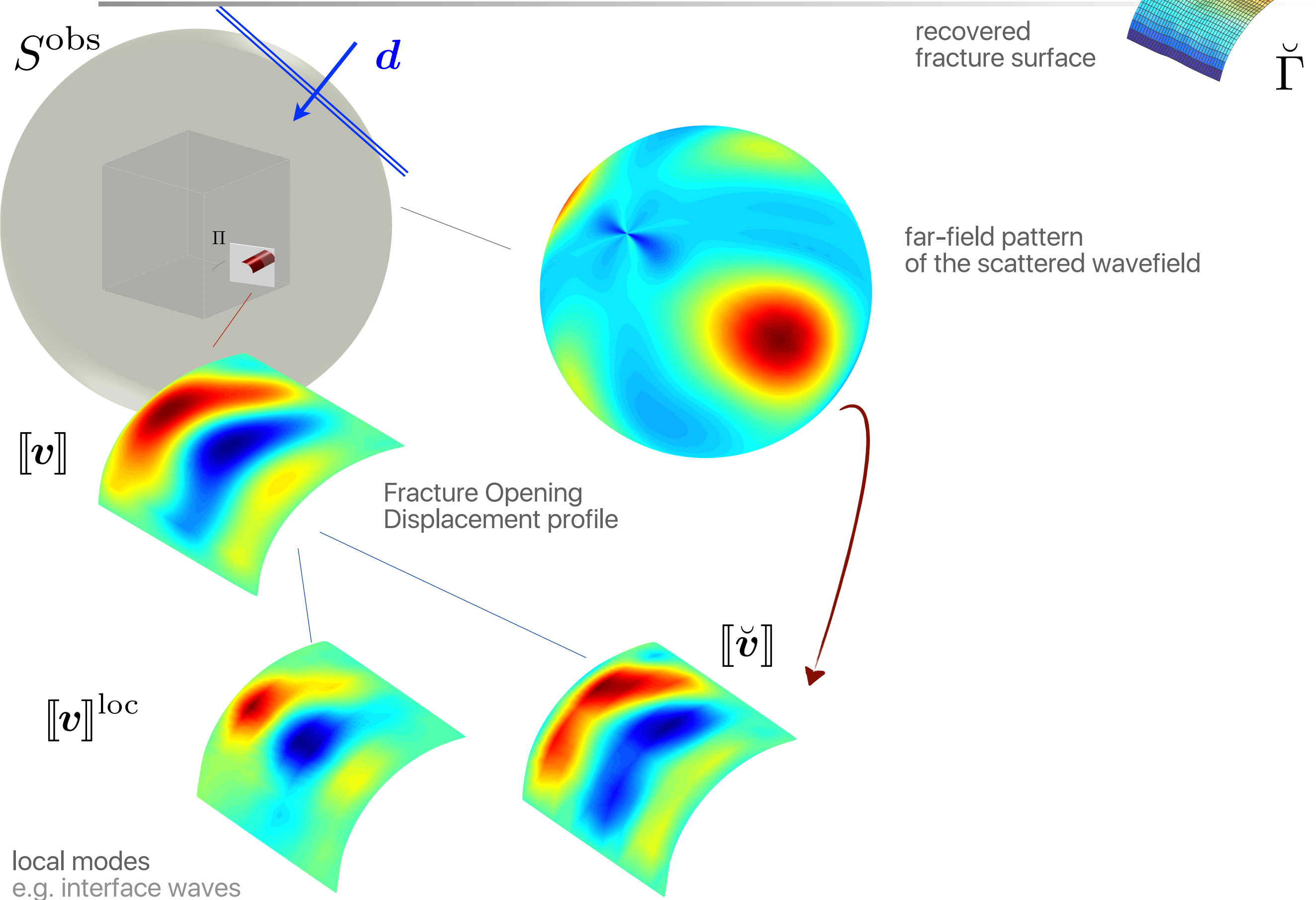


far-field pattern
of the scattered wavefield

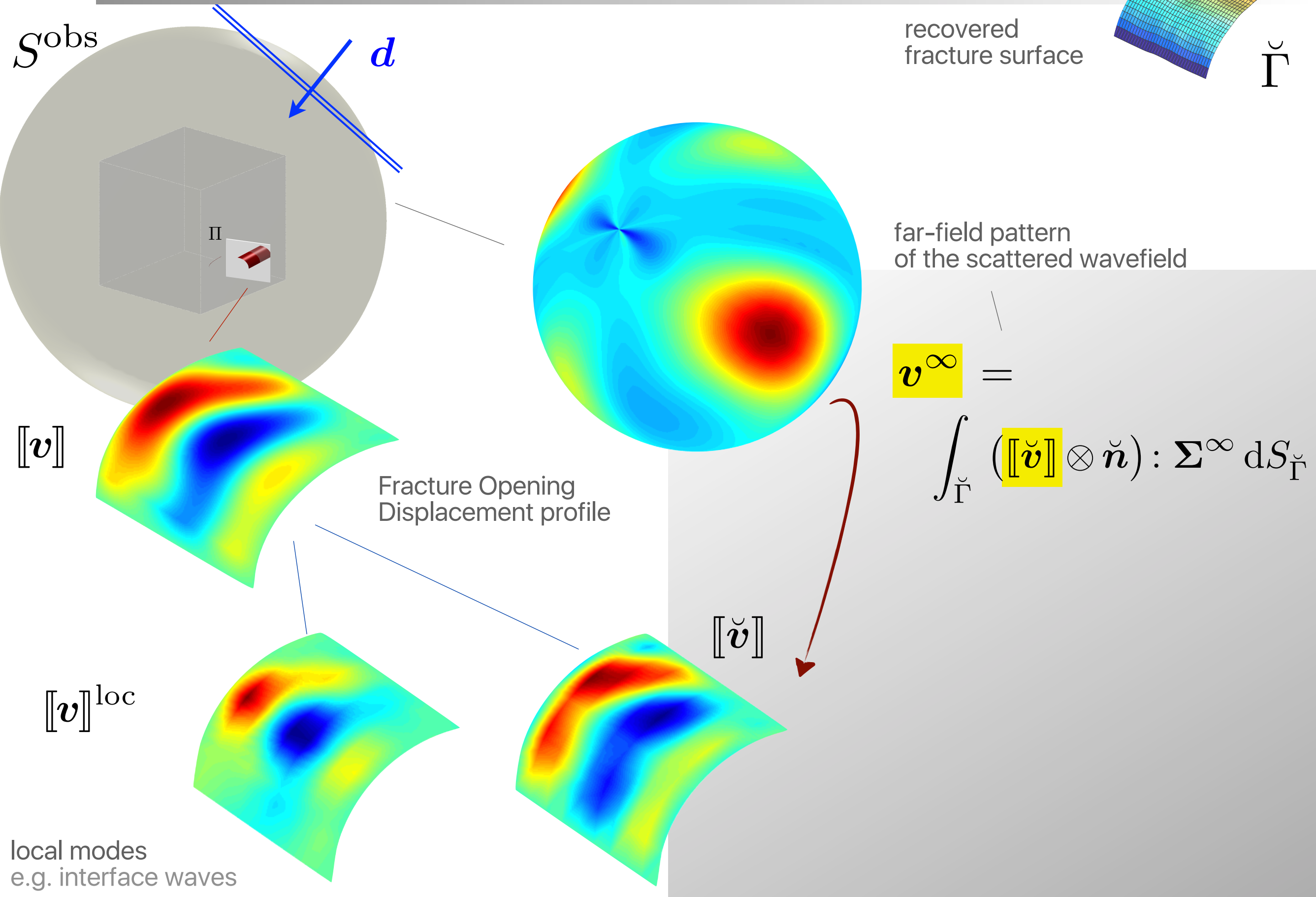
FOD Reconstruction



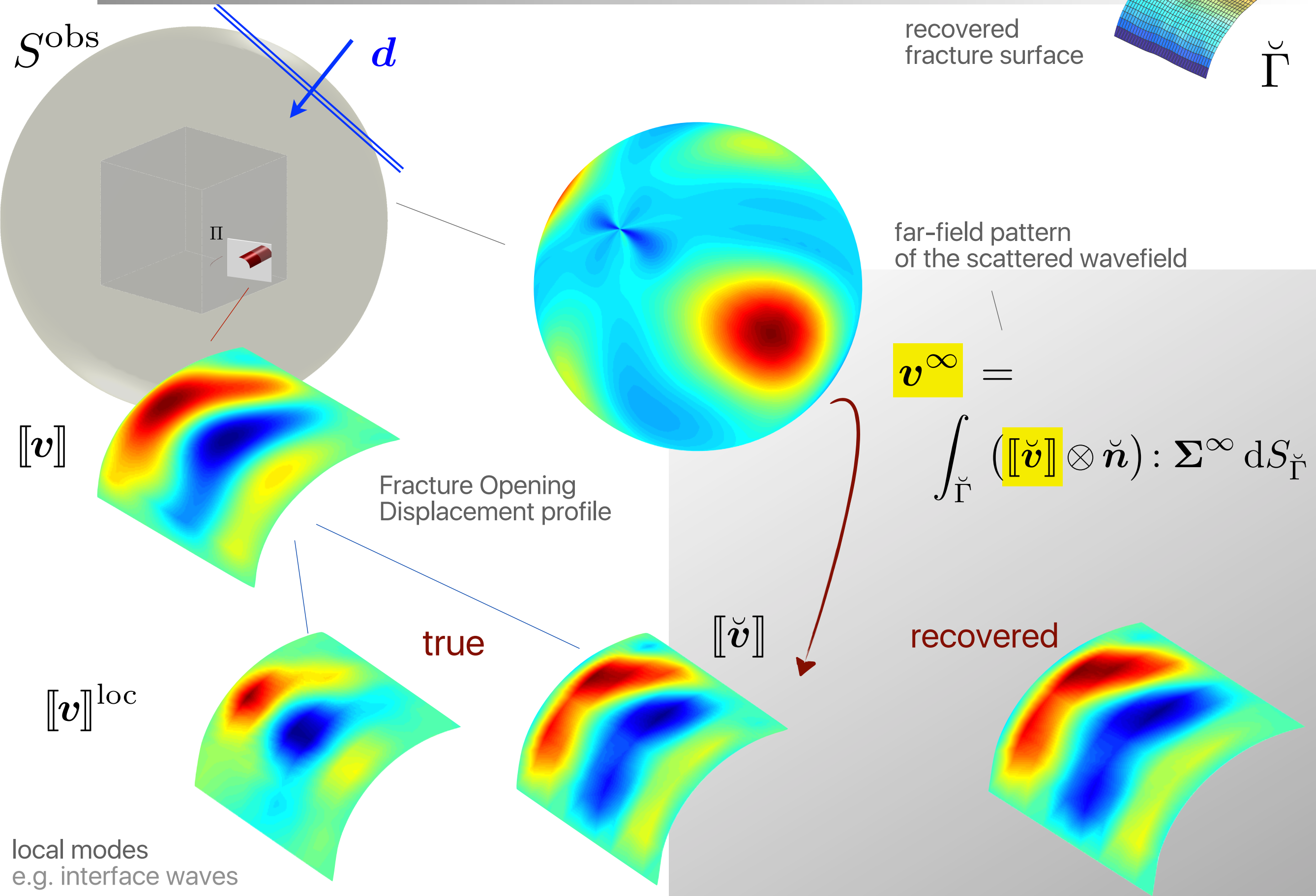
FOD Reconstruction



FOD Reconstruction



FOD Reconstruction



Reconstruction of \mathbf{K}

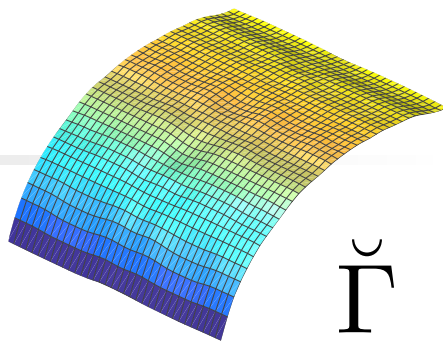
TBIE representation

$$t^i(\xi) - \check{\mathbf{K}} \cdot [\![\tilde{\mathbf{u}}]\!](\xi)$$

free field
traction

$$= \check{\mathbf{n}} \cdot \mathbf{C} : \int_{\check{\Gamma}} \Sigma : D_x [\![\tilde{\mathbf{u}}]\!](x) dS_x - \\ \rho \omega^2 \check{\mathbf{n}} \cdot \mathbf{C} : \int_{\check{\Gamma}} \mathbf{U} \cdot ([\![\tilde{\mathbf{u}}]\!] \otimes \check{\mathbf{n}})(x) dS_x$$

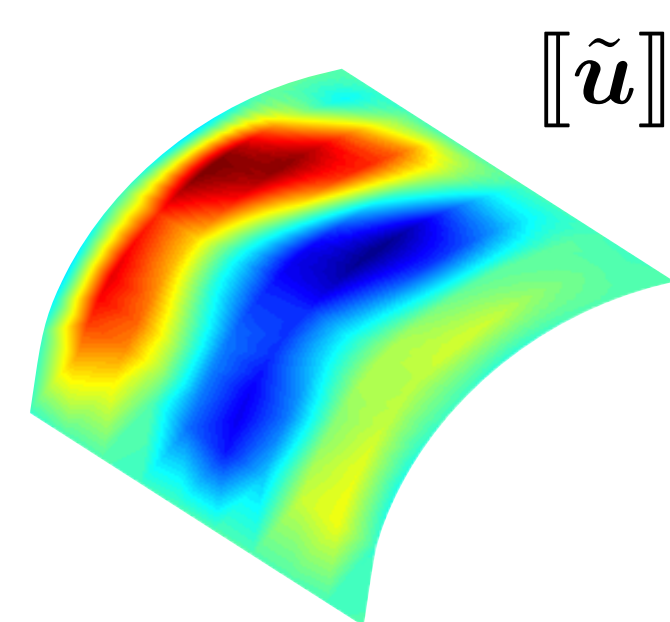
recovered
fracture surface



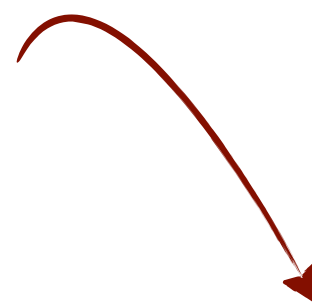
FEM of BEM simulation

Regularization

Reconstructed FOD
(propagating modes)

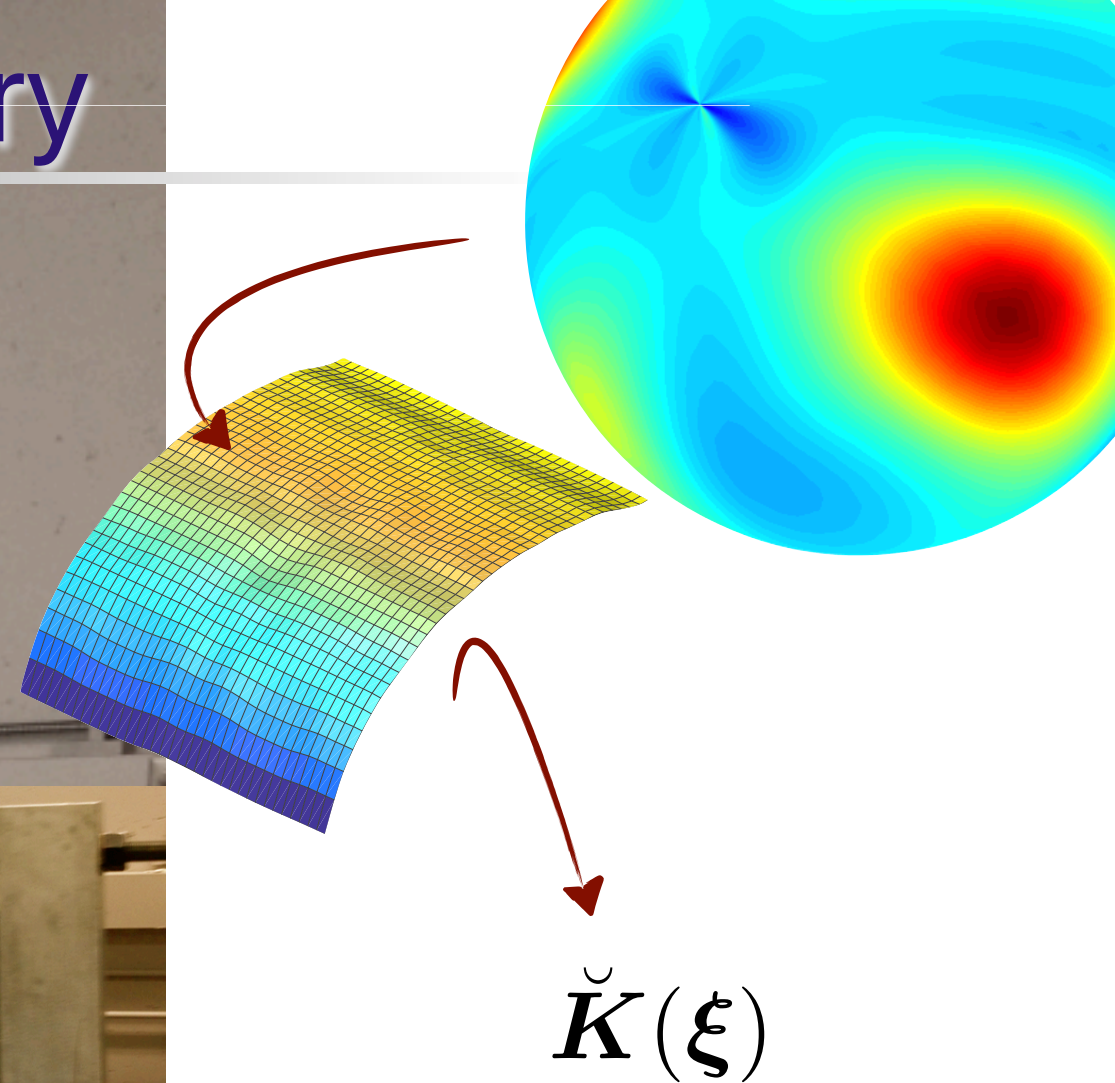
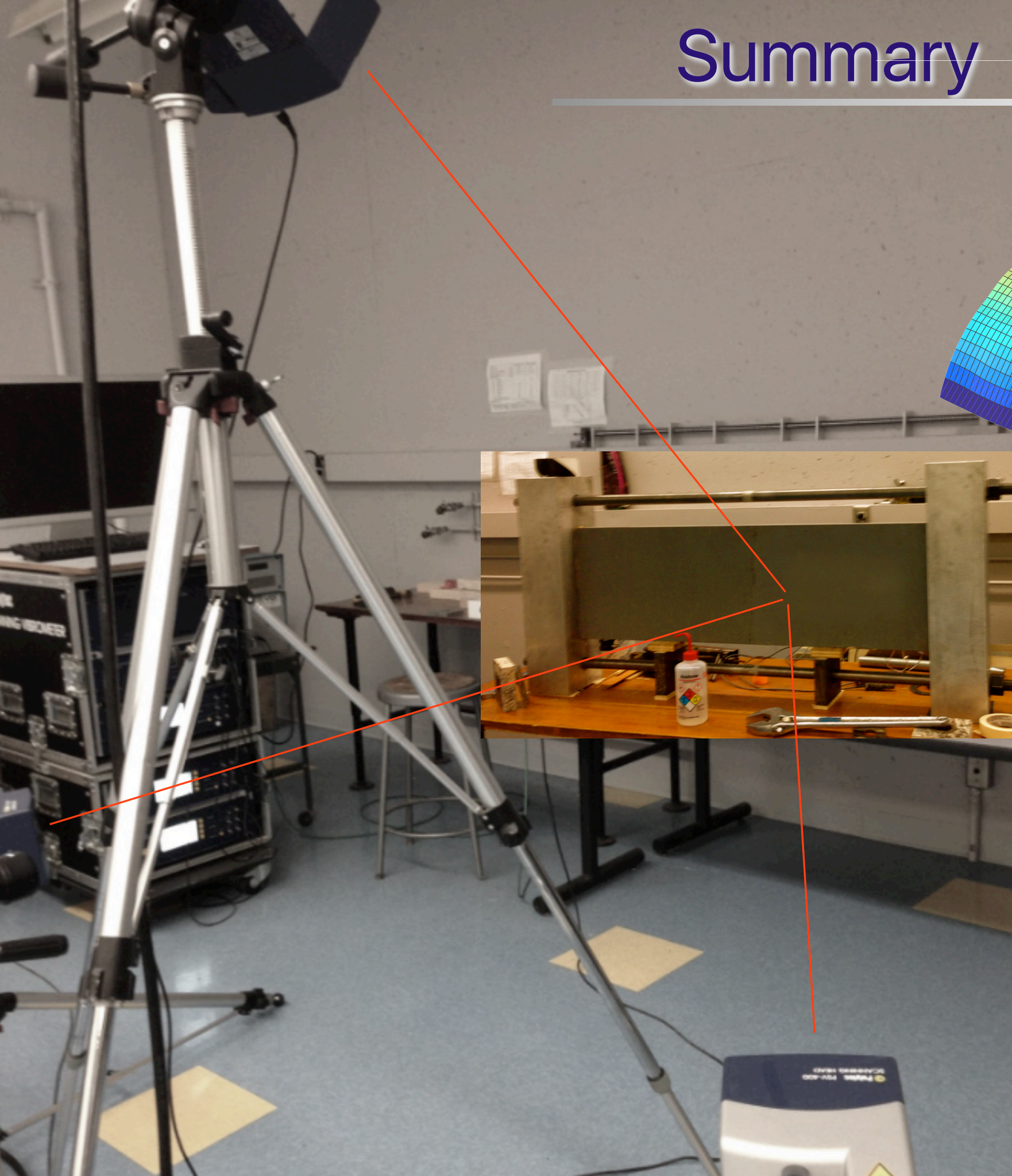


[\![\tilde{\mathbf{u}}]\!]



Solve for $\check{\mathbf{K}}(\xi)$

Summary



- low sensitivity to noise
- flexibility in sensing configuration
- no restriction on frequency regime of illumination
- active and non-iterative
- point-by-point characterization of the fracture interfacial condition